Evaluating the Safety and Mobility Impacts of American Dream Complex: Phase I (Feasibility Study, and Data Acquisition)

FINAL REPORT
April 2021

Submitted by:
Mohammad Jalayer, Ph.D.
Assistant Professor

Deep Patel
Research Assistant

Parisa Hosseini
Research Assistant

Abdelkader Souissi
Research Assistant

Ghulam Rasool, Ph.D.
Assistant Professor

Nidhal Carla Bouaynaya, Ph.D.
Professor & Associate Dean for Research and Graduate Studies

Department of Civil and Environmental Engineering
Department of Electrical and Computer Engineering
Rowan University,
Glassboro, NJ, 08028

External Project Manager
Joseph Weiss, Transportation Safety Analyst
New Jersey Division of Highway Traffic Safety

Disclaimer Statement

1. Report No. CAIT-UTC-REG31	2. Government Accession No.	3. Recipient's Catalog No.
4. Title and Subtitle Evaluating the Safety and Mobility Impacts of American Dream Complex: Phase I (Feasibility Study, and Data Acquisition)		5. Report Date April 2021
7. Author(s) Mohammad Jalayer (https://orcid.org/0000-0001-6059-3942) Deep Patel (https://orcid.org/0000-0001-7595-7489) Parisa Hosseini (https://orcid.org/0000-0003-3488-3895) Abdelkader Souissi (https://orcid.org/0000-0002-4740-2563) Ghulam Rasool (https://orcid.org/0000-0001-8551-0090) Nidhal Carla Bouaynaya (https://orcid.org/0000-0002-8833-8414)		6. Performing Organization Code CAIT/Rowan University
		8. Performing Organization Report No. CAIT-UTC-REG31
9. Performing Organization Name and Address Department of Civil and Environmental Engineering Dept. of Electrical and Computer Engineering Rowan University, Glassboro, NJ, 08028		10. Work Unit No.
		11. Contract or Grant No. 69A3551847102
12. Sponsoring Agency Name and Address Center for Advanced Infrastructure and Transportation Rutgers, The State University of New Jersey 100 Brett Road Piscataway, NJ 08854		13. Type of Report and Period Covered Final Report 12/01/2019 – 03/31/2021
		14. Sponsoring Agency Code
15. Supplementary Notes U.S. Department of Transportation/OST-R 1200 New Jersey Avenue, SE Washington, DC 20590-0001		

16. Abstract

Traffic congestion and motor vehicle crashes are perceived as pivotal concerns that are particularly difficult to manage in high-density urban areas. Thus, mitigating traffic congestion and improving users' safety on roadways are top priorities of the United States Department of Transportation (USDOT). American Dream Complex, located outside New York City, is an entertainment and retail center that was officially opened in October 2019. The complex is expected to attract over 40 million annual visitors once fully operational, which may potentially result in substantial mobility and safety issues for road users in the area. The present research work evaluates the mobility and safety concerns of the transportation network in the vicinity of the American Dream Complex due to its partial official opening. In terms of mobility, the performance of four surrounding corridors was explored by incorporating travel time inflation (TI) as a performance measure. Based on the results obtained from the mobility analysis, no considerable congestion was observed on the opening day of the American Dream Complex on surrounding corridors. Additionally, StreetLight data was also explored for Interstate 95, NJ Route 3, and NJ Route 120 for a period of 120 days before and 120 days after the opening of the complex. Findings showed an increase in the trips made after the opening; however, the travel duration was not significantly impacted due to the opening. To achieve the second goal of this study, the research team developed an innovative artificial intelligence (AI)-based video analytic tool to assess intersection safety using surrogate safety measures. To extract the trajectory data, the proposed work integrates a real-time AI detection algorithm, YOLO-V5, with tracking using the Deep SORT algorithm. The proposed approach achieved a relative accuracy between 95 and 98 percent in detecting and tracking vehicle trajectories.

17. Key Words Mobility, Safety, Conflict, American Dream Complex		18. Distribution Statement	
19. Security Classification (of this report) Unclassified	20. Security Classification (of this page) Unclassified	21. No. of Pages 90	22. Price

Table of Contents

List of Figures

List of Tables

EXECUTIVE SUMMARY

In recent years, traffic congestion and motor vehicle crashes have become major concerns that are particularly difficult to manage in high-density urban areas. Thus, mitigating traffic congestion and improving user safety on roadways are top priorities of the United States Department of Transportation (USDOT). American Dream Complex, located outside New York City, is an entertainment and retail center located within the Meadowlands Sports Complex in East Rutherford, New Jersey. With a building footprint exceeding 3 million square feet, it is the second-largest retail and entertainment complex in the nation, and it is located within five miles of New York City. The complex officially opened in October 2019 and is expected to attract over 40 million annual visitors once fully operational. This will potentially result in substantial mobility and safety issues for pedestrians and motorists in the area. The main objective of this study is to evaluate the mobility and safety concerns of the transportation network in the vicinity of this complex due to its partial official opening. To achieve the study objectives in terms of mobility, firstly, the performance of four surrounding corridors was explored by incorporating travel time inflation (TI) and its counterpart, the Corridor Travel Time Inflation (CTI), as performance measures. Then, TI for each corridor on a monthly basis was provided to explore the impact of the partial opening of the American Dream Complex on the surrounding corridors using probe data. Moreover, for a better visualization of the congestion, day-by-day Corridor Increase in Mean Travel Time (CIMTT) heatmaps were developed.

Based on the results obtained from monthly based TI, Interstate 95, NJ Route 3, and NJ Route 120 experienced an increase in TI due to the partial opening of the American Dream Complex during both non-peak and peak hours. However, results from the CIMTT heatmaps showed that no considerable congestion was observed on the opening day of the American Dream Complex on surrounding corridors. Average speed heatmaps also showed a decreased pattern for some cases and an increased pattern for some other cases due to the opening of the complex.

Similarly, StreetLight data was also explored for Interstate 95, NJ Route 3, and NJ Route 120 for a period of 120 days before and 120 days after the opening of the American Dream Complex. To investigate the impact of the complex opening on the roadways, changes in the travel duration of trips were examined. Findings showed an increase in the trips made after the opening; however, the travel duration was not significantly impacted due to the opening.

To achieve the second goal of this study, the research team developed an innovative artificial intelligence (AI)-based video analytic tool to assess intersection safety using Surrogate Safety Measures(SSM). Surrogate safety measures (e.g., Post-encroachment Time and Time to Collision) are extensively used to identify future threats, such as rear-end collisions due to vehicle and road users' interactions. To extract the trajectory data, the proposed work integrates a real-time AI detection algorithm, YOLO-V5, with tracking using the Deep SORT algorithm. 180-minutes of high-resolution video data were collected from two intersections near the American dream

complex. Non-compliance behaviors, such as red-light running and pedestrian jaywalking, are captured to better understand the risky behaviors at intersections. The proposed approach achieved a relative accuracy between 95 and 98 percent in detecting and tracking vehicle trajectories. Also, results demonstrated that the developed tool could be used to assess the safety of a signalized and non-signalized intersection.

CHAPTER 1. INTRODUCTION AND THE PROBLEM STATEMENT

Traffic congestion and motor vehicle crashes are major global challenges being faced every day. This is especially problematic in urban areas, where infill development will increase traffic volume in the region, thus impacting both congestion and crash frequency. Even as new developments are being constructed, reducing congestion and enhancing traffic safety on America's transportation roads are top priorities of the United States Department of Transportation (USDOT). According to the American Transportation Research Institute (ATRI), New Jersey has the worst traffic bottleneck in the country (Truckinginfo, 2019). Moreover, the state of New Jersey ranked second in the nation with respect to the ratio of pedestrian fatalities to the total number of motor vehicle deaths (NHTSA, 2018), necessitating further investigations. Therefore, it is especially important to understand on a quantitative level how major commercial development will impact the densely populated, highly congested region.

The American Dream Complex is an entertainment and retail center located within the Meadowlands Sports Complex in East Rutherford, New Jersey. With a building footprint exceeding 3 million square feet, once complete, American Dream Complex will be the second-largest retail and entertainment complex in the nation. The ongoing commercial development is located within 10 miles of New York City, NY. The American Dream Project (initially known as the Meadowlands Xanadu) was proposed by Mills Corporation in 2003, and the project construction began in 2004. However, in 2007, due to the Mills Corporation's bankruptcy, Colony Capital took over the project. Eventually, in July 2013, Triple Five Group, the owners of the two largest malls in North America, officially took control of the project. Despite the delays and obstacles, the American dream complex officially opened at about 10% capacity to the public on October 25, 2019 (Wikipedia, 2021). The American Dream Complex consists of four phases:

Phase 1: Phase 1 of the American Dream Complex is the Nickelodeon Universe and Theme Park opened on October 25, 2019. The Park is located on the Westernmost section of the American Dream Complex and houses many attractions packed within its 8.5-acre facility. The facility is accessible either by car or through mass transit. Additionally, The Rink, an NHL regulation ice-rink, was also opened on October 25, which features various family activities, including both open and figure skating, as well as hockey tournaments and other events.

Phase 2: The second phase of the American Dream complex is the Dreamworks Water Park, which was initially planned to open on March 19, 2020. The water park is located South of the Nickelodeon Universe Theme Park. This park was opened on October 1, 2020. According to American Dream's website, the park is home to over 40 waterslides and 15 attractions, including SurfRiders and a lazy river. American Dream also states that the facility will house the world's largest wave pool of 1.5 acres and the tallest indoor body slide of 142 feet.

Phase 3: This phase of the American Dream complex is the Big Snow Indoor Snow Park, a facility that was opened on December 5, 2019. The Big Snow Indoor facility is located in the North Wing

of the American Dream Complex. The Big Snow Indoor facility holds the honor of being North America's first indoor real-snow, snowboard, and ski center.

Phase 4: The fourth phase of the American Dream Complex is the final phase of the American Dream's grand opening, which involves the grand opening of the rest of the complex. This phase is set to include the debut of over 350 retail stores and additional entertainment facilities. Entertainment facilities include the LEGOLAND Discovery Center, SEA LIFE Aquarium, Angry Birds MiniGolf, and CXM Luxury Theatres. The opening of this section of the complex was delayed due to the COVID-19 pandemic, but it was finally opened on October 1, 2020. This phase marks the completion of the majority of American Dream facilities outlined in the phase planning model. On the map of the American Dream Complex, the location slated for retail stores is located at the heart of the complex as it will take up a majority of the facility.

Once fully open, American Dream Complex is expected to attract over 40 million visitors annually. This will potentially result in substantial mobility and safety issues for pedestrians and motorists in the area, which need to be further studied.

In order to assess the mobility issues, probe vehicle data can be used to evaluate the congestion performance of roadways going to and coming from the American Dream Complex. This type of data is being used as a common data source for measuring the regional performance of roadway networks. By developing a performance evaluation method based on these data, the health of the roadway system can be monitored, and future improvement plans can be established. Probe data is a valuable source of speed information in terms of temporal and spatial coverage (Brennan et al., 2019). This type of data is increasingly incorporated in transportation analytics.

There are a number of situations that can have an immediate impact on the prevailing traffic conditions. Crash incidents, weather events, construction, and congestion, all impact a roadway network almost daily (Brennan et al., 2015). Reliable traffic information obtained from probe vehicles has been used to assess travel time variation resulting from these daily traffic fluctuations due to specific conditions. Traditionally, a trip generation model is produced when specific land use is designated to ascertain the traffic impact in the immediate area. With the advent of probe vehicle telematics, these normally modeled impacts can now be measured. It is understood that the opening of a large commercial complex will affect the traffic conditions of the adjacent roadways, which is supported by the ITE Trip Generation manual. What is not known is how much of an impact this type of opening will have on a complex this large, whose retail and entertainment construction is being phased. Investigating the changes in traffic conditions of adjacent roadway networks due to the opening of a major development provides a means to proactively manage traffic congestion and improve users' safety on roadways. Therefore, it is especially important to understand on a quantitative level how major commercial development will impact densely populated, highly congested regions.

In terms of accomplishing a successful design, plan, and management of a safe traffic system, it is essential to have a broad understanding of road user behavior and its effect on the safety of traffic flow. In order to do that, several studies have been researched for identifying diverse Surrogate Safety Measures (SSM) using micro stimulations and video processing techniques. Generally, SSM can be characterized as either time-based or non-time-based (Gettman and Head, 2003). SSM is an extensively used method for recognizing future threats that may arise due to conflict among road users (Tak et al., 2018). Perkins and Harris first proposed the procedure for recording and identifying the traffic conflicts at an intersection and also defined traffic conflict as all possible accident condition that leads to the elusive action like swerving or braking (Perkins and Harris, 1967). Later, Amundson and Hyden (1977) revised the definition and is recognized by FHWA and other international agencies as "an observable situation in which two or more road users approach each other in time and space to such an extent that there is a risk of collision if their movements remain unchanged" (Gettman et al., 2008). There are a long history and current research work that ample efforts have been put into the improvement of methodology, connecting the conflicts and crashes to the design and expansion of surrogate measures (Gettman et al., 2008). In context to the study, this section will provide an overview of the traffic confits and an understanding of the surrogate conflict measures, including Time to Collision (TTC), Post-Encroachment Time (PET), etc. Moreover, this section will also deliver an overview of the existing studies that have tried to examine the surrogate conflict measures using the video analysis technique.

Research Goals and Objectives:

This project mainly focused on identifying the traffic and safety issues associated with the American Dream complex. The main objectives of this study can be summarized as follows:

- to conduct a feasibility study by evaluating the traffic operations and safety concerns of the transportation network in the vicinity of this complex

- to collect relevant data representing existing issues over a period of time to compare to the first benchmark phase of data collection since the opening of the complex

- to conduct initial analytics to assess mobility and safety issues, and

- to develop a video analytics framework to identify the conflicts between different road user groups, such as drivers and pedestrians, by using Artificial Intelligence (AI) tools

CHAPTER 2. LITERATURE REVIEW

In this chapter, a comprehensive literature review is provided to synthesize existing information on the American Dream Complex, traffic and safety data collection/analysis methods, video analytics, and strategies to alleviate congestion and safety issues specific to the American Dream Complex. The summary of previous studies herein is divided into two sections, mobility and safety.

2.1 Mobility

The application of probe vehicle data in performance evaluation of highways and arterial roads has drawn considerable research interest over the last decades. A summary of previous studies on the application of probe vehicle data is provided as follows:

Dynamic Freeway Travel-Time Prediction with Probe Vehicle Data: Link Based Versus Path Based

(Mei Chen and Steven I. J. Chien)

Proposing a path-based travel time model using probe vehicle data is the main objective of this study. To do so, the Kaman filtering technique was employed to develop the model. This technique is based on the real-time records obtained from probe vehicles. Then, the performance of the proposed model was compared with the conventional link-based travel time estimation models. It was shown that the proposed path-based model in this study outperformed normal traffic flow. It was also concluded that the variance of the reports obtained from probe vehicles increased when road traffic volume was near its capacity. This condition led to more errors in travel time estimation. This study also showed that increasing probe vehicle percentage can slightly result in more accurate travel time estimations for path- and link-based approaches (e. g., 3% improved accuracy for increasing probe vehicle percentage from 1% to 3%) (Chen and Chien, 2001).

Application of Probe-Vehicle Data for Real-Time Traffic-State Estimation and Short-Term Travel-Time Prediction on a Freeway

(Chumchoke Nanthawichit, Takashi Nakatsuji, and Hironori Suzuki)

This study suggests a new model for traffic state estimation by using probe vehicle data and detector data. The proposed model is based on the Kalman filtering technique. In this technique, "a microscopic traffic flow model" served as state equations. Various traffic conditions were considered for testing the proposed approach. This approach is able to conduct state estimation even if some probe data is missing for a specific segment. Results showed that the proposed approach could lead to state estimations with smaller errors (70% to 85% reduction error). Moreover, the proposed model was implemented to estimate short-term travel time by converting the estimated speeds. Afterward, the results were compared with the estimations obtained from

three conventional approaches. It was found that the proposed method in this study outperformed by decreasing the estimation error (MARE < 0.04) (Nanthawichit et al., 2003).

Variability of Travel Time Estimates using Probe Vehicle Data

(Toshiyuki Yamamoto, Kai Liu, and Taka Morikawa)

This study focuses on how reliable travel time can be estimated for roadways or links using probe vehicle data with different frequencies. An urban route located in Japan was selected as the case study, and a six-month probe vehicle data was collected for this arterial. By deleting probe data with higher frequency, probe data with lower frequency was incorporated to conduct simulations for probe data variability assessment. Results indicated that using probe data with lower frequency can result in smaller variance for links exactly before the signalized intersections. Results also showed that using probe data with lower frequency, the accuracy level of predicting the travel time for roadway segments is almost the same as those predicted by using probe data with higher frequency (Yamamoto et al., 2006).

Estimating Delay Time at Signalized Intersections by Probe Vehicles

(Kai Liu, Toshiyuki Yamamoto, and Taka Morikawa)

The main objective of this study is to conduct a sensitivity analysis of delay measurement by using probe vehicle data with different transmission intervals at an intersection. A total of six-month probe vehicle data with high frequency (five-second intervals) from ten probe taxis in Japan was obtained. By deleting some parts of the data, lower-frequency data (from 10 s to 60 s intervals) was also obtained for further analysis. Then, two algorithms were developed to calculate the travel time delay for both high-frequency and low-frequency data. It was found that the dataset with 10 s transmission intervals is capable of estimating travel time 74% correct with an average error of 12%. However, the dataset with 60 s intervals predicted delays 37% correct with an average error of 47%. These findings proved that as the transmission interval increases, the accuracy level of delay time estimation decreases (Liu et al., 2006).

Bayesian Mixture Model for Estimating Freeway Travel Time Distributions from Small Probe Samples from Multiple Days

(Klayut Jintanakul, Lianyu Chu, and R. Jayakrishnan)

The main objective of this study is to propose a new hierarchical Bayesian model to predict the distribution of freeway travel time from small samples of probe data. In order to address the heterogeneous nature of the travel time and its skewed or multimodal distribution, two normal components were considered in this study. An initial dataset consisting of a small sample of travel time from probe data (gathered for 20 days over a specific time duration) was utilized prior to determining the model parameters. A simulation was also conducted to verify the results. Six mi

of I-405, located in Orange County, California, was simulated using PARAMICS. Results indicated that the proposed model is capable of predicting the distribution of travel time for each interval (Jintanakul et al., 2009).

Monitoring travel times in an urban network using video, GPS, and Bluetooth

(Li Jie, Henk van Zuylenb, Liu Chunhua, and Lu Shoufeng)

In this study, the performance of different methods for estimating travel time in urban networks in Changsha, China, was explored. Travel time distributions were measured by incorporating different methods, and the results were compared. In this study, considered methods include Bluetooth scanners, video observations, GPS devices in 6000 taxis, private cars, busses (with 30 s polling interval), and GPS devices installed in a few probe cars (with 3 Hz measuring frequency). Results revealed that the quality of estimated travel time from Bluetooth scanners is not acceptable due to two main reasons, the existence of outliers that cannot be deleted easily and the difficulty in distinguishing Bluetooth devices belonging to different passenger groups. Results also indicated that standard GPS devices are effective tools for estimating link travel times. It was found that the average speed data obtained from GPS can be effectively utilized to measure the average travel time for a link. Traffic counts obtained from video recordings were found to be more accurate compared to ones obtained from loop detectors. The cumulative count method was applied to evaluate the accuracy of GPS devices installed in a few probe vehicles. It was concluded that the travel times measured with GPS devices are in agreement with those measured by the suggested method (Jie et al., 2011).

Probe Vehicle Data for Characterizing Road Conditions Associated with Inclement Weather to Improve Road Maintenance Decisions

(Alexander M. Hainen, Stephen M. Remias, Thomas M. Brennan, Christopher M. Day, and Darcy M. Bullock)

This paper discusses the feasibility of using probe vehicle data in characterizing roadway conditions impacted by inclement weather along a segment. In this study, eight portable devices for data collection were installed with about ten miles spacing along the I-65 in Indiana to collect Bluetooth MAC Addresses. The selected stations are located within the boundaries of ice and snow maintenance units. In order to collect the data from vehicles traveling both Southbound and Northbound of the I-65, the data collection devices were installed in the median. Data were collected in 2011 during two storm events. Since the travel time is dependent on segment length, space means speed (SMS) was considered as the performance measure of road segments in this paper. Afterward, the statistical distribution of SMS for the selected segment was plotted, which are "intellectually sound but visually intuitive graphs." Results showed that during the storm, SMS experienced a 20 mph decrease, and the interquartile experienced a four mph increase. This paper proved the applicability of emerging probe vehicle data in determining the effect of a weather

condition on the roadway and providing alternative strategies for the roadway condition (Hainen et al., 2012).

Probe Vehicle-Based Statewide Mobility Performance Measures for Decision Makers

(Thomas M. Brennan, Jr., Stephan M. Remias, Gannon M. Grimmer, Deborah K. Horton, Edward D. Cox, and Darcy M. Bullock)

This paper proposes several techniques to create performance measures of current freeway conditions. These performance measures can be used at a state agency level for decisions such as the arrangement of capital program investments, the scheduling of lane closures, and the management of snow removal. This paper discusses techniques for the use of commercial probe data in the assessment of congestion of seven Indiana Interstate highways for a total of 1,866 lane miles. In this paper, three congestion performance measures, including "congestion hours," "distance-weighted congestion hours," and "the congestion index" was employed to assess congestion and evaluate the performance of roadway systems. The probe data was also utilized to determine the user delay and its related costs. It was shown that the delay cost for some portion of I-65 (7.4 miles) during an 18-month period was $32 million (Brennan et al., 2013).

Travel time estimation for urban road networks using low frequency probe vehicle data

(Erik Jenelius, and Haris N. Koutsopoulos)

A statistical model was suggested in this study in order to predict network travel time by incorporating low-frequency probe data. In this study, a multivariate normal distribution was presumed for link travel time. The suggested network model was capable of modeling the trip travel times as "link travel time" and "intersection delays." The proposed model considered a spatial moving average (SMA) structure basis for the associations between travel times of various links. The proposed model was then, employed for an arterial network located in Stockholm as the case study. It was shown that the probe vehicle data with low frequency could be utilized for performance evaluation and monitoring of urban transport systems. It was also concluded that one could monitor very small variations of travel times on a daily, seasonally, and also yearly basis (Jenelius and Koutsopoulos, 2013).

Performance Characterization of Arterial Traffic Flow with Probe Vehicle Data

(Stephen M. Remias, Alexander M. Hainen, Christopher M. Day, Thomas M. Brennan, Jr., Howell Li, Erick Rivera-Hernandez, James R. Sturdevant, Stanley E. Young, and Darcy M. Bullock)

This study focuses on the application of probe data in determining the most applicable adaptive control objectives and evaluating their effectiveness. To do so, four case studies were considered, and their proposed techniques of data collection for performance evaluation of adaptive control systems were reviewed. The proposed techniques in these case studies include "reidentification

with pavement sensors," "reidentification with Metropolitan Affairs Coalition address matching," and "crowd-sourced data." The study also addressed the weaknesses and the strengths of each implemented technique. As a result, it was suggested that the commercial data providers supply more useful probe data information by providing detailed base maps. It was also found that the probe data provides the richest information under the condition that the distributions are performed for links determining control or approach delay of every signalized intersection. This study proved the idea that the probe data distribution can be utilized to determine the appropriate control objectives for a corridor (Remias et al., 2013).

Urban link travel time estimation based on sparse probe vehicle data

(Fangfang Zheng and Henk Van Zuylen)

This paper attempts to estimate travel time by using probe vehicle data having a low polling frequency of 1 min or 5 min. Since this kind of low-frequency probe data results in estimating partial travel time for a link, this study aims to overcome this issue and estimate the complete travel time. To achieve this goal, an artificial neural network-based model with three layers was developed for each probe vehicle using the probe data. Link IDs, time stamps, speeds, and probe positions were considered as input data for the neural network model. Then, an analytical model proposed by Hellinga et al. (2008) was selected as the comparative study. Moreover, VISSIM simulation software was implemented to conduct the performance evaluation of the proposed model and the analytical model suggested by Hellinga et al. (2008). Results indicated that the proposed neural network-based model had better performance than the proposed model by Hellinga et al. (2008). This result can be explained by the higher number of parameters, which the neural network-based model applies as inputs. Results also revealed that the position parameter is the underlying input for the neural network-based model, and the model's accuracy directly relies on this parameter (Zheng and Zuylen, 2013).

Spatially Referenced Probe Data Performance Measures for Infrastructure Investment Decision Makers

(Stephen M. Remias, Thomas M. Brennan, Christopher M. Day, Hayley T. Summers, Deborah K. Horton, Edward D. Cox, and Darcy M. Bullock)

The main objective of this study is to assess the application of crowdsourced probe vehicle data and its performance measures in developing and visualizing the congestion from the spatial and temporal perspectives so that decision-makers can take benefit of them in order to perform an evaluation study of past and potential future investments. To achieve this goal, I-80-I-90 corridor located in Northwest Indiana was considered, and the congestion changes during a bridge construction over this corridor in 2011 and 2012 were accessed by developing three performance measures. Developed performance measures include travel time (TT), segment speed, and travel time deficit (TTD). Estimated costs caused by congestion were also calculated in this study by

adding the costs for passenger cars, and truck and commercial vehicles, and the costs related to carbon dioxide emissions. Consequently, the TTD was developed for I-80 for 2012 at a national level, and the congestion distribution for different states along this corridor was discussed (Remias et al., 2014).

Performance Measures to Characterize Corridor Travel Time Delay Based on Probe Vehicle Data

(Thomas M. Brennan, Jr., Stephen M. Remias, and Lucas Manili)

This study aims to develop a visualization-based methodology in order to characterize congestion along a corridor. To this end, I-80 Located in Northern New Jersey, was considered a case study, and over 90 million speed records for 2013 were gathered for further analysis. In this study, a variable speed threshold was considered for each traffic message channel (TMC). According to this approach, the threshold was calculated by considering the 70th percentile of the 15-min average speeds. Congestion hours (VCH) corresponding to TMCs that are below the congestion threshold were also calculated. Furthermore, travel time inflation (TI) was employed as the performance measure to perform the analysis. Then, due to the deficiency of TI in showing the time of the day, corridor travel time inflation (CTI) was calculated and visualized for I-80 corridor. The authors suggested that the visualization techniques that they developed by using crowdsourced probe vehicle data provide the decision-makers with a useful tool for roadway management-related tasks (Brennan et al., 2015).

Characterizing Bridge Functional Obsolescence Using Congestion Performance Measures Determined from Anonymous Probe-Vehicle Data

(Andrew J. Bechtel, Thomas M. Brennan Jr., and Jhenifer Mesquita de Araujo)

The main purpose of this study is to evaluate the congestion condition along obsolete bridges by using anonymous probe data. 37 bridges located in Burlington County, New Jersey, were selected for further analysis. The selected bridges had poor deck geometry ratings based on the rating system defined by the National Bridge Inventory (NBI). In order to determine congestion measures, the authors analyzed about 35 million speed records obtained for selected bridges and calculated congestion hours with the speed threshold of 70th percentile space mean speed (SMS). Then, the results were compared to NBI ratings. The study concluded that out of the 37 bridges that were expected to have a high degree of congestion, 28 bridges had congestion of less than 100 hours, 2 had more than 100 hours of congestion, and 7 had no congestion hours. These results proved the fact that the rating system suggested by NBI cannot be a representative indicator for congestion. The proposed methodology, as well as the NBI rating, were then employed to illustrate the capability of congestion analysis as a useful tool for bridge management purposes (Bechtel et al. 2016).

Probe data-driven travel time forecasting for urban expressways by matching similar spatiotemporal traffic patterns

(Zhihao Zhang, Yunpeng Wang, Peng Chen, Zhengbing He, and Guizhen Yu)

This study suggests a pattern-matching approach for estimating travel time. This method consisted of multiple steps for estimating travel time which benefits from a matching process of spatiotemporal traffic patterns on a large scale. In the first step, the method applied the Gray-Level Co-occurrence Matrix (GLCM) to obtain the spatiotemporal features of traffic. Secondly, the distance of similar traffic patterns was measured using the Normalized Square Distance (NSD). Thereafter, patterns matching the best were selected using a screening process. Consequently, the travel times were predicted by implementing a negative exponential weight for each selected pattern. This method, finally, was applied to a 32-km expressway located in China by matching the speed patterns. Results proved the applicability of the suggested method in predicting travel times for different traffic conditions. This method had better performance compared with other conventional methods such as Naïve KNN and Historical Average (Zhang et al., 2017).

Multiple Factor Based Sparse Urban Travel Time Predictions

(Xinyan Zhu, Yaxin Fan, Faming Zhang, Xinyue Ye, Chen Chen, and Han Yue)

This study suggests a new multi-factor-based methodology by incorporating a neural network with three layers in order to predict travel time. The proposed methodology consisted of three steps. In the first step, the probe data for a traveling taxi was collected during the business days for a targeted link. Then, the feature associations between the target link and the adjacent ones were explored during 30 min intervals. In this step, approximately 225 thousand records were collected. As the second step, an artificial neural network with three layers was developed by considering eight neurons in the input layer and one neuron in the output layer. The impact of different factors such as speed expectation, link length, time instant, and weather information was also explored in this step. In the third and final step, the travel time for the target link was estimated using the trained neural network. For results verification, the authors incorporated the probe vehicle data for Wuhan, China, gathered from May to July 2014. It was concluded that recommended methodology in this study could perform well under the condition of having sparse data. It was also found that the factors, including the 30 min interval selected for a day, the day of the week, and the expected speed for adjacent links, are the most influential factors in the estimation of travel time for the target link (Zhu et al., 2018).

Performance Measures for Characterizing Regional Congestion using Aggregated Multi-Year Probe Vehicle Data

(Thomas M. Brennan Jr., Mohan M. Venigalla, Ashley Hyde, and Anthony LaRegina)

This study details the regional congestion assessment by using aggregated probe speed data during an extreme condition, Hurricane Sandy. To this goal, probe speed data obtained for 10 miles of coastline covering five counties in New Jersey in 2012 (including 614 TMCs and 90 million speed records) was analyzed in this study. The results, afterward, were compared with the congestion data for 2013, 2014, and 2016. The speed threshold considered in this study was 70% of the base free-flow speed (BFFS). Regional travel time inflation (RTI), showing the spatial congestion distribution on a regional level, was taken into account as the performance measure and was calculated by adding all travel time inflation (TI) of each TMC. The study proved the applicability of RTI and TI as performance measures in determining the congestion of roadway systems. Subsequently, the regional increase in mean travel time (RIMTT) was proposed to perform the congestion on a yearly basis for 2016. The study showed that RIMTT is a useful visualization tool that can characterize and indicate congestion changes throughout the day or the year (Brennan et al., 2018).

Exploring Travel Time Distribution and Variability Patterns Using Probe Vehicle Data: Case Study in Beijing

(Peng Chen, Rui Tong, Guangquan Lu, and Yunpeng Wang)

The main contribution of this study is to prove the usefulness of probe vehicle data in investigating "travel time distribution and variability patterns." To this goal, 200 links in China covering major roads, secondary roads, urban expressways, and auxiliary urban expressways were selected as case studies, and probe vehicle data were obtained for them. Different distributions, then, were developed for unit distance travel time. Among all the developed distributions, the lognormal distribution was selected by conducting three different goodness-of-fit tests (chi-squared test, Anderson-Darling test, and Kolmogorov-Smirnov test). Moreover, in order to examine "the day-of-week travel time variability pattern," four reliability measures (including punctuality rate (PR), buffer time index (BTI), coefficient of variation (CV), and unit distance travel time) were employed in this study. It was indicated that major roads and auxiliary roads of urban expressways have the same reliable travel time variability patterns in the daytime. However, at nighttime, urban expressways showed the most reliable pattern. It was also concluded that all types of roads except for secondary roads experience distinguishable morning and afternoon peaks (Chen et al., 2018).

Assessing Highway Travel Time Reliability using Probe Vehicle Data

(Piotr Olszewski, Tomasz Dybicz, Kazimierz Jamroz, Wojciech Kustra, and Aleksandra Romanowska)

This article attempts to apply probe vehicle data to identify the performance measure for examining the frequency and severity of traffic congestion that occurs along a roadway. To do so, firstly, a pilot survey was carried out on an A2 motorway located in Poland in order to confirm the reasonable accuracy of probe vehicle data as well as its applicability for examining traffic conditions. Expressway S6 located in Poland was, then selected as a case study, and a new method was proposed to calculate free-flow speed (FFS) in the off-peak period (FFS) by utilizing traffic counts and probe vehicle data. To find the segments having higher delay and lower reliability, the authors determined the travel time indexes and reliability rates in 2016. It was found that only two segments of Expressway S6 had a reliability rating under 90%, indicating that this roadway has a good travel time reliability. Consequently, a new reliability indicator named delay index was introduced, and the delay map graphs illustrating the special and temporal distribution of congestion were suggested in this study (Olszewski et al., 2018).

Using anonymous probe-vehicle data for a performance indicator of bridge service

(Andrew J Bechtel, Thomas M Brennan, Kevin Gurski, and Jessica Ansley)

This study aims to propose a congestion metric as a performance indicator for bridges by employing anonymous probe vehicle data. To this goal, 2211 bridges located in New Jersey were selected, and the congestion metrics were calculated for them. In this study, any drop in speed that was below a threshold (70th percentile of space mean speed) was considered as a congestion occurrence. The US National Bridge Inventory (NBI) defines a performance indicator for bridges, namely functionally obsolete (FO) designation. The authors, as the next step, compared the proposed congestion metric with FO designation. Results obtained from comparison indicated that only a few FO bridges (4%) had congestion metrics exceeding 200h in 2014. Moreover, only 55% of FO or structurally deficient (SD) bridges had congestion metrics exceeding 2500h. It was also concluded that bridges located closer to large cities in New Jersey experienced higher congestion metrics. This study finally suggested that the congestion metrics can appropriately serve as performance indicators (Bechtel et al., 2018).

Use of Multi-sensor Data in Modeling Freeway Travel Time: Variability Analysis and Prediction

(Zhen Chen)

The aims of this study are as follows: finding the most suitable travel time reliability (TTR) measure, investigating the pattern of travel time variability by taking into account different factors,

and finally proposing a new machine learning-based methodology, namely XGBoost model, to predict the distribution of travel time. Different factors, including "weather condition," "time of the day," and "day of the week" were considered in the model. Eight segments of I-77 located in Charlotte, North Carolina, were selected as a case study, and travel time data of this corridor was obtained from the Regional Integrated Transportation Information System (RITIS) website. The planning time index (PTI) was considered as the travel time reliability measure in the travel time variability analysis. Results obtained from the variability analysis showed that the travel time variability for weekends is lower compared to weekdays for the segments of the corridor having a considerable peak hour pattern. Finally, results obtained from travel time prediction analysis showed that the efficiency and accuracy of the computation for travel time estimation could be improved by using XGBoost model (Chen, 2019).

Probe vehicle performance measures for assessing travel time reliability

(Kyle Robert Thompson)

This study aims to propose different metrics for assessing travel time reliability by utilizing probe vehicle data obtained from INRIX. To this end, by reviewing previous studies and FHWA rulemaking, ten various reliability metrics for travel time were obtained and calculated for interstate segments located in Iowa. Results then, were compared, and three similar reliability metrics were determined. The three selected metrics include "buffer time index," "the standard deviation of segment travel time index (TTI)," and "the 15th-85th percentile range of TTI". Afterward, the three selected metrics and two metrics from FHWA ("the level of travel time reliability and peak over travel time reliability") were incorporated to conduct a reliability analysis of an interstate network in Iowa by determining the most unreliable segment and developing choropleth maps. Results showed that unreliable segments determined by each metric are not consistent. This can be attributed to the sensitivity of considered metrics to TTI distribution characteristics. Moreover, by combining three selected metrics in different groups as composite metrics, a new method was proposed to assess the reliability of travel time. Results revealed that the combination of "the 15th-85th percentile range of TTI" and "standard deviation of TTI" can serve as useful metrics for travel time reliability assessment (Thompson, 2019).

Visualizing and Evaluating Interdependent Regional Traffic Congestion and System Resiliency, a Case Study Using Big Data from Probe Vehicles

(Thomas M. Brennan Jr., Ryan A. Gurriell, Andrew J. Bechtel, and Mohan M. Venigalla)

This study applied aggregated probe data in order to conduct traffic congestion analysis under the condition that a traffic-related event occurred on the roadway network. The sites where the study was conducted spanned across the Mercer, Burlington, and Camden Counties in New Jersey. The reason these counties were specifically chosen is that they are in close proximity to I-276, a bridge that had been closed for a period of time. The data collection for this experiment was performed

between January 1 and March 31 of 2017, leading to the data yielding over 90 million unique speed records. Mean Percent Increase in TMC Travel Time (MTT) was used as a traffic congestion measure in this study. Heat maps showing the bridge closure were obtained using probe vehicle data and were illustrated for three counties. It was found that for Mercer County, the bridge closure resulted in a considerable increase in MTT (Brennan et al., 2019). Table 1 tabulates a summary of conducted studies on the application of probe vehicle data for performance evaluation.

Table 1 Summary of studies on probe vehicle data application.

Studies	Year	Variables Analyzed
Chen and Chien	2001	Real-Time Estimation of Travel Time
Nanthawichit et al.	2003	Travel-Time Prediction, Traffic-State Estimation
Yamamoto et al.	2006	Variability of Link Travel Time Estimates
Liu et al.	2006	Travel Time Delay
Jintanakul et al.	2009	Travel Time Distribution Prediction
Jie et al.	2011	Travel Time Distribution Prediction
Hainen et al.	2012	Space mean Speed, Temporal Variation Impact
Brennan Jr. et al.	2013	Congestion Hours, Distance-Weighted Congestion Hours, Congestion Index, User Delay, and Cost
Jenelius and Koutsopoulos	2013	Link Travel Time Prediction
Remias et al.	2013	Travel Time, Travel Time Reliability
Zheng and Zuylen	2013	Travel Time Prediction
Remias et al.	2014	Travel Time (TT), Segment Speed, Travel Time Deficit (TTD), Cost
Brennan Jr. et al.	2015	Congestion Hours; Travel Time; Travel Time Inflation (TI)
Bechtel et al.	2016	Congestion Hours, Deficiency Score, Travel Time
Zhang et al.	2017	Future Travel Time Prediction
Zhu et al.	2018	Segment length, Standard Deviation of Speed, Travel Time Prediction
Brennan Jr. et al.	2018	Base Free Flow Speed, Base Free Flow Travel Time, Total Travel Time Inflation (TI), Regional Travel time Inflation
Chen et al.	2018	Day-of-Week Travel Time, Buffer Time Index (BTI), Unit Distance Travel Time, Punctuality Rate (PR), Coefficient of Variation (CV)
Olszewski et al.	2018	Traffic Speed, Travel Time Reliability, Free Flow Speed

Bechtel et al.	2018	Travel Time Reliability Rate, Delay Index,
Chen	2018	Travel Time Distribution, Time of Day, Day of Week, Year, Weather Condition
Thompson	2019	11 Travel Time Reliability Metrics (such as Buffer Time Index (BTI), the Standard Deviation of Segment Travel Time Index (TTI), the 15th-85th Percentile Range of TTI)
Brennan Jr. et al.	2019	Base Free Flow Speed, Travel Time, Travel Time Inflation, Regional Increase in Mean Travel Time (MTT)

2.2 Safety

Examining intersection safety using Surrogate Safety Measures has been implemented in many studies over recent years. A summary of previous studies that evaluated SSM's using video data is provided as follows:

Large-scale automated proactive road safety analysis using video data

(Paul St-Aubin, Nicolas Saunier, and Luis Miranda-Moreno**)**

This study demonstrates a real-world outline for the application of an automated, high-resolution, video-based traffic-analysis system. This is predominantly focused on researchers for behavioral studies and road safety analysis. The study collects massive amounts of microscopic traffic flow data from ordinary traffic using CCTV and consumer-grade video cameras and offers the tools for showing basic traffic flow studies as well as more advanced, pro-active safety and behavior studies. This study developed a methodology to evaluate a large and detailed study of roundabouts. Results demonstrated an 85-95 percent of tracking accuracy (St-Aubin et al., 2015).

Safety evaluation of unconventional outside left-turn lane using automated traffic conflict techniques

(Yanyong Guo, Tarek Sayed, Mohamed Zaki, and Pan Liu)

This article focuses on the evaluation of the safety impacts of unconventional outside left-turn lanes at signalized intersections. The assessment is shown using an automatic video-based traffic conflict technique. Video data are collected from a signalized intersection, where both old inside and alternative outside left-turn lanes are installed on two intersection approaches. The article compared the frequency and severity of conflict for left-turning vehicles as well as the proportion of vehicles involved in conflicts from the inside and outside left-turn lanes. The results showed that the intersection approaches with outside left-turn lanes had noticeably more conflicts compared to approaches without outside left-turn lanes. The approaches with outside left-turn lanes had a much higher conflict. The trade-off between the improved mobility and the negative

safety impact of outside left-turn lanes should be considered before future installations (Guo. et al., 2016).

Calibration and validation of a new time-based surrogate safety measure using fuzzy inference system

(Navid Nadimi, Hamid Behbahani, and HamidReza Shahbazi.)

This article focused on Post-Encroachment Time (PET) and Time-to-collision (TTC), the two important time-based SSM's classifying the probability of a rear-end collision, head-on, and right-angle collisions. The study showed that the indicators could be used as a warning strategy in collision avoidance systems. It can be developed using a new index that combines the properties of both TTC and PET. Multiple variables were considered in this article, including DRAC, PSD, and CPI. Results showed that evasive maneuvers due to the driver errors of the following car (clearance, relative speed, and vehicle speed) could be detected by collision avoidance systems (Nadimi et al., 2016).

Measuring Crosswalk Safety at Non-signalized Crossings During Nighttime Based on Surrogate Measures of Safety: A Case Study in Montreal, Canada

(Ting Fu, Luis Miranda-Moreno, and Nicolas Saunier)

This paper evaluates the safety method of crosswalks at nighttime by using thermal video sensors in downtown Montreal, Quebec. Thermal video data was collected in both daytime and nighttime conditions for a total number of 16.8 hours, and video data processing was carried out using the tracker, then road user trajectories were obtained. Vehicle speed within the marked crosswalk area was calculated. Results showed that the proposed thermal-video-based surrogate safety methodology is effective in collecting and analyzing pedestrian-vehicle interactions at night, regardless of lighting conditions. Also, evaluated that the average vehicle speed and percentage of dangerous conflicts were higher during nighttime compared to daytime, indicating that pedestrians were at higher risk during nighttime (Fu et al., 2016).

Surrogate Safety Analysis of Pedestrian-Vehicle Conflict at Intersections Using Unmanned Aerial Vehicle Videos

(Peng Chen, Weiliang Zeng, Guizhen Yu, and Yunpeng Wang)

This study examines the practicability of considering the Unmanned Aerial Vehicle video for the surrogate safety analysis at an urban intersection in Beijing, China. The study team collected an Arial video roughly 100 m from the ground for 60 minutes. GoPro Hero Black Edition:3 camera with a 1920 x 1080 resolution was attached to a Phantom 2 UAV for a video recording. The frequency, location, and severity of the pedestrian-vehicle conflicts are determined by calculating two surrogate safety measures, Post-Encroachment Time (PET) and Relative Time to collision

(RTTC). Results showed relatively risky behavior of right-turn vehicles around the corner and high exposure of pedestrians to traffic conflict both outside and inside the crosswalk. Additionally, findings also depicted that UAV can support the assessment of an intersection's safety in an accurate and cost-effective way (Chen et al., 2017).

Automatic Traffic Data Collection under Varying Lighting and Temperature Conditions in Multimodal Environments: Thermal versus Visible Spectrum Video-Based Systems

(Ting Fu, Joshua Stipancic, Sohail Zangenehpour, Luis Miranda-Moreno, and Nicolas Saunier)

The purpose of this article is to compare existing computer vision methods to the performance of thermal video sensors under different lighting and temperature conditions. Thermal and regular video data was collected at the same time under different conditions across different places. The regular video sensor did slightly better than the thermal sensor during the day. The performance of the thermal sensor is much better for low visibility and shadow conditions, mainly for pedestrians and cyclists. Thermal speed measurements were constantly more accurate than for the regular video, regardless of light exposure. Thermal video is not affected by lighting and pavement temperature. Thermal sensors may help solve issues associated with visible light cameras for traffic data collection and offer other benefits, such as insensitivity to glare, privacy, storage space, and lower processing requirements (Fu et al., 2017).

A Comparison Analysis of Surrogate Safety Measures with Car-Following Perspectives for Advanced Driver Assistance System

(Sehyun Tak, Sunghoom Kim, Donghoun Lee, and Hwasoo Yeo)

This study performs an analysis using three different surrogate safety measures to determine the relationship between human driving behavior and collision risk. Wherein, collision risk is calculated by Time to Collision (TTC), Deceleration-based Surrogate Safety Measure, and Stopping Headway Distance (SHD) based on two different car-following theories, such as the action point model and asymmetric driving behavior model. To do so, the study team used the Next Generation Simulation (NGSIM) trajectory dataset, which was obtained from a segment of U.S. Highway 101 in Los Angeles, California, for 65 minutes. The segment length is 640 m with five lanes. Data comprises microscopic traffic information on individual vehicular movements' trajectories, including speed, position, space headway, vehicle type and acceleration/deceleration, and at 0.1 sec time intervals. The results show that the estimated collision risks of the TTC and SHD only partially match the pattern of human driving behavior. Additionally, the SHD and TTC overemphasize the collision risk in the deceleration process, predominantly when the focus vehicle is faster than its preceding vehicle. While the DSSM shows well-matched results to the pattern of human driving behavior (Tak et al., 2018).

Can post encroachment time substitute intersection characteristics in crash prediction models?

(Lakshmi Peesapati, Michael P. Hunter, and Michael O. Rodgers)

This research looks at the effectiveness of Post-Encroachment Time (PET) as an SSM for possible left-turn to opposing through vehicle conflicts. This article compares the use of PET both as the only forecaster of crashes and with a mixture of other characteristics of an intersection. PET data for this study was composed of videos that were recorded using high-definition cameras and from a higher viewpoint. Video data collected at the intersections were analyzed in a lab using a traditional frame-by-frame video reduction software program. The article concluded that models merging PET and traffic volume characteristic data have improved predictive power than the models containing only PET (Peesapati et al., 2018).

A Surrogate Video-Based Safety Methodology for Diagnosis and Evaluation of Low-Cost Pedestrian-Safety Countermeasures: The Case of Cochabamba, Bolivia

(Lynn Scholl, Mohamed Elagaty, Bismarck Ledezma-Navarro, Edgar Zamora, and Luis Miranda-Moreno)

In this article, researchers use an automated video analytics tool to investigate surrogate traffic safety measures and assess the usefulness of inexpensive countermeasures at selected pedestrian crossings at risky intersections. BriskLUMINA, a computer vision software, is used to process countless hours of video information and generate data on road users' speed and trajectories. It was found that motorcycles, turning movements, and roundabouts are the key issues related to pedestrian crash risk. The applied treatments were effective at four-legged intersections but not at traditional-design roundabouts. This study shows the applicability of the surrogate methodology based on automated video analytics in the Latin American context, where traditional methods are challenging to implement. The methodology could help to quickly understand short-term treatments before they are applied (Scholl et al., 2019).

Surrogate safety indicator for unsignalized pedestrian crossings

(Piotr Olszewski, Paweł Dąbkowski, Piotr Szagała, Witold Czajewski, and Ilona Buttler)

In this article, pedestrian and vehicle traffic was filmed at two unsignalized pedestrian crossings. The path of vehicles and pedestrians was found based on video processing. Many variables describing pedestrian-vehicle conflicts were calculated, such as speed, post-encroachment time, the distance between the participants, decelerations, etc. Identification of encounters was based on interactions of pedestrians and vehicles, drivers yielding to pedestrians, and vehicles passing near pedestrians. Criteria for determining unsafe encounters were considered with the assumption that it should be possible to automate the calculation process. The selected variables were pedestrian-

vehicle passing distance and the vehicle speed at that moment. Other criteria were used in cases of abrupt braking. A Dangerous Encounter Index was proposed as a surrogate safety indicator for pedestrian crossings. It relates the occurrence of dangerous events to exposure, defined as the number of pedestrian-vehicle encounters (Olszewski. et al., 2020).

Analysis of the transition condition of rear-end collisions using time-to-collision index and vehicle trajectory data

(Ye Lia, Dan Wua, Jaeyoung Leea, Min Yangb, and Yuntao Shia)

The purpose of this paper is to look at transition conditions like driver behaviors of either the lead driver or the following driver and to figure out how they contribute to the risk. It also investigates how the time to collision (TTC) changes during these times, as well as which factors change the TTC the most. Video data were collected from tall buildings and was extracted automatically by specialized software. 13 types of transition conditions were categorized based on the speed of the front vehicle, the speed of the following vehicle as well as speed difference. Two parameters were employed for selecting data. The first was that neither car should switch lanes, and the second was that a vehicle must be following for at least 10 seconds. The article provided an understanding of minimizing rear-end collision risks. In the past, TTC index was used for possible risk analysis. With one TTC value, it was only capable of determining safeness at one specific time point, but with the transition conditions analyzed in this study, more factors became available (Lia et al., 2020).

A Modified Post Encroachment Time Model of Urban Road Merging Area Based on Lane-Change Characteristics

(Weiwei Qi, Wei Wang, Bin Shen, and Jiabin Wu)

This article is about a Traffic Conflict Technology (TCT) method used to estimate the safety level of the merging areas on urban roads. It mainly focuses on lane-change characteristics. A modified Post Encroachment Time (PET) model is proposed to reveal the relationship between time, speed, and distance in the process of traffic conflict in order to figure out lane-change characteristics as well as accurately forecast traffic safety in the merging area. The traffic data of Guangyuan Road in Guangzhou were collected by cameras at peak hours (Qi et al., 2020)

2.3 Findings

According to the literature review conducted over the past years, the following findings were obtained:

Mobility:

- Probe vehicle data is one of the reliable data sources for evaluating the performance of highways and arterials.

- Many performance measures can be defined for developing performance evaluation.
- Travel time is one of the widely used performance measures suggested by many previous studies.

Safety:

- Surrogate measures have been extensively used for evaluating the safety of a road segment.
- Post-Encroachment Time (PET) could be a very useful method to identify the safety effect of an intersection design.

CHAPTER 3. METHODOLOGY

3.1 Mobility Analysis

3.1.1 Data

3.1.1.1 Probe Vehicle Data

Probe vehicle data requires both a spatial component and a temporal component. The spatial attributes are defined by Traffic Message Channels (TMCs), which are pre-defined locations along roadways (Table 2). As a telematics device traverses a TMC, the vehicle speed is captured along with a number of other attributes, including TMC code, vehicle speeds, date-time stamp, c-value, and confidence score (Table 2). In this study, four major routes consisting of state routes, interstate highway/turnpike, and major arterials were selected. Then, probe vehicle data for the selected roadways was obtained from the Regional Integrated Transportation Information System (RITIS) database (RITIS, 2020). The probe data analytic suite on the RITIS website provides various attribute selection choices and formats for downloading the raw probe data. For the purpose of this study, a total of 60 TMCs were selected surrounding the American Dream Complex. Figure 1 presents selected TMCs in the study area for four roadways. All the TMC segments have continuous coverage of RITIS data for 24-hours a day from September 1, 2019, to January 31, 2021.

Table 2 Example of obtained TMCs attributes for Interstate 95

TMC Code	Road	Direction	State	Start Latitude	Start Longitude	End Latitude	End Longitude	Length (miles)
120+04603	I-95	NORTHBOUND	NJ	40.75777	-74.1166	40.79844	-74.0774	3.488163
120-04603	I-95	SOUTHBOUND	NJ	40.80966	-74.0634	40.802	-74.0733	0.741292
120-04604	I-95	SOUTHBOUND	NJ	40.81378	-74.056	40.81363	-74.0563	0.021945
120-04605	I-95	SOUTHBOUND	NJ	40.82479	-74.0324	40.81465	-74.0534	1.325885

Table 3 Example of TMCs recorded speed data for Interstate 95

TMC Code	Date Time Stamp	Speed	Average Speed	Confidence Score	C Value
120+04603	9/1/2019 0:00	65.99	60	30	100
120-04603	9/1/2019 0:00	61.28	57	30	100
120-04604	9/1/2019 0:00	60.9	58	30	100
120-04604	9/1/2019 0:00	60.9	58	30	100
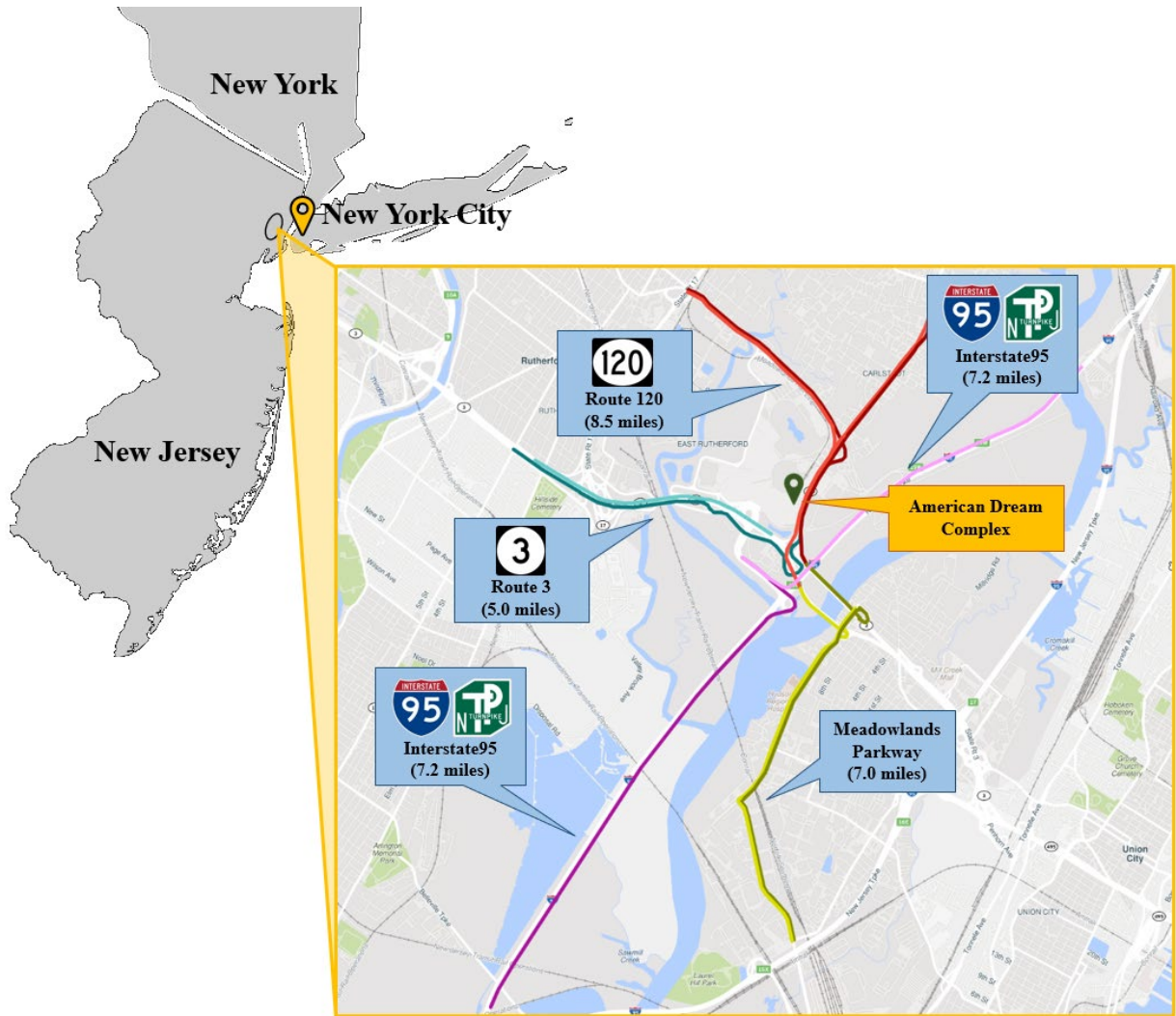
Figure 1 Study area around the American Dream Complex with 60 TMC segments

Based on previous studies (Brennan et al., 2015; Brennan et al., 2018), only speed data with a confidence score value of 30 and a c-value of 100 were considered. The values mentioned above for confidence score and c-value can be attributed to the condition where the recorded speed is in accordance with the probe measurements with high confidence. Considering high confidence indicates the real conditions of the roadway network.

3.1.1.2 Streetlight Data

To identify the possible changes in the trip attributes and travelers' attributes after the opening of the American Dream Complex, we accessed the Street light's insight database and compared the before and after opening data. Streetlight insight database uses cell phones and other driving devices to obtain the data point and transfers them to trips using proprietary algorithms (Streetlight Inc.). As a part of this study, trip data was extracted for 120 days before and after the opening of the complex to evaluate the difference in trip attributes due to the opening of the American Dream

Complex. To extract the data from the Streetlight Inc database, the predefined origin/pass-through gates were created near the major road segment that leads up to American Dream Complex. As shown in Figure 2, gates were created considering the road width, distance to exit or entry ramp, and the traffic flow direction. Trip and traveler data from June 27th, 2019 to February 22nd, 2020 was extracted from the database for each day and each road segment, as shown in Table 4.
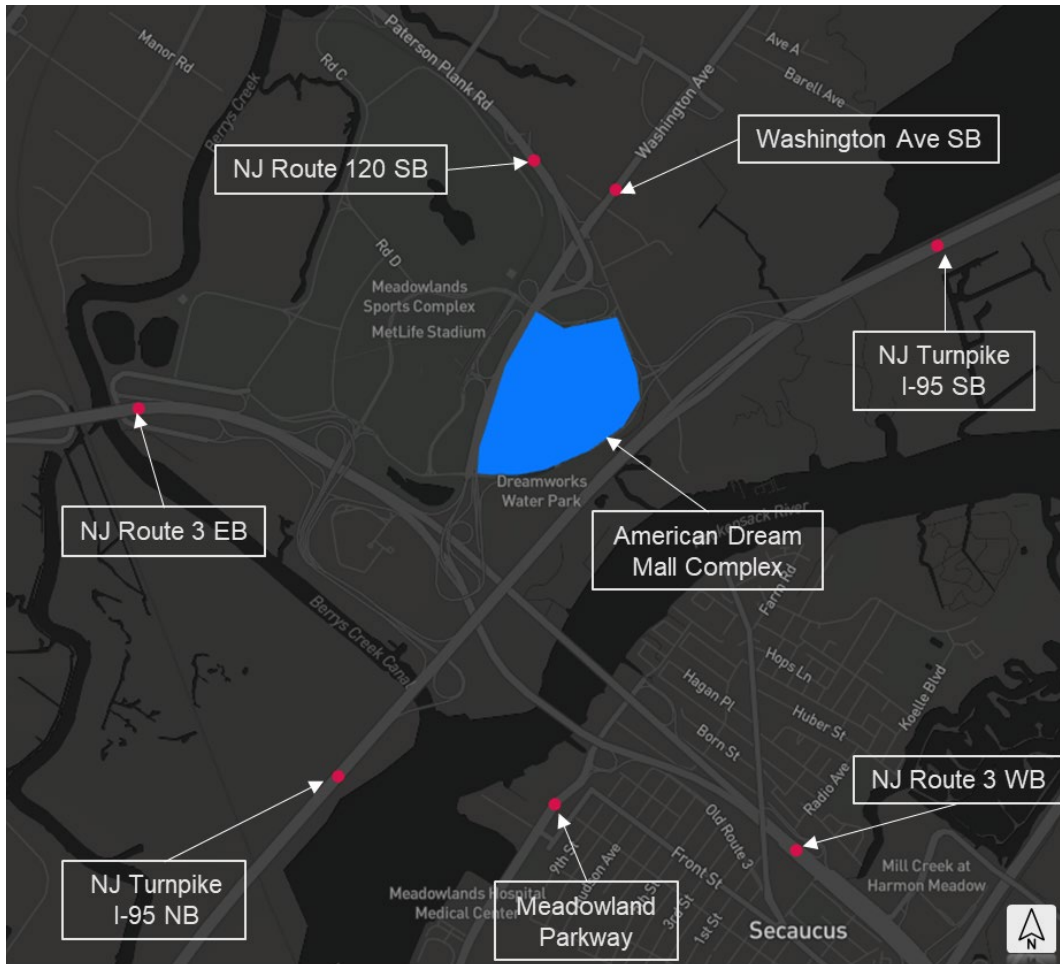
Figure 2 Representation of origin/pass through gates and the destination region

Table 4 Description of the predefined Origin/Pass-Through Gates

Origin/Pass-Through Gates	Distance to American Dream Complex (Miles)	Based Travel Time to American Dream Complex (Minutes)	Location Latitude	Location Longitude
NJ Route 3 EB	1.9	4	-74.089846	40.810985
NJ Route 3 WB	1.8	3	-74.056994	40.793400
NJ Turnpike I-95 NB	2.5	5	-74.080427	40796014
NJ Turnpike I-95 SB	1.3	2	-74.044698	40.817563
NJ Route 120 SB	1.2	4	-74.069022	40.820275
Washington Ave SB	1.3	3	-74.065079	40.818628
Meadowlands Parkway	1.9	4	-74.068910	40.795005

3.1.2 Traffic Performance Measures using Probe Data

The main focus of this section is to assess the performance of corridors located near the American Dream Complex. Generally, congestion for a TMC can be defined as "70% of the average segment speed during periods where congestion is unlikely" (Brennnan et al., 2015). According to previous studies, a congested TMC can be referred to as a TMC that experiences space mean speed below a pre-defined value (45 mph for major highways) during a period. This value agrees with the general definition of congestion (70% of 65 mph). However, by considering a constant threshold, the variety of different factors, including spatial location, roadway type, and geometry, is ignored. Hence, to overcome this issue, a variable speed threshold is considered. This threshold can be calculated as 70% of the base free-flow speed (BFFS). BFFS can be determined using the following equation (Brennan et al., 2018):

$$v_{ia} = 0.7 \frac{1}{n_j} \sum_{j \in F} v_{ij} \tag{1}$$

v_{ia}: Variable speed threshold for TMC i
n_j: Total number of 15-intervals within free-flow time F
v_{ij}: Recorded speed for each TMC i

As part of this study, instead of using a benchmark base free-flow time, this research calculated a variable speed threshold for each corridor by considering the whole study period. A base travel time (BTT), then, was calculated for each TMC. BTT can be a proportion of variable speed threshold and each TMC's length. BTT was calculated using the following equation (Brennan et al., 2018):

$$BTT_i = \frac{x_i}{v_{ia}} \tag{2}$$

BTT_i: Base travel time for each TMC i (hours)
x_i: Length of each TMC i (miles)

Travel time for each TMC can be determined as follows (Brennan et al., 2018):

$$TT_{ij} = \begin{cases} \frac{x_i}{v_{ij}}, & v_{ij} < v_{ia} \\ 0, & v_{ij} \geq v_{ia} \end{cases} \tag{3}$$

TT_{ij}: Travel time for each TMC i (hours) during the time period j

In this study, travel time inflation (TI) was selected as a performance measure. TI can be defined as the difference between the TT and the BTT. TI can be calculated as follows (Brennan et al., 2018):

$$TI_i = \sum_{j \in K}(TT_{ij} - BTT_i); \quad for\ TT_{ij} > 0 \tag{4}$$

TI_i: *The total travel time inflation for each TMC i (hours) for all the 15-min time period j during the analysis period K*

Equation 4 calculates TI for each TMC i. For determining TI for the whole corridor, the following equation can be applied (Brennan et al., 2018):

$$CTI = \sum_{i \in C}TI_i \tag{5}$$

CTI: *The total travel time inflation for all TMCs (hours) for a corridor during the analysis period K*

In order to have a better view of congestion day by day during the entire study period, a normalized form of the TI named the Corridor Increase in Mean Travel Time (CIMTT) is considered. To do so, the TI is divided by the travel time calculated for each TMC. Given this information, CIMTT can be determined using the following equation (Brennan et al., 2018)**:**

$$CIMTT_{ij} = \sum_{n}\frac{TI_i}{BTT_i} \tag{6}$$

$CIMTT_{ij}$: *The corridor increase in mean travel time for all TMCs (min) for a corridor*

3.2 Safety Analysis

3.2.1 Video Data

In terms of testing the developed safety analysis tool, video data was collected at two intersections near the American Dream Complex. First, Hampton Inn at Paterson Plank Rd. is a 4 leg signalized intersection located on NJ Route 120/Paterson Plank Rd with no left turn. Paterson Plank Rd. is a two-way road with two moving lanes in the North and South directions. There is a dedicated divergent that provides a left-turning facility for moving vehicles. The second intersection, Murray Hill Pkwy and Paterson Plank Rd., is also a 4 leg signalized intersection with no left turn. At the intersection of Paterson Plank Rd. has 3 moving lanes in the north and south directions and a dedicated right-turning divergent. At the same time, Murray Hill Pkwy has one moving lane, one right-turning lane, and one left-turning lane for East and West directions.

Murray Hill Pkwy & Paterson Plank Road

American Dream Complex

NORTH

Hampton Inn at Paterson Plank Road
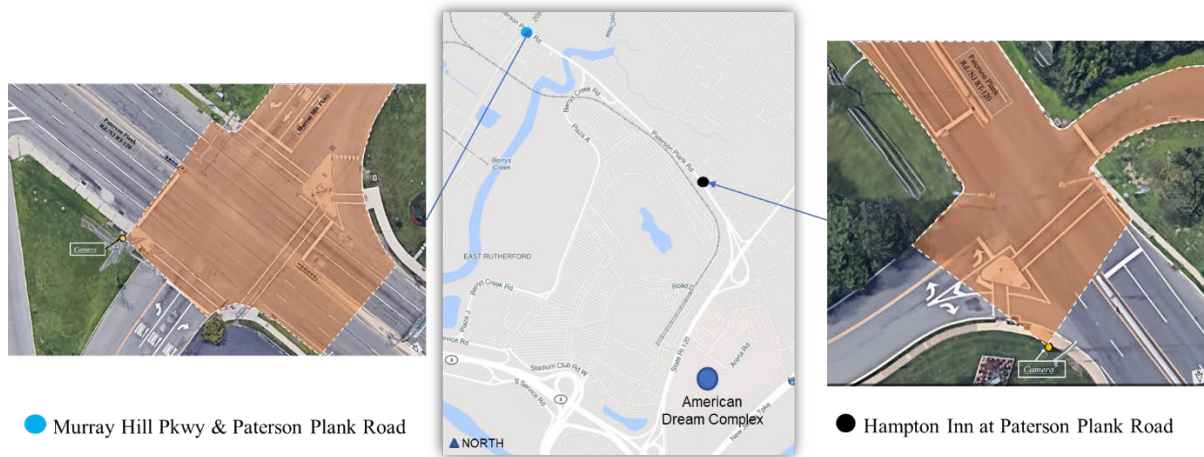
Figure 3 Study Intersection

Figure 3 shows the camera position and its vision coverage. The camera was set up on the pole near the intersection, as shown in Figure 3. A high-resolution (2704 X 1520) video for 180 minutes was recorded by a Go Pro Hero 9 at 30 FPS. The video was recorded between 2:40 PM to 5:40 PM

3.2.2 Detection & Tracking

Real-time object detection and tracking algorithms have been widely used to achieve traffic management objectives and evaluate traffic safety. This algorithms' main goal is to locate the positions (i.e., X, Y coordinates) and the moving object's size in a video or an image. Detecting an object is an initial step in all detection and tracking methodology. As part of this study, the Yolo-V5 (You Only Look Once) Algorithm was used to detect road users in the video (Jocher et al., 2021).

YOLO algorithm is a deep learning network for real-time detection that performs its main two tasks in a series pattern. The algorithm first identifies the location of the object pixels, and then based on the pre-trained weights, it classifies the object. YOLO considers the image pixel values as the inputs and predicts the bounding boxes and class probability of the object as an output result. The algorithm uses only a single neural network to perform the tasks at a high processing speed. YOLO-V5 is built on a PyTorch framework instead of the original Darknet framework used in the previous version (Redmon et al., 2016; Redmon et al., 2018; Jocher et al., 2021).
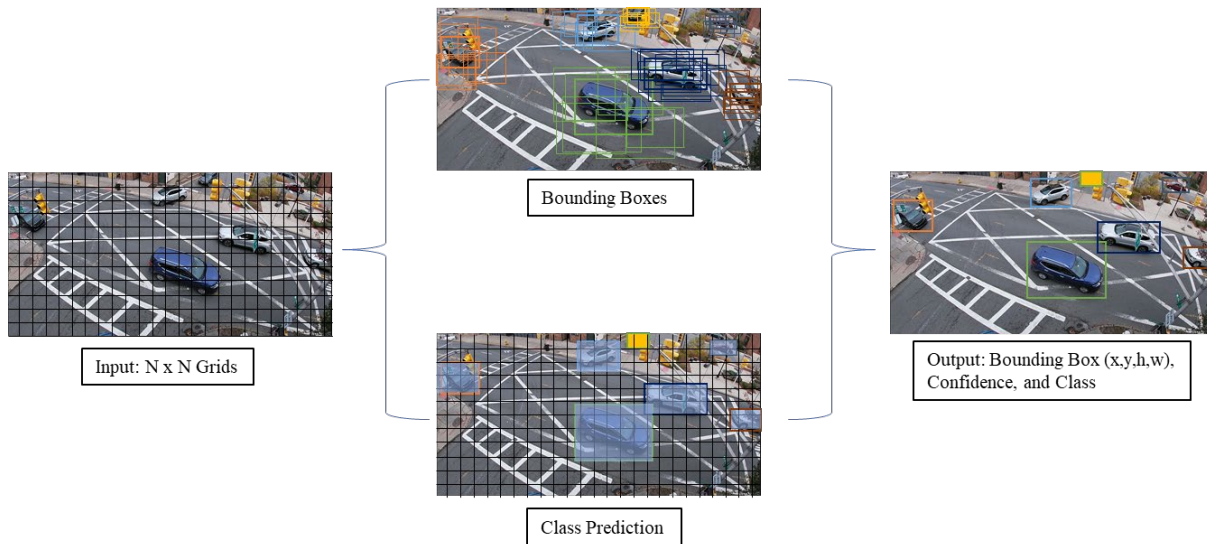
Figure 4 YOLO Algorithm process flow chart

Figure 4 shows the process principle of the YOLO algorithm. First, Algorithm takes a frame/image as an input and divides it into NxN grids. Each cell in the grid is processed to predict the bounding box for all the objects in a frame. Simultaneously, it also looks for the class probabilities for the identified bounding boxes. Lastly, each bounding box provides X & Y coordinates, height & width, confidence score, and the class value. As a part of this study, we have considered the detection confidence score threshold to be 80 percent.

In terms of processing speed, YOLO-V5 archives the inference time as fast as 0.007 seconds per image for 140 Frame Per Second (FPS) video while upholding detection accuracy like previous versions. YOLO-V5 has a weight file of 27 MB, which is 90 percent smaller in size compared to previous versions. Optimized YOLO-V5 is based on PyTorch and can easily be compiled to ONNX and CoreML to make mobile deployment easy. Overall, using YOLO-V5, detection can be carried out in a wider area with fewer space constraints (Wang et al., 2020).

Object tracking has been recognized as the most critical task in all computer vision projects. There has been extensive research work being conducted for visual object tracking; however, there has been a lot of difficulty in handling changes in tracking the detected object. For instance, the occurrence of occlusion, changes in bounding box dimension, variation in illuminations, camera motion, etc., cause a lot of errors in tracking. As part of this study, DeepSORT, a Simple Online and Real-time Tracking (SORT) algorithm, is used for tracking multiple objects frame by frame. DeepSORT uses the Hungarian and Kalman filter algorithm to track a detected object (Bewley et al., 2016). The baseline process flow of the DeepSORT algorithm is as follows (Hou et al., 2019):

- Track Estimation: A DeepSORT algorithm uses the Kalman Filter method to predict the position of the object bounding box in the current frame. Additionally, DeepSORT uses a standard version of the Kalman Filter that considers the constant velocity and linear

regression. Spatial information is only used by the track estimation, i.e., the X and Y coordinates of the bounding box.

- Appearance Descriptor: To attain the detection and tracks appearance details, an appearance descriptor is used. It is a pre-trained Convolutional Neural Network of a massive scale of re-identification dataset. Wherein, the network is able to identify the features identifies that are similar to previously detected objects and/or far away from each other.
- Data Association: Further, based on the results from the track estimation and appearance descriptors, it is possible to see the correlation between the old and newly detected objects' current frames. Remarkably, DeepSORT algorithm uses a detection confidence threshold to filter out all detection. Additionally, the Algorithm uses the cost matrix to represent spatial and appearance similarities between each existing and new detection track. As a focus of this study, IOU_machting, NN_matching, class, and average detection confidence threshold functions were used to improve the accuracy of the tracking algorithm.
- Track Handling: Object's tracked from the data association are taken care of during the track handling. For instance, if the newly tracked object is not associated with the old tracks, then the track will be tentatively held until it does not satisfy all the conditions for getting a new track id. Once it satisfies all the requirements, then a new track id is updated. Otherwise, the tentative track will be removed.

3.2.3 Traffic Count

As the scope of this study, a system to predict the traffic flow that counts and classifies the vehicle base on the direction flow was developed. As discussed previously, detection and tracking of the vehicle were extracted using YOLO-V5 and DeepSORT algorithm. Furthermore, to obtain the flow direction of the vehicles, a predefined zone is created. Wherein each unique pixel value from the zone was extracted and matched with the complete trajectories extracted from the algorithm. Figure 5. represents the zones that are created using the OpenCV library and polygon plotting method. The flow direction of the tracked objects was determined based on the start and endpoints of each track id.

(Location: Hampton Inn at Paterson Plank Road)
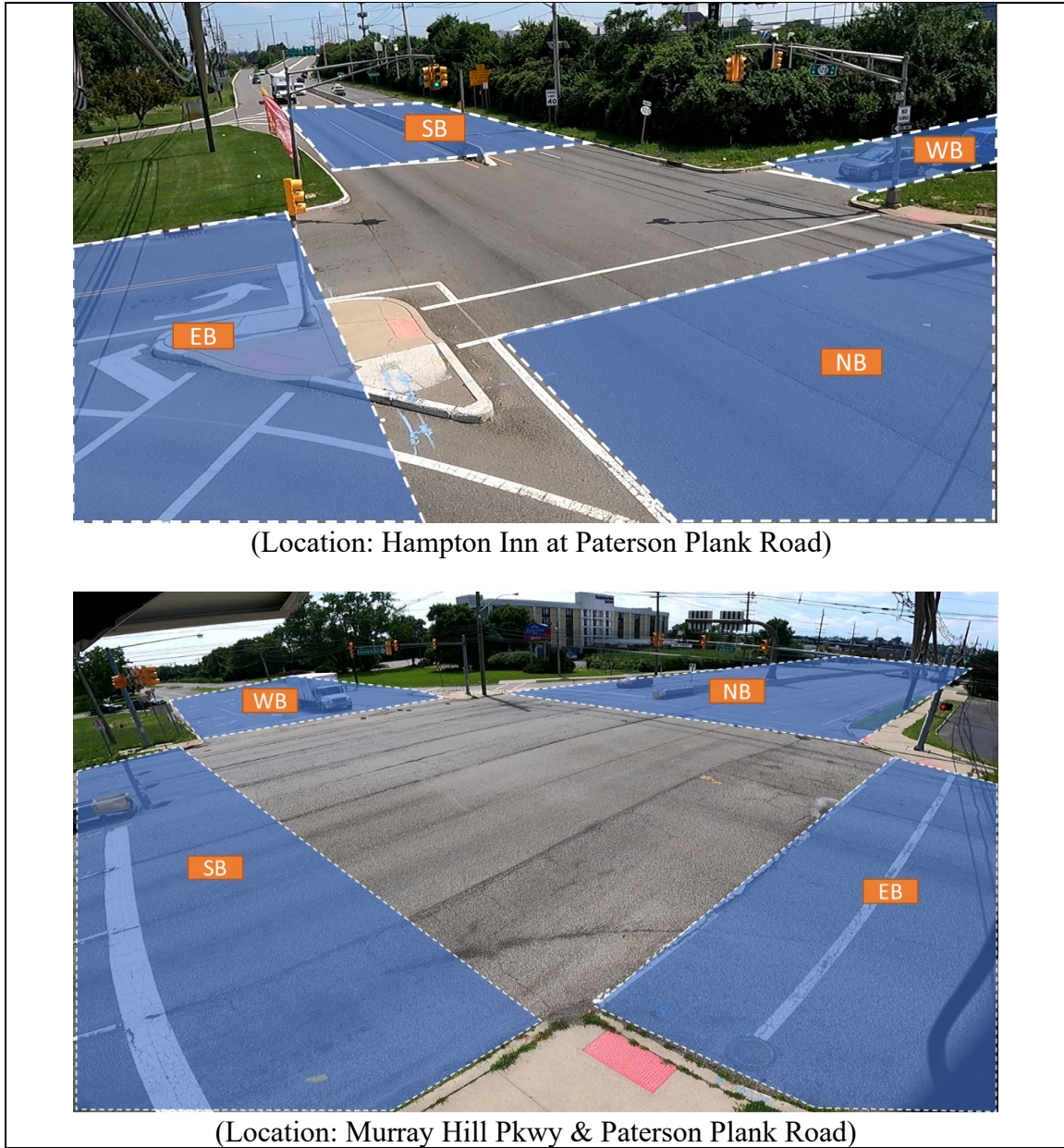
(Location: Murray Hill Pkwy & Paterson Plank Road)
Figure 5 Predefined zones at the study intersection

3.2.4 Traffic Violation

As a part of safety analysis, traffic violations such as a vehicle running red lights and pedestrian jaywalking events are crucial concerns at an intersection. A system was developed to achieve the study objectives wherein one of the traffic lights was detected, and the condition was implemented for the violation bars based on the traffic signal phases. During the signal's red phase, vehicles passing the Northbound violation bar or the Southbound violation bar are considered vehicles running red light events. While during the signal's green phase, vehicles passing the Eastbound

violation bar and the Westbound violation bar are considered as vehicles running red light events. Figure 6 shows the violation bars' position and the detected traffic light for the two study locations.

(Location: Hampton Inn at Pateson Plank Road)

(Location: Murray Hill Pkwy & Paterson Plank Road)
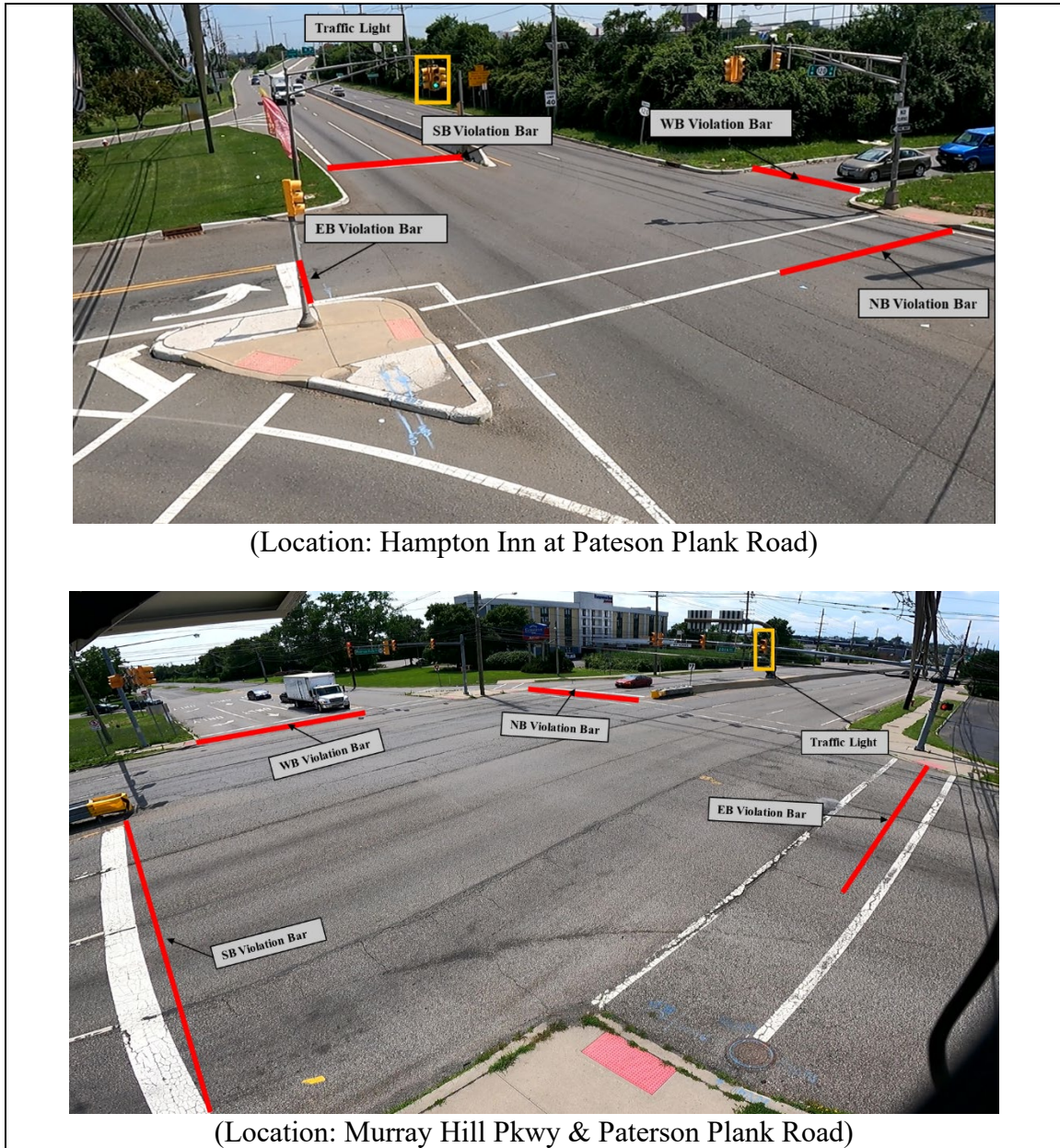
Figure 6 Positions of violation bars and the detected traffic light

For evaluating pedestrian jaywalking events, a system using the OpenCV library and polygon plotting function was developed. A predefined region was created on the frame that covered all the crosswalks and the sidewalk area. Then a condition algorithm was implemented to the extracted trajectory data of the pedestrians. Coordinate values, i.e., the position of pedestrians obtained from the YOLO-V5 and DeepSORT were checked if they were inside or outside the predefined region. For instance, if any of the coordinate values were observed outside the region, it was considered a

jaywalking event. Figure 7 shows the predefined polygon region created on the frame for the two intersections.

(Location: Hampton Inn at Paterson Plank Road)

(Location: Murray Hill Pkwy & Paterson Plank Road)

Figure 7 Polygon region created for identifying the Jaywalking event

3.2.5 Surrogate Safety Measures

Surrogate Safety Measure (SSM) is one of the widely used approaches for identifying future threats and evaluating safety. Each SSM is calculated based on the occurrence of conflict events between two road users. Conflict is defined as an observable point, line, or area where two or more road users intersect each other in time and space with a possibility of colliding with each other if the speed and direction of both road users remain unchanged (Amundsen and Hyden, 1977). SSMs

are considered as the best safety evaluation methods that help identify the near-miss conflict events at the study location and compare the results with the historical crash data for recommending countermeasures. There are several SSMs that are used for evaluation, including Time to Collision, Post-Encroachment Time, Maximum Speed, Speed difference, and deceleration rate.

As a purpose of this study, Post-Encroachment Time (PET) was formulated for accessing the vehicle-to-vehicle conflict events and their severity at the test location. PET is defined as the time difference between a departing vehicle and the arriving vehicle following or intersecting in the conflict area. In terms of processing the trajectory data, PET is calculated as a function of the paired vehicles. A time-space diagram to calculate the PET for vehicle-to-vehicle conflict is represented in Figure 8.
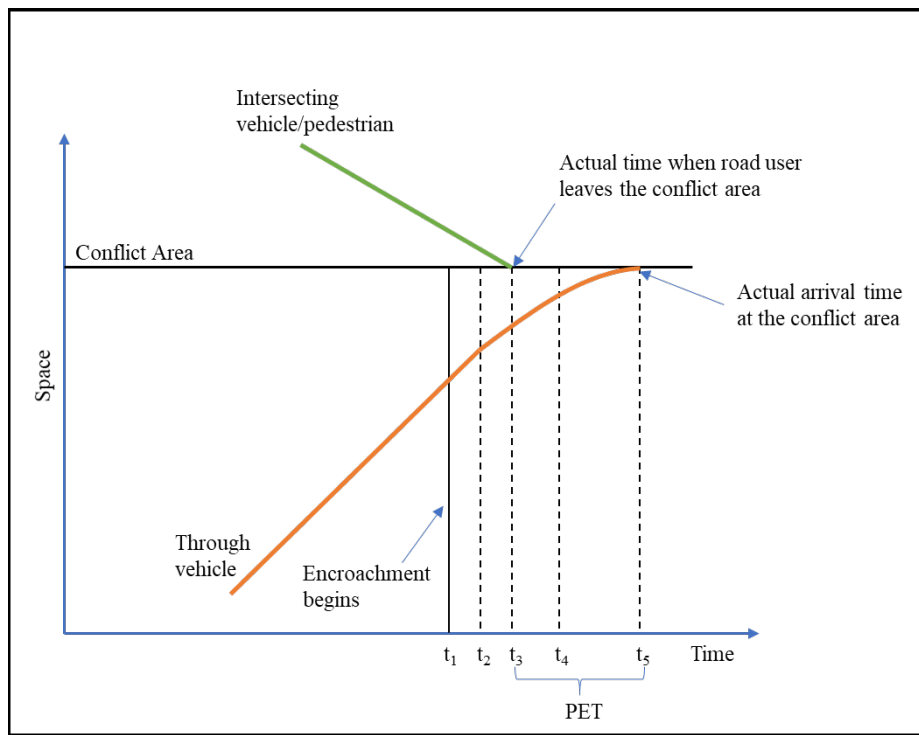
Figure 8 Time-space diagram to identify the Post-Encroachment Time (PET)

PET for paired vehicles at conflict area is obtained as:

$$PET = t_5 - t_3 \qquad (7)$$

Note for calculating the PET from the obtained trajectory and bounding box centroid data, the front and the back (i.e., the front and the rear of the vehicle) points of the bounding box were calculated and considered for paired vehicles. Similar to the previous studies, PETs with less than 5 seconds counted as a conflict, and PETs with less than 1.5 seconds were considered as dangerous conflict

(Fu. et al., 2016; Zangenehpour et al., 2015). Additionally, the study also considered the 20 seconds as the arbitrary threshold for identifying all potential risks for vehicle-to-vehicle collisions at the intersection.

CHAPTER 4. RESULTS AND DISCUSSION

4.1 Mobility Analysis

Developing a performance evaluation of a roadway system during the occurrence of a specific event can provide useful information about the effect of the event on the congestion condition of the roadway. In this study, travel time inflation (TI) was selected as a performance measure in the analysis. By considering variable threshold speed for each TMC, TI was calculated for the entire four corridors each month during both non-peak and peak hours. The hours for Am peak are 06:00 to 09:00 am and for pm peak 16:00 to 19:00. CTI was determined for a month before the October 25, 2019 opening and three months after the opening. Calculated monthly CTIs for four selected roadways are presented in Figures 9, 10, 11, and 12.
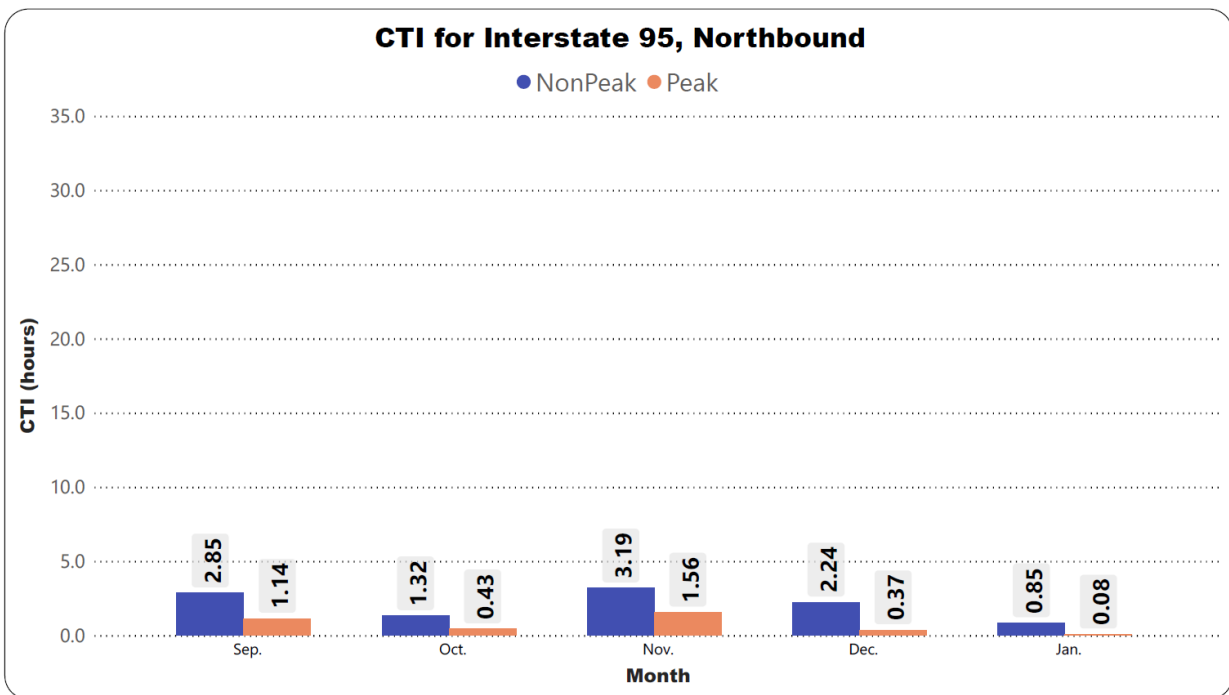
a) Northbound
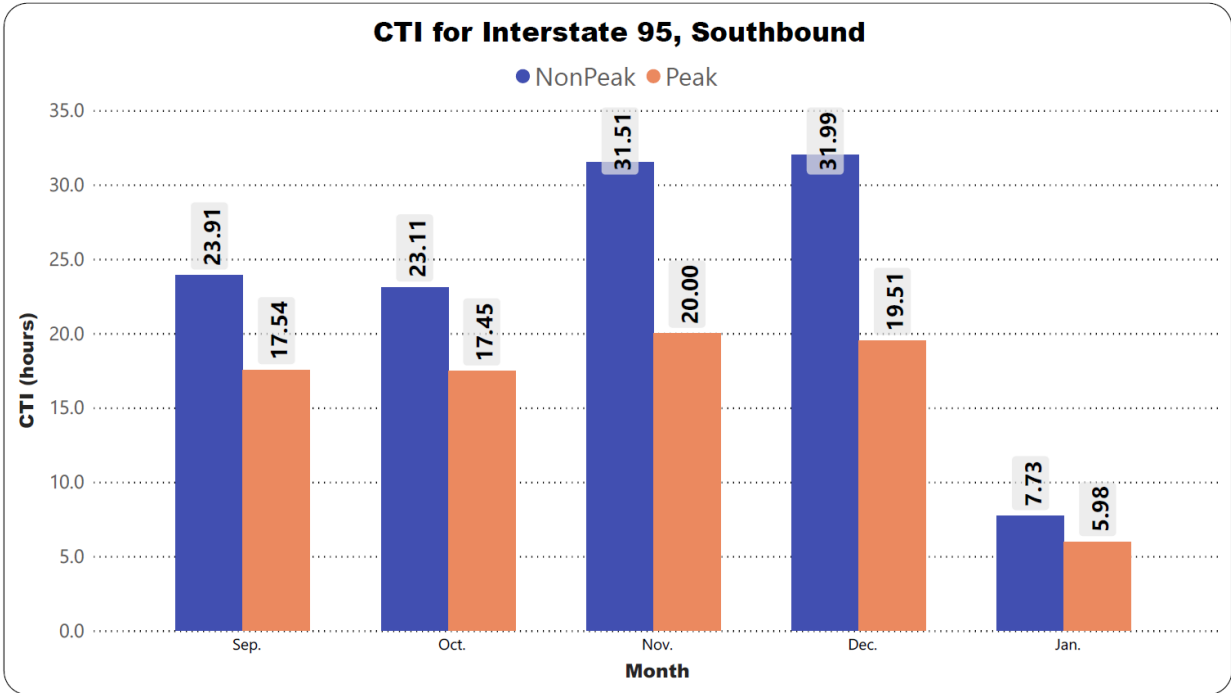
b) Southbound
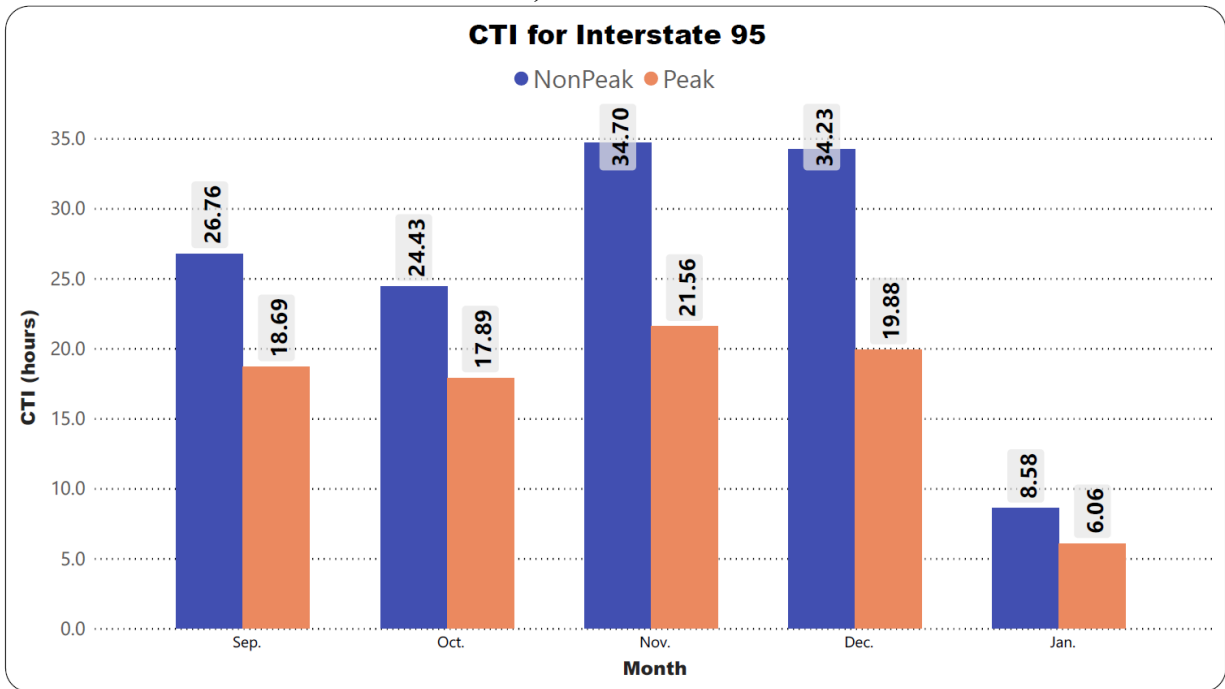
c) Both North & Southbound
Figure 9 Monthly CTI for Interstate 95

As shown in Figure 10, CTI for both Northbound and Southbound of Interstate 95 experienced an increase after the opening of the American Dream Complex for both non-peak and peak hours.

From December to January, a sharp decrease was observed in CTI for both Northbound and Southbound as well as the entire corridor. This can be explained by the new year's holidays.

After the opening of the American Dream Complex, CTI for Northbound of Meadowlands Pkwy decreased slightly during non-peak hours (from 4.22 to 4.02 hours), as illustrated in Figure 10. However, this value increased slightly during peak hours for Southbound after the official opening. Considering the entire corridor, CTI remained almost the same during non-peak hours and increased slightly from 3.36 to 3.54 hours after the official opening. A decreasing pattern was also observed in CTI of the entire corridor from December to January.
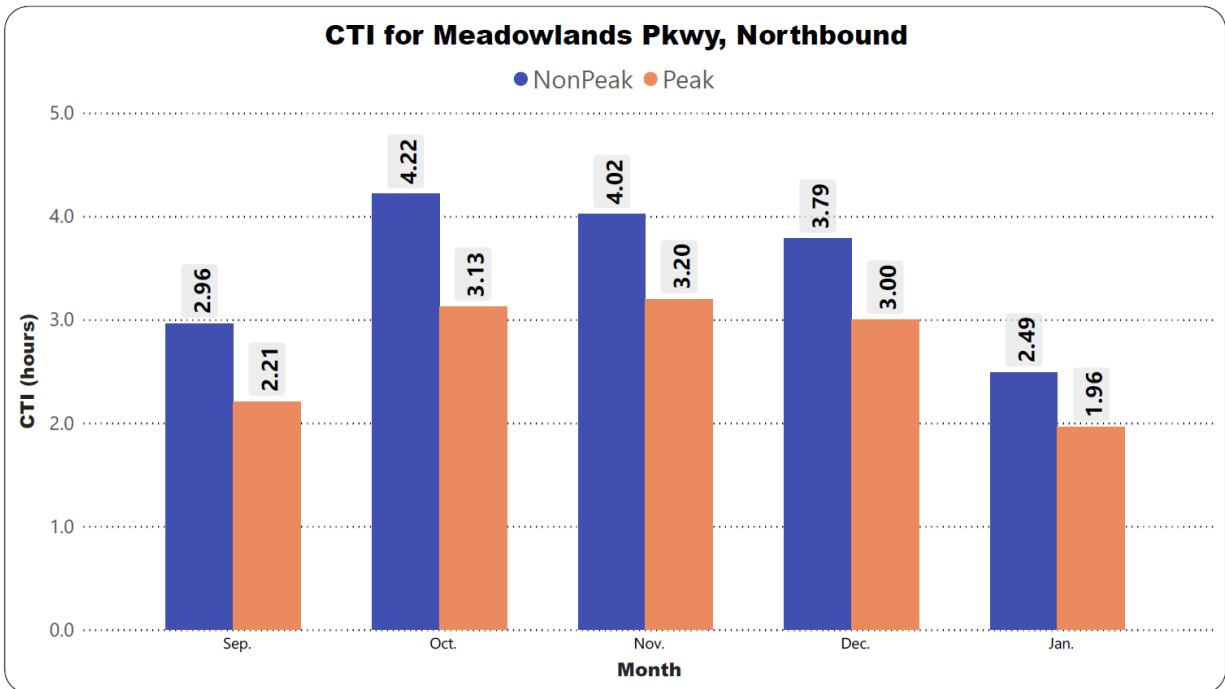
a) Northbound
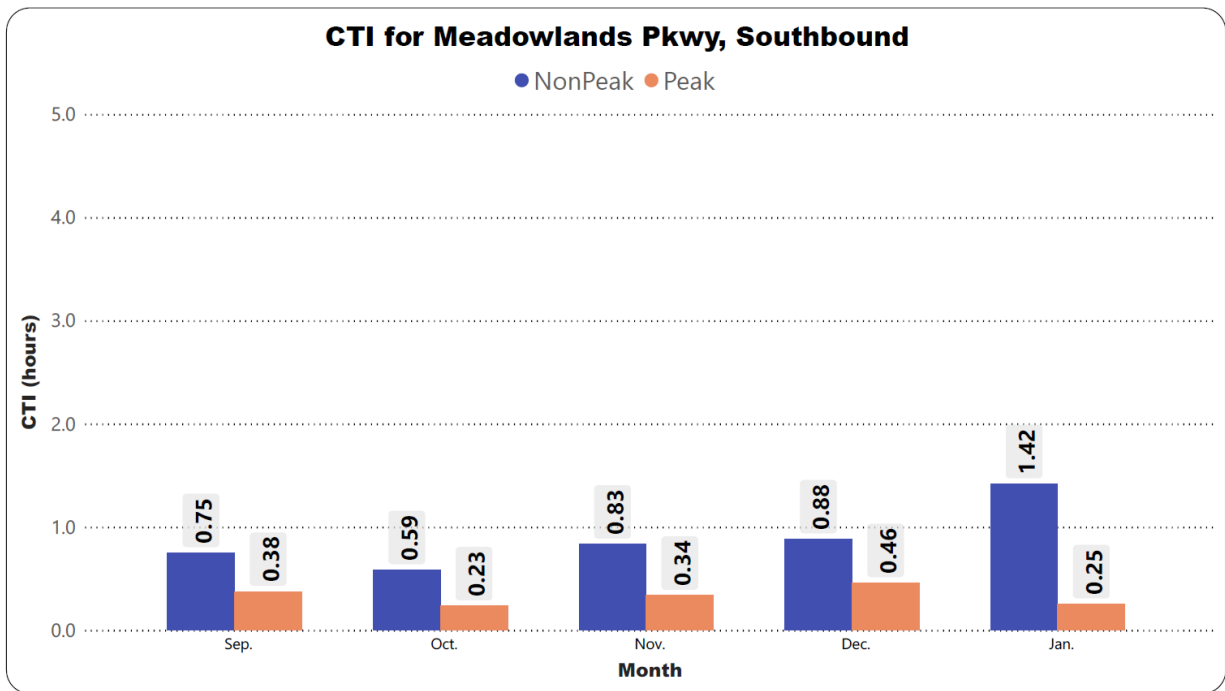
b) Southbound
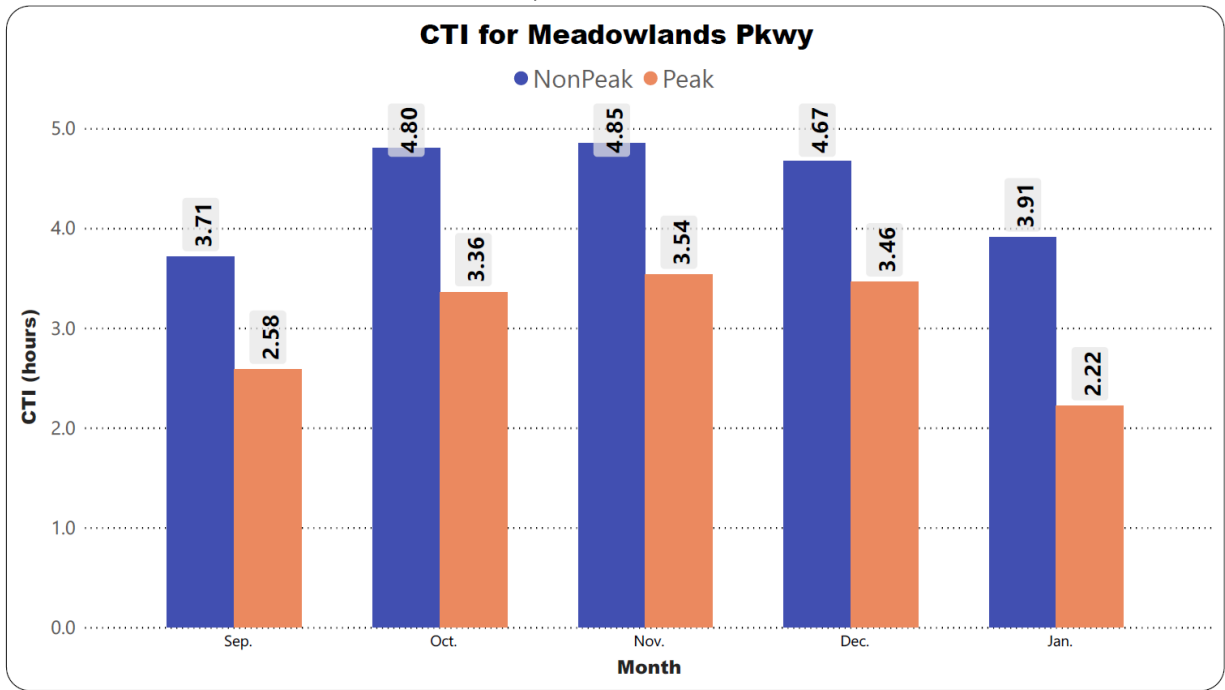
c) Both North & Southbound

Figure 10 Monthly CTI for Meadowlands Pkwy

From October to November, CTI followed an increasing pattern for both Eastbound and Westbound of NJ Route 3 as well as the entire corridor (both non-peak and peak hours). A decreasing pattern was also observed for NJ Route 3, with the beginning of holidays during non-peak and peak hours (shown in Figure 11).
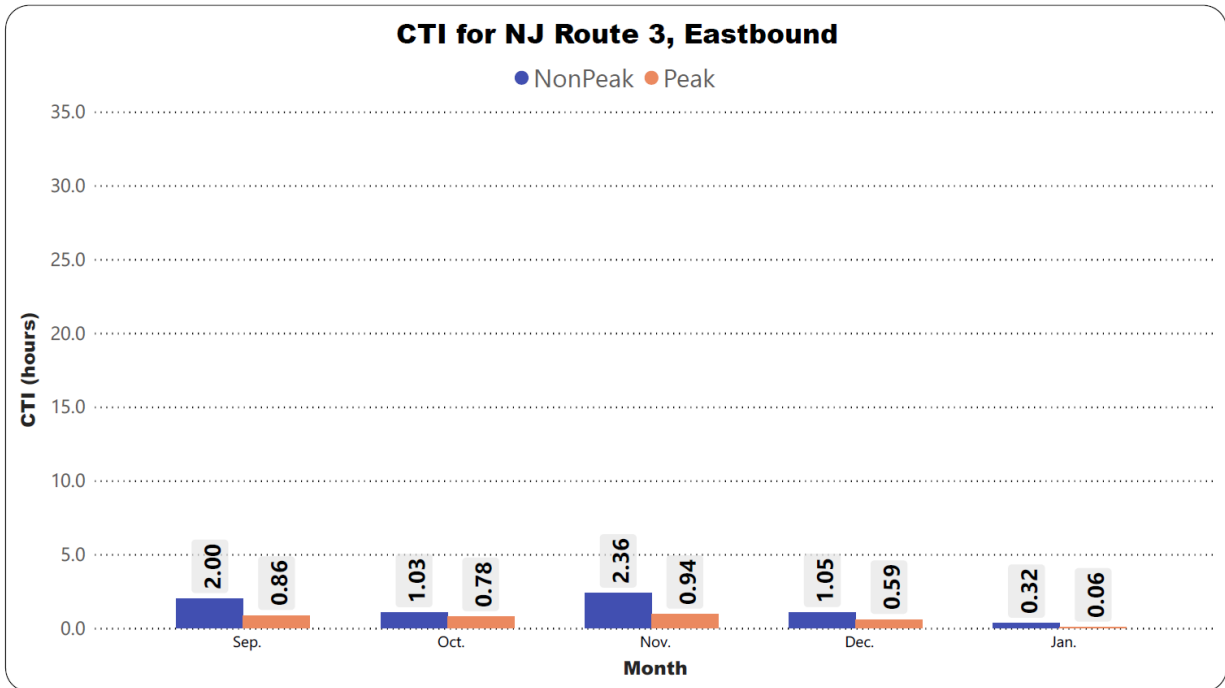
a) Eastbound

b) Westbound

45
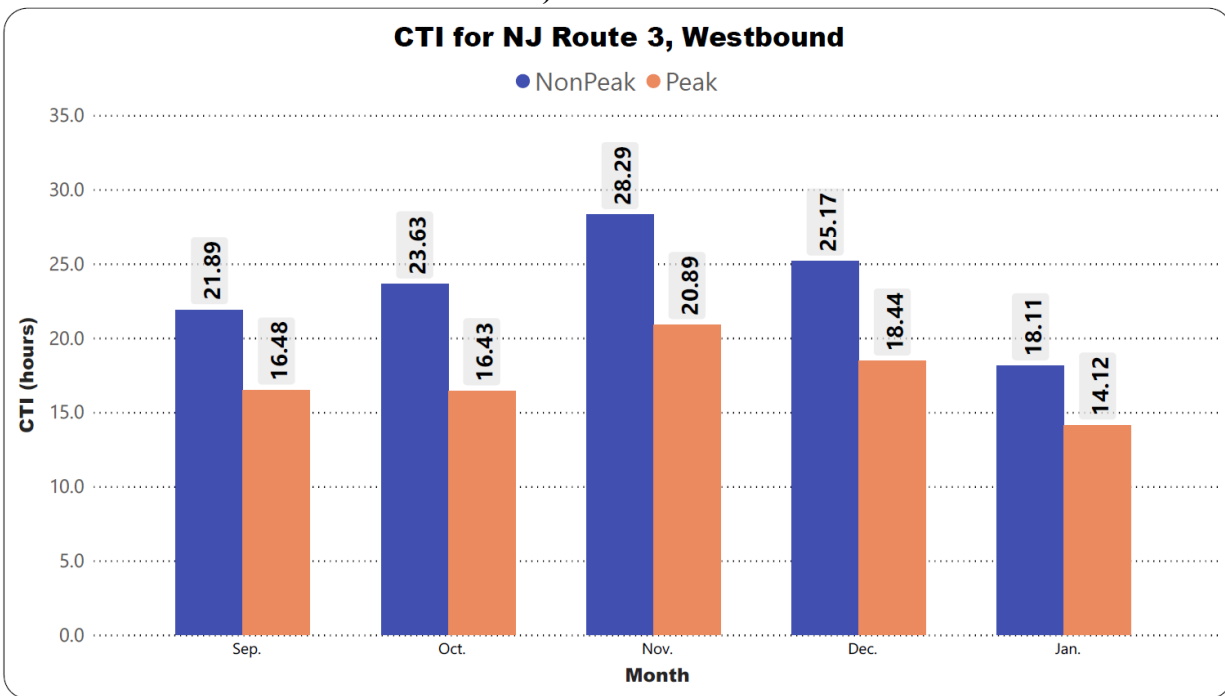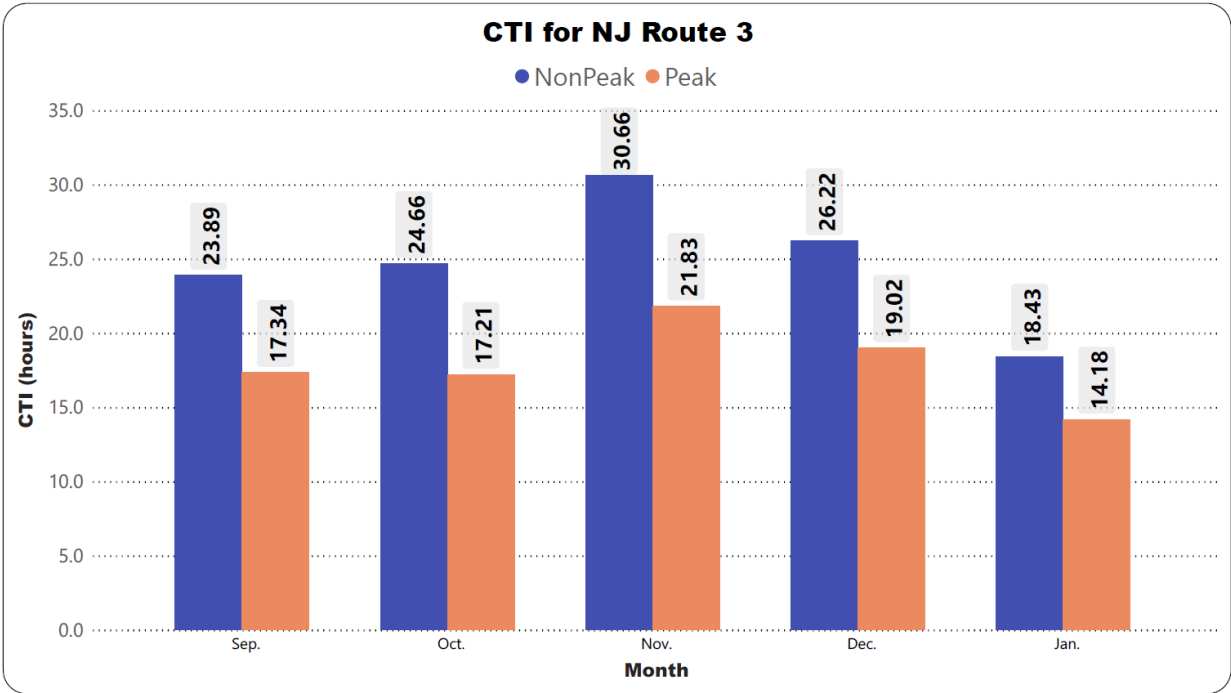
c) Both East & Westbound
Figure 11 Monthly CTI for NJ Route 3

In Figure 12, the same increasing pattern was observed for NJ Route 120 after the official opening of the American Dream Complex. The same decreasing pattern was also observed in CTI due to the holidays.
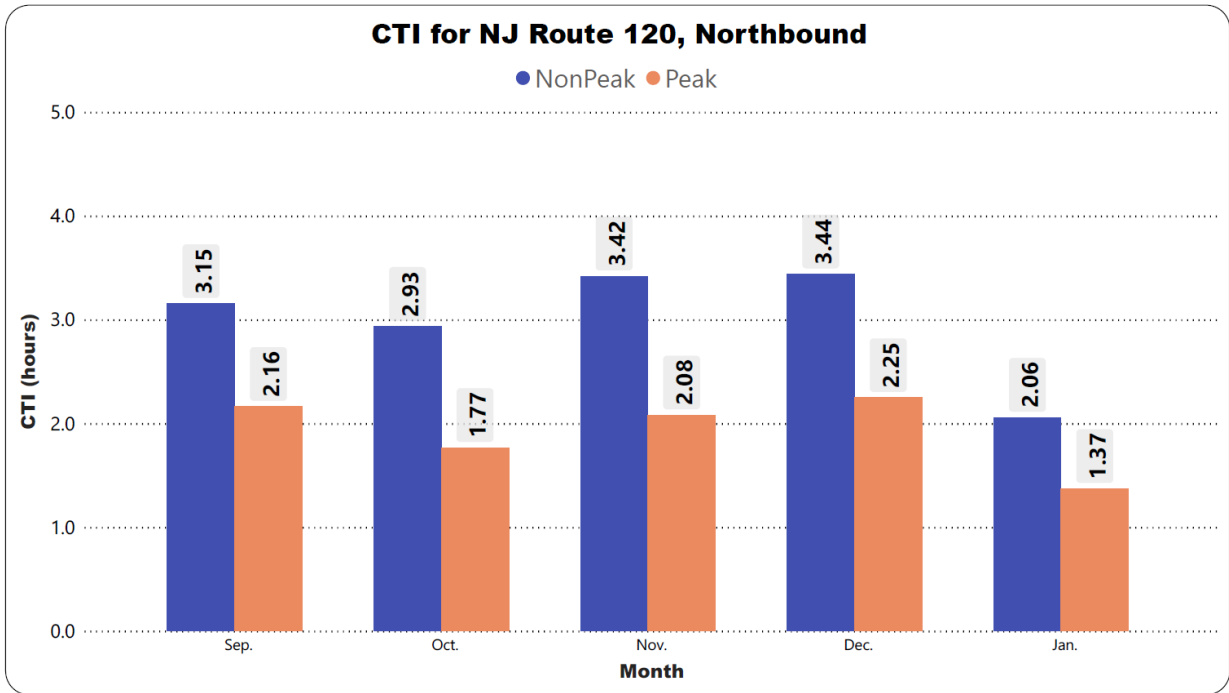
a) Northbound
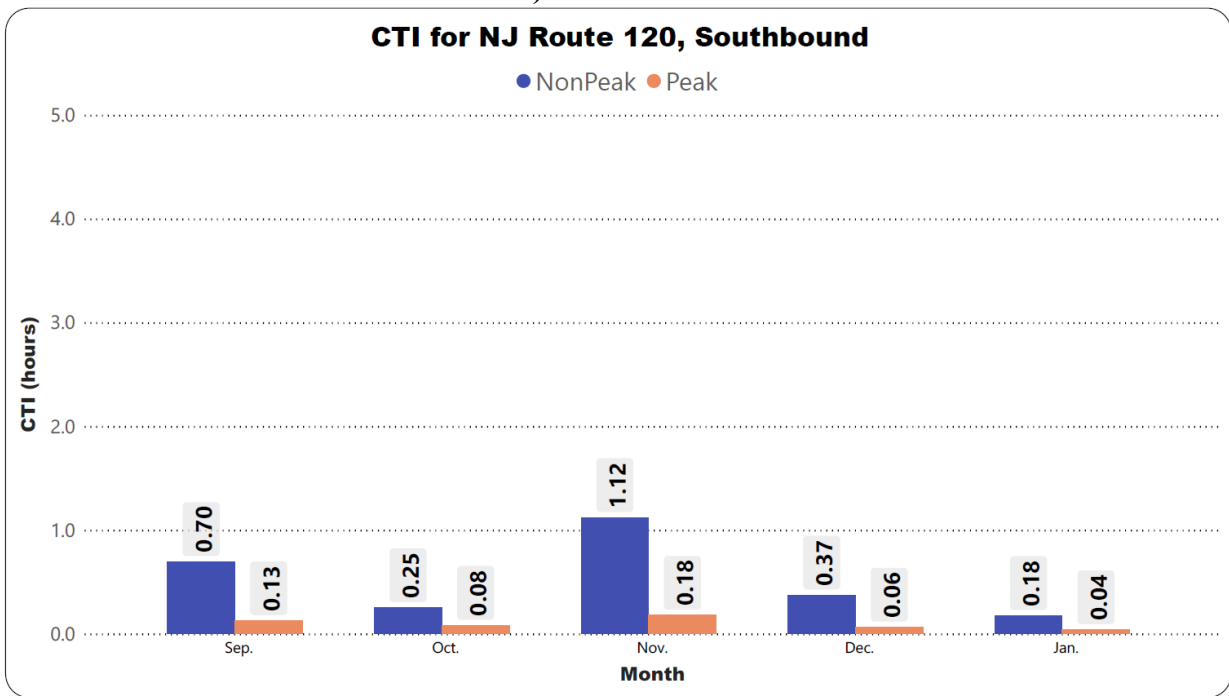
b) Southbound
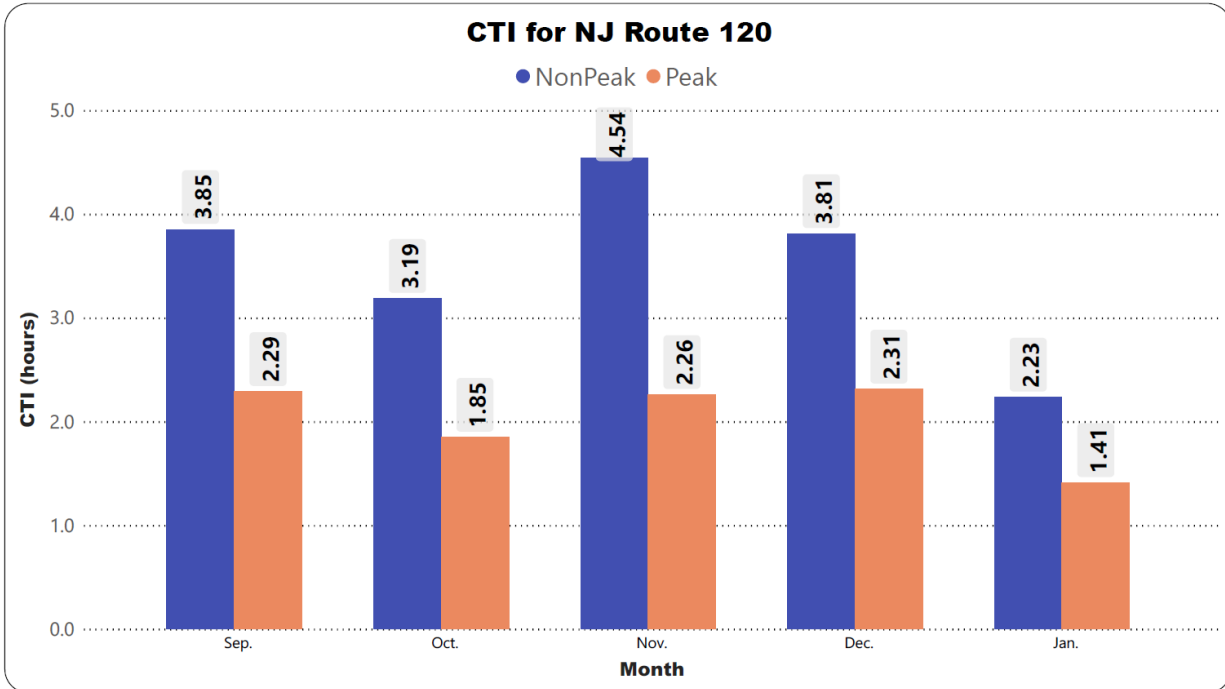
c) Both North & Southbound
Figure 12 Monthly CTI for NJ Route 120

The individual TI was also calculated for all 60 TMCs of four corridors during the entire study period (Sep. 2019 to Jan. 2020) and indicated in Figures 13 and 14 for non-peak and peak hours, respectively. These figures, as an illustration of TI distribution, can provide useful information on the exact location of congestions in the study areas. Based on this figure, some TMCs along the NJ Route 3 and Interstate 95 experienced high values of TI during both non-peak and peak hours. On the other hand, most of the TMCs along the Meadowlands Pkwy and NJ Route 120 experienced low values of TI.
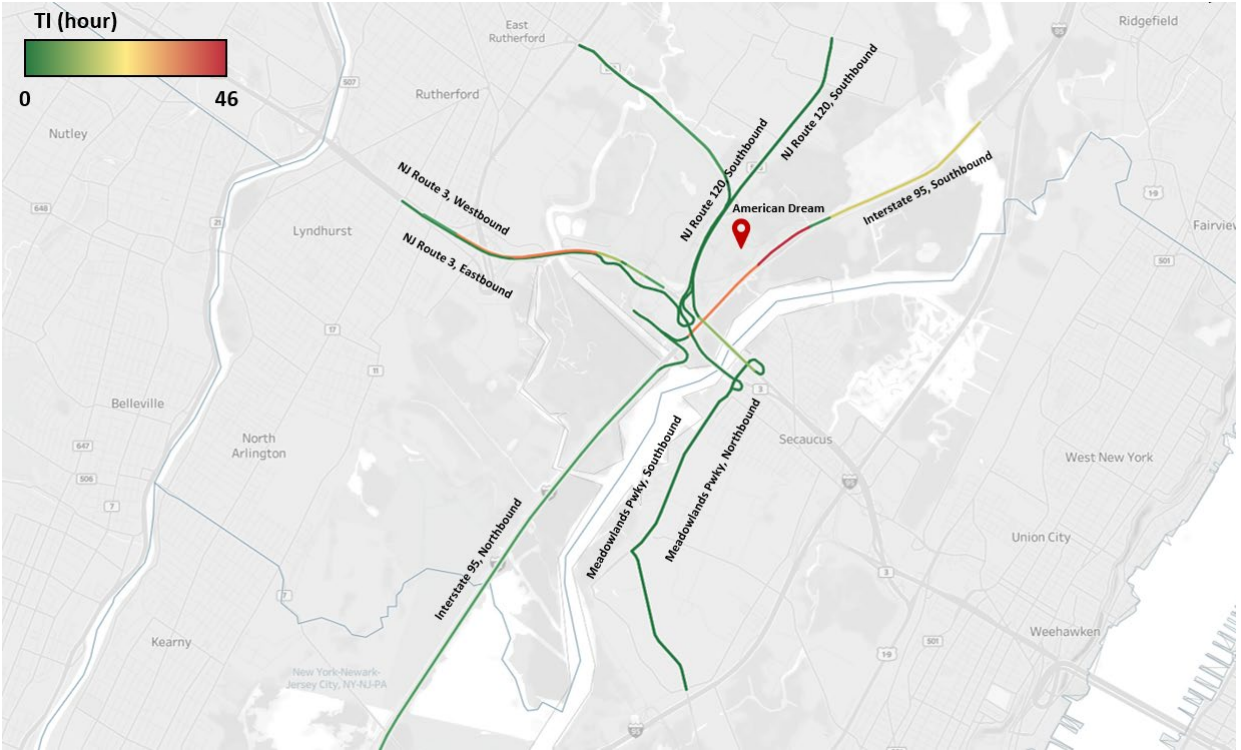
a) Non-peak Hours
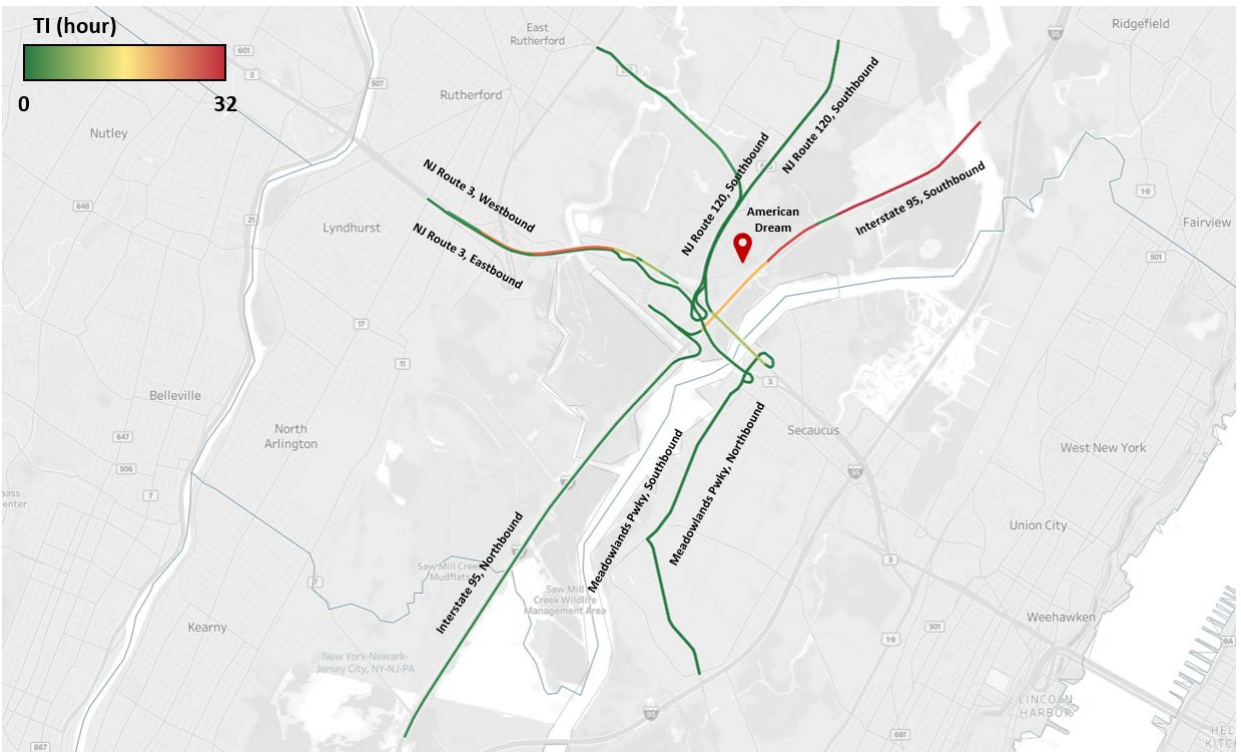
b) Peak Hours
Figure 13 TI for all 60 TMCs during the entire study period

In order to have a better visualization of congestion and compare it day by day during the entire study period for the selected sites, travel time was normalized and divided by the calculated base travel time of each TMC. This performance measure for each corridor is visualized using the heatmaps shown in Figures 14, 15, 16, and, 17. It is noted that no reliable speed data were obtained from 10 pm to 6 am, as represented by the blank spaces. In these heatmaps, y-axis represents the hour of the day (15-min bin), and x-axis represents the day of the week. Generally, it is expected to observe an increase in congestion due to the opening of any new development. Based on the ITE Trip Generation Manual, an equivalent land use (LU-820 'Shopping Center') would generate about 46.12 and 21.10 trips on Saturday and Sunday, respectively, for every 1,000 Square feet of retail space. For this case, the increase will be phased, which offers a unique perspective on the gradual opening of a major development that impacts the surrounding area.

As illustrated in Figure 14, for both Northbound and Southbound Interstate 95, major congestions occurred during pm peak hours. No considerable congestion was observed during the am peak hours for the entire study period. Furthermore, based on the CIMTT graphs, the partial opening of the complex did not have an immediate, major, impact on the congestion of this corridor despite the granular increase found in the T.I. calculations. However, congestion during the pm peak hours decreased due to the new year's holidays (December 24 to January 1) for both bounds of Interstate 95.

Based on Figure 15, there is not a considerable congestion pattern for the northbound of Meadowlands Pkwy during am peak hours; however, a steady pattern of congestion was observed for the pm peak hours of this bound. For the Southbound, interestingly, no considerable congestion was observed for both am and pm peak hours. The partial opening of the complex did not have a considerable effect on the congestion pattern for both am and pm peak hours. On the other hand, the new year's holidays decreased the congestion. The congestion pattern after the holidays is the same as before the holidays for both bounds of this corridor.

According to Figure 16, NJ Route 3, Eastbound, experienced only some minor congestions on some specific days. A steady pattern of very high congestion was recorded during the pm peak hours for NJ Route 3, Westbound. Similar to the other corridors, the partial opening did not affect the congestion pattern at NJ Route 3. The new year's holidays considerably decreased the congestion at this route, as they did at other corridors.

And finally, as shown in Figure 17, a steady pattern of congestion was only observed for pm peak hours of NJ Route 120, Northbound. For the Southbound of this route, almost no congestion were observed. The same as the other corridors, NJ Route 120's congestion was not affected by the partial opening of the complex. Eventually, the new year's holidays only decreased the congestion during pm peak hours of NJ Route 120, Northbound.

Data loss from about 10 pm at night to 6 am in the morning for all corridors was another notable observation from these heatmaps.
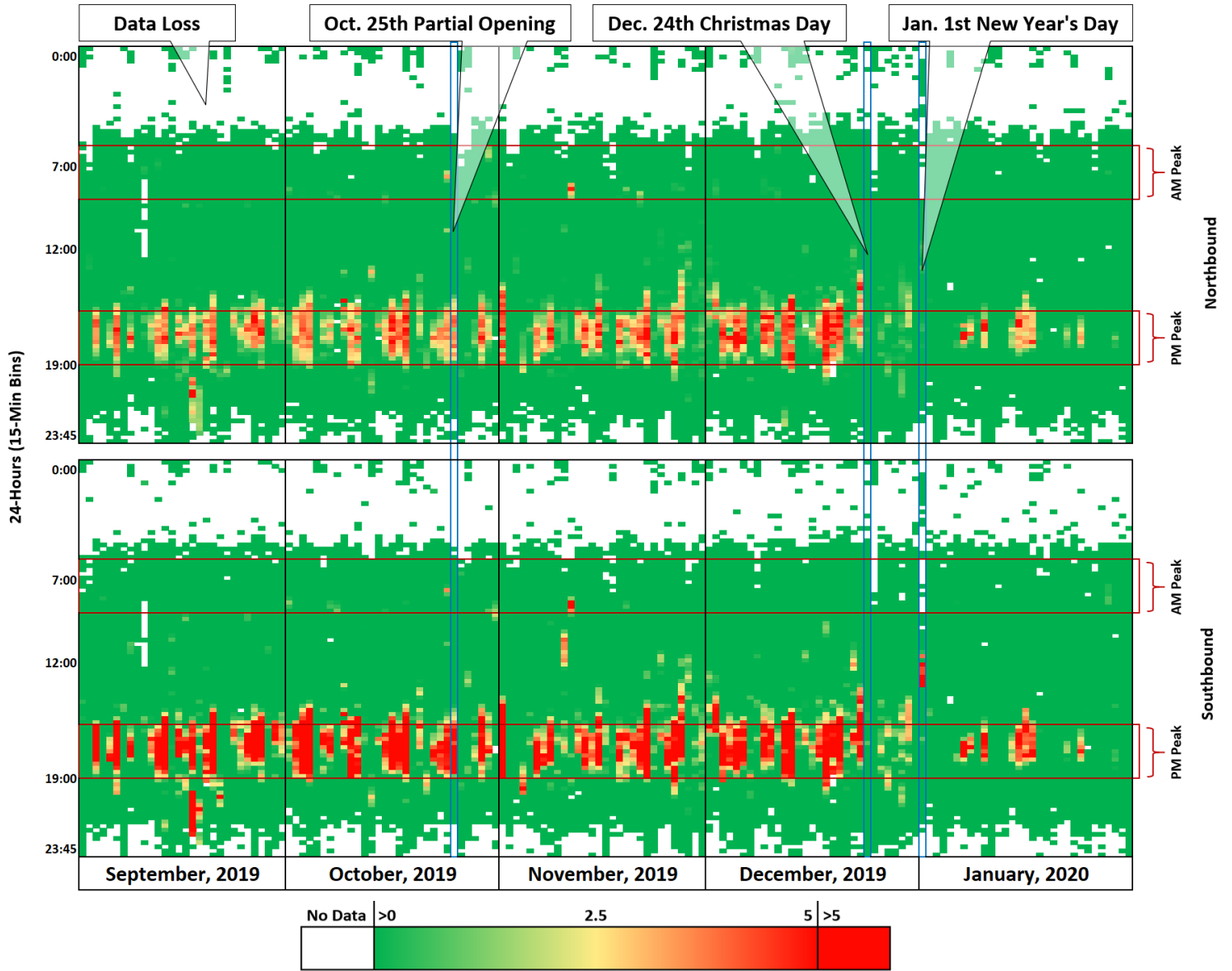
Figure 14 Daily CIMTT for Interstate 95 in 15-min bin
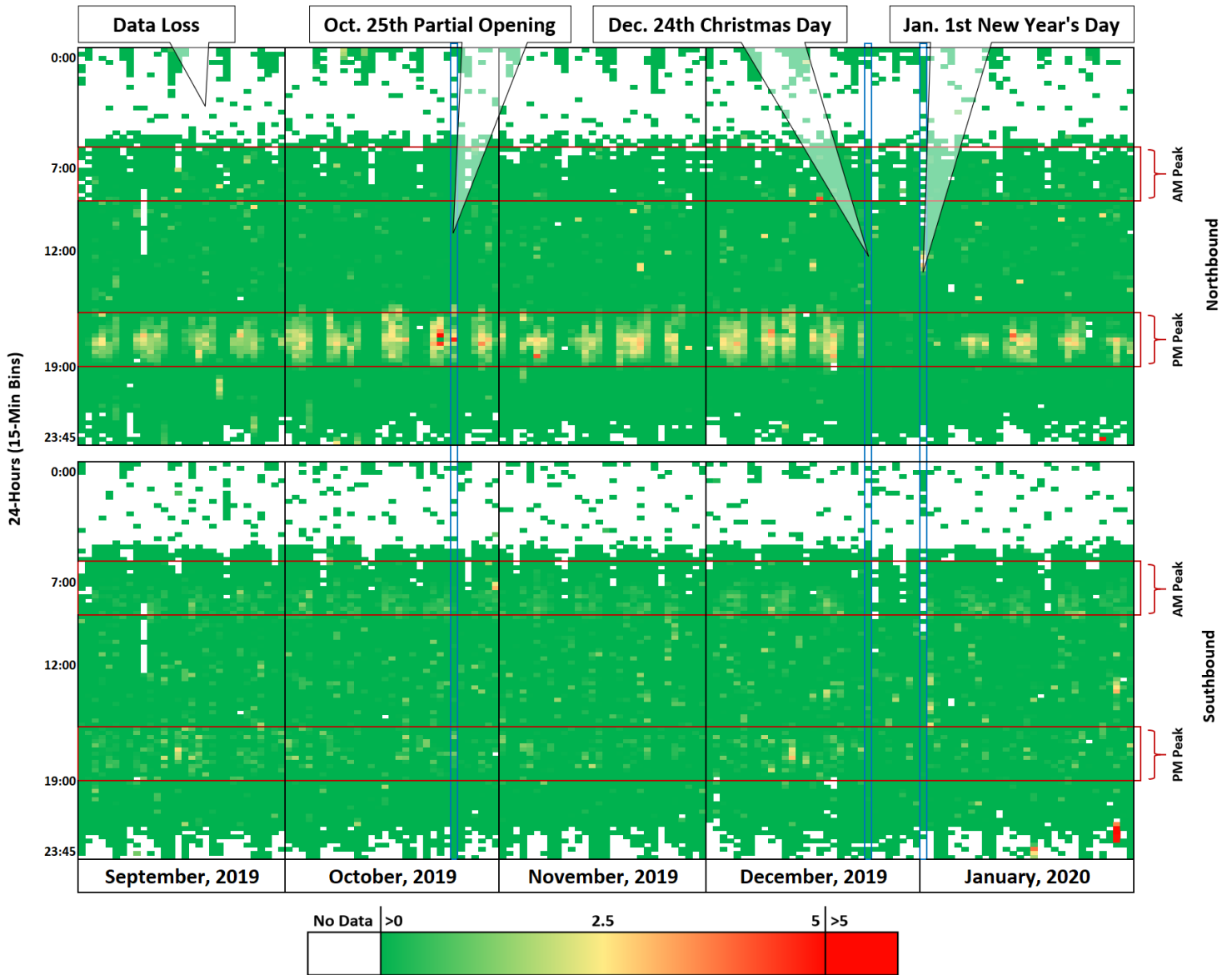
Figure 15 Daily CIMTT for Meadowlands Pkwy in 15-min bin
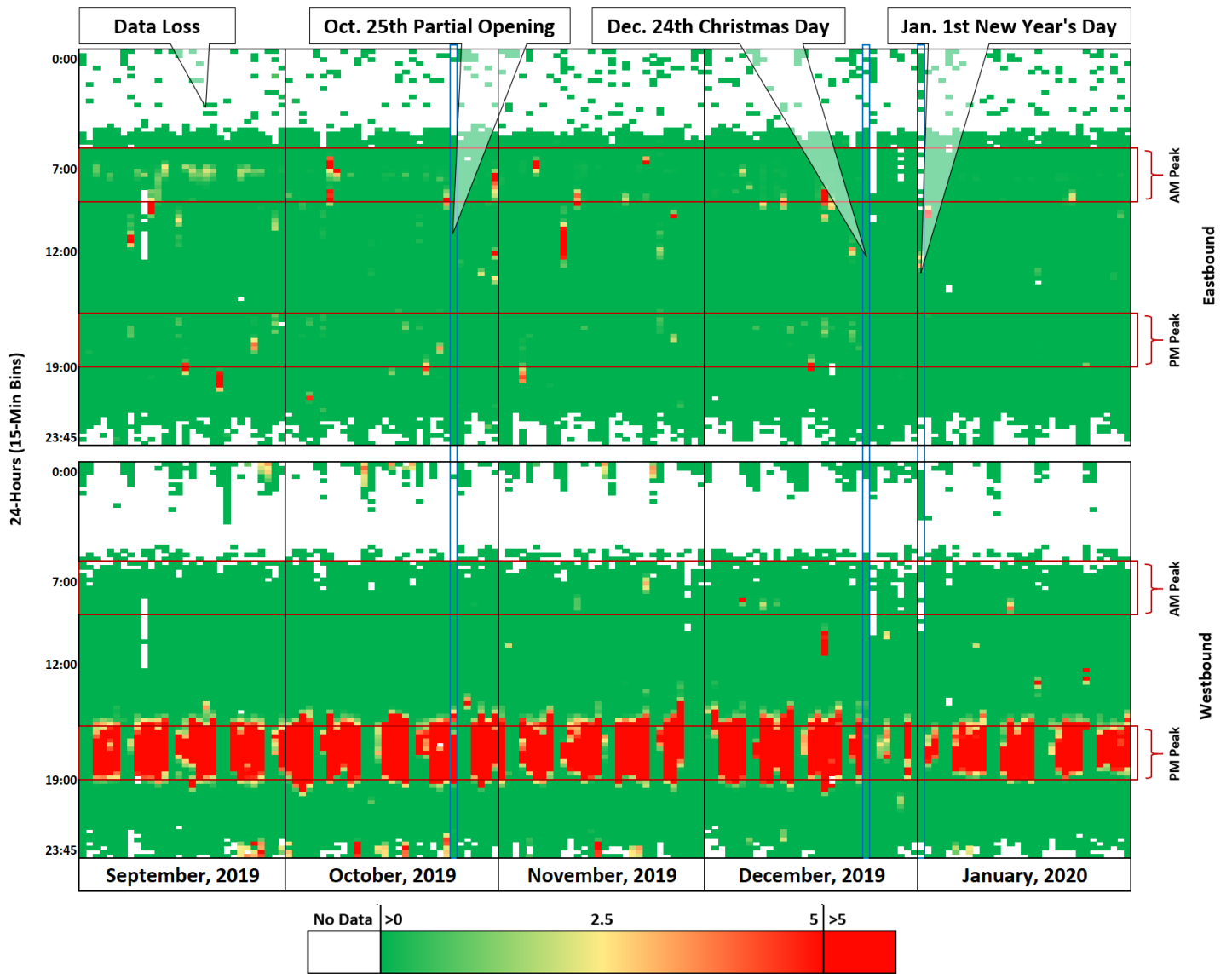
Figure 16 Daily CIMTT for NJ Route 3 in 15-min bin
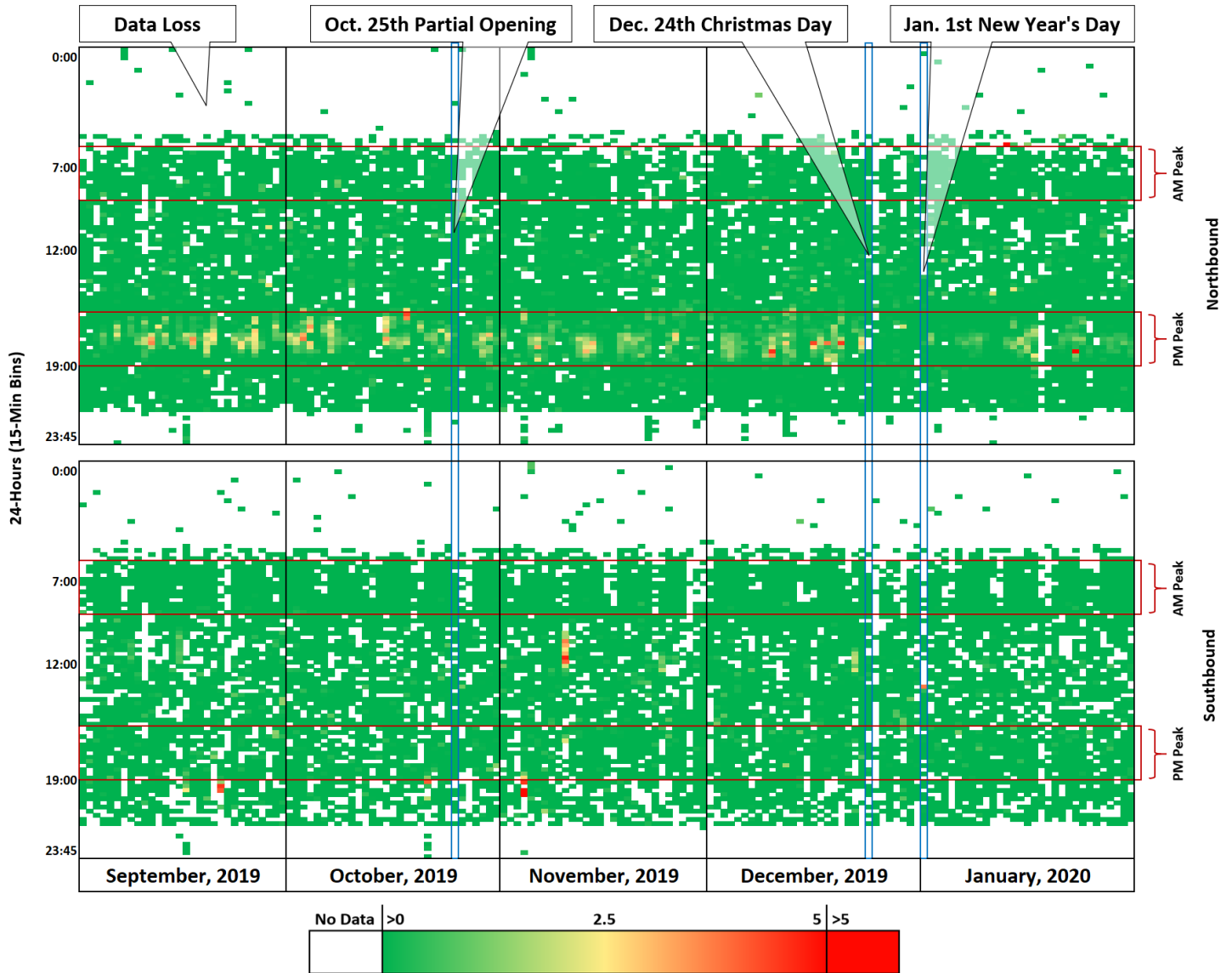
Figure 17 Daily CIMTT for NJ Route 120 in 15-min bin

In addition to CIMTT heatmaps, the speed heatmaps were also developed for better analyzing the congestion condition of the surrounding corridors. To do so, only the TMCs with the same speed limits within each corridor was considered and averaged. Hence, each cell represents the average speed for their bin. Illustrations of the considered TMCs for each corridor are shown in Figures 18 to 21. The average speed records were then visualized as the heatmaps shown in Figures 22 to 25. Moreover, in order to have a better insight into the comparison of the opening day speeds with other days, the speed records cells during am peak, pm peak, and mid-day hours for seven Fridays before (September and October) and nine Fridays (November and December) after the opening Friday (October 25) were extracted from the heatmaps and averaged. Then the values were compared with each other to investigate how the traffic speed changed due to the opening of the

complex. Tables 5 to 12 tabulate the average speed records for different Fridays before and after opening day for all selected corridors. Finally, the average speeds during the entire peak hours (both am and pm peak hours) for the selected routes were also extracted from the heatmaps. Tables 13 to 16 summarise the average speeds during the am and pm peak hours.
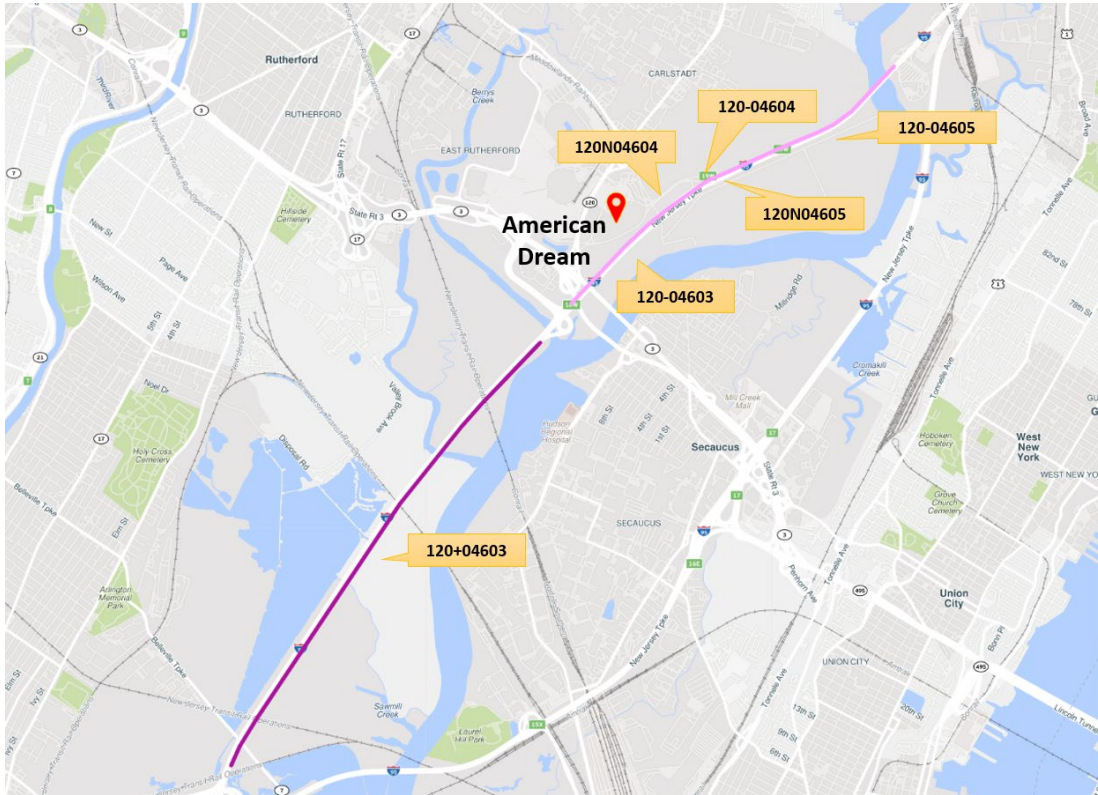
Figure 18 Considered TMCs for speed heatmaps for Interstate 95
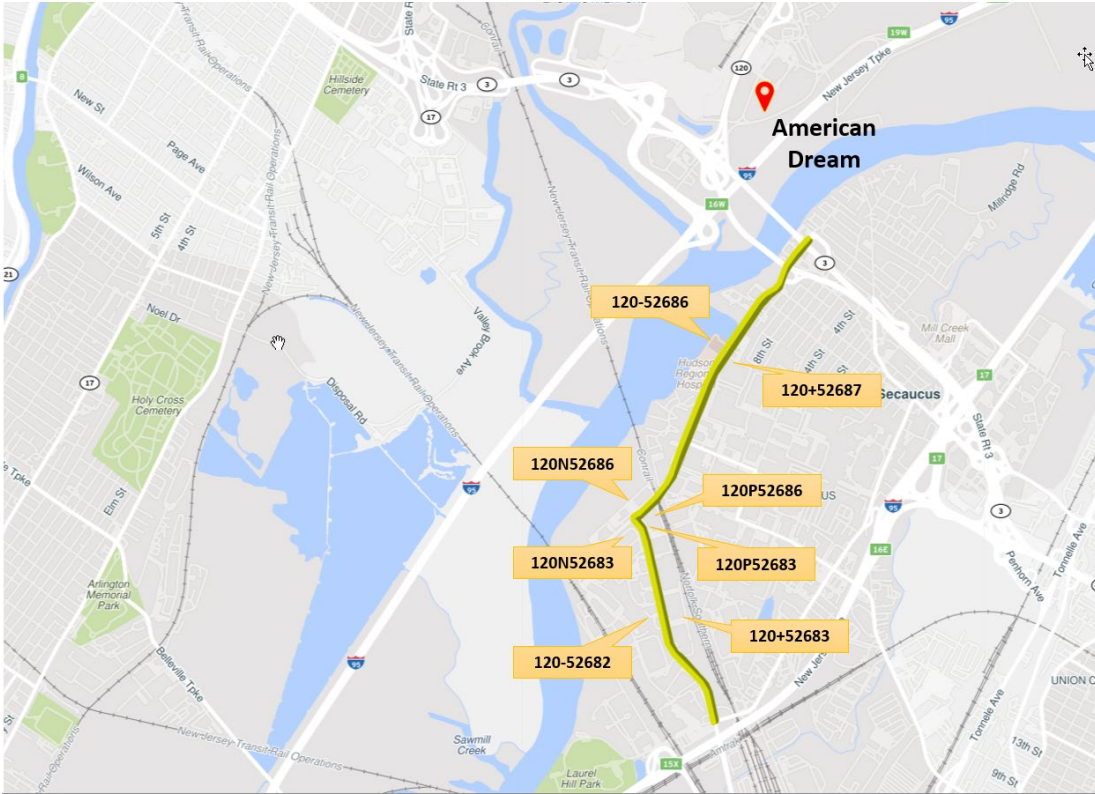
Figure 19 Considered TMCs for speed heatmaps for Meadowlands Pkwy
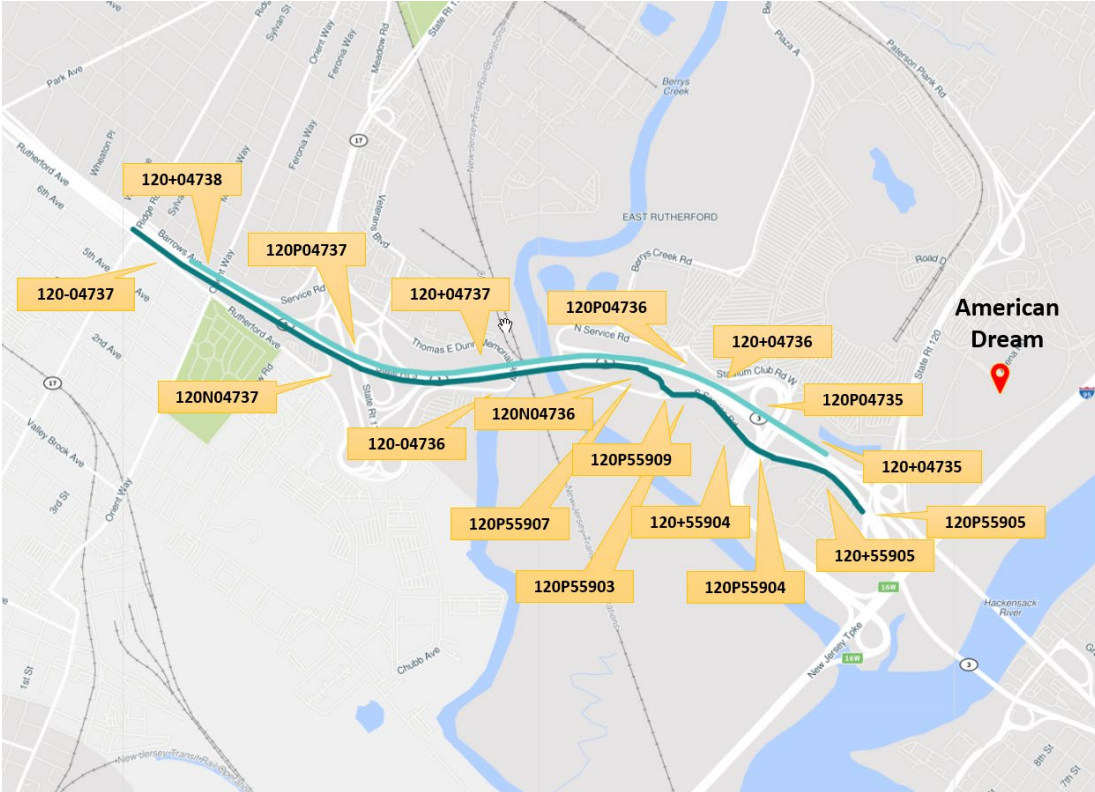
Figure 20 Considered TMCs for speed heatmaps for NJ Route 3
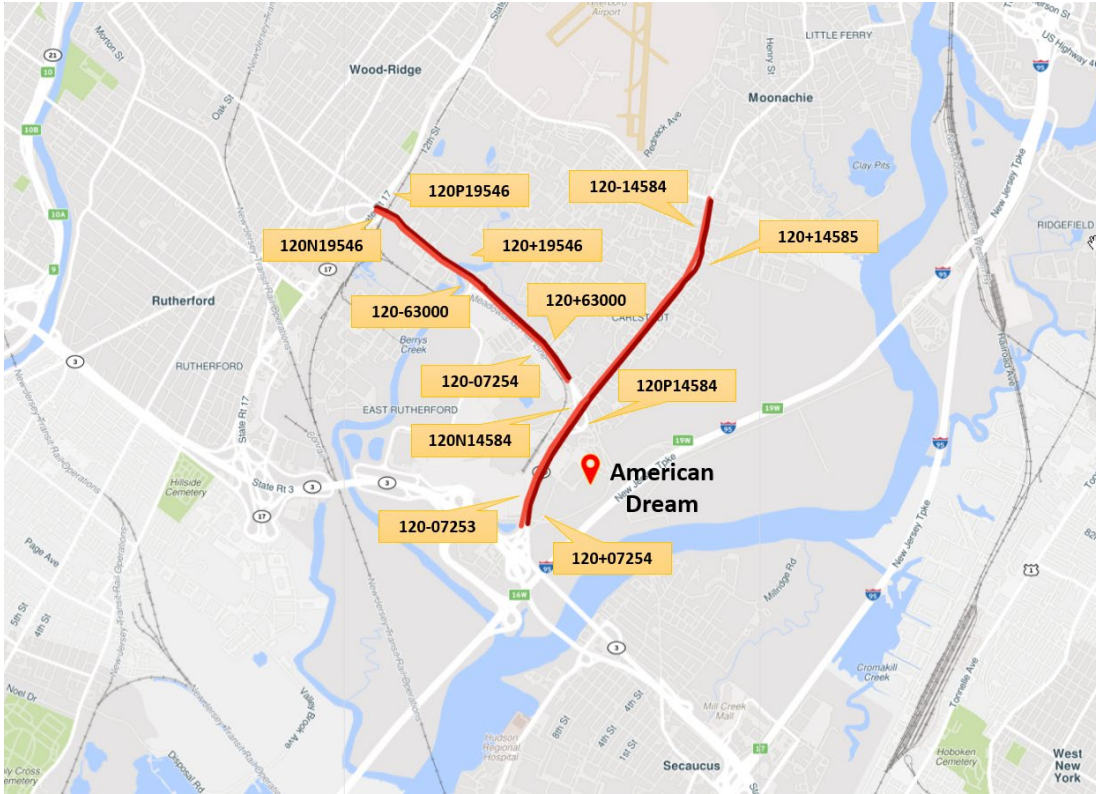
Figure 21 Considered TMCs for speed heatmaps for NJ Route 120

As can be seen in Figure 22, for Northbound Interstate 95, low traffic speeds were only observed on some specific days. However, for the Southbound of this corridor, low values of speed were only observed during the pm peak hours showing the traffic congestion during this time. For both bounds, after the new year's holidays, the traffic congestion decreased, having high values of average speed records.

Based on Tables 5 and 6, for the Eastbound of Interstate 95, the average speeds of all Fridays during September had values of greater than 60 mph, with an average of 61.29 mph for the entire September. Then in October, they decreased to the average of 59.22 mph and 59.87 on the opening Friday. After the opening, the speeds increased to an average of 61.91 mph on Fridays during both November and December. However, during the mid-day and pm hour peak hours, the opening Fridays recorded the highest average speed compared to other Fridays. For the Westbound of this corridor, opening Friday had the highest average speed during am peak and mid-day hours in comparison with other Fridays. For pm peak hours, on the other hand, averagely, the opening Friday speed was almost equal to the average speed of both September and October.

According to Figure 23, some data loss was observed during the entire study period for the selected TMCs for speed heatmaps of both Northbound and Southbound. Moreover, almost no abrupt and

considerable congestion of the traffic was recorded for this corridor. Also, from the heatmaps, the opening did not have a notable effect on the traffic condition of this corridor.

As provided in Tables 7 and 8, when the average Fridays of September and October were compared to the opening Friday, the am and pm peak hours of both Northbound and Southbound of Meadowlands Pkwy experienced a decrease. However, the mid-day of this corridor recorded an increase in average speeds. Moreover, the am peak hours of both bounds had an increase, while the mid-day and the pm peak hours experienced a decrease in average speed after the opening.

As shown in Figure 24, the pattern of traffic was the same as the pattern observed in CIMTT heatmaps for both Eastbound and Southbound. In terms of the statistics and according to Tables 9 and 10, the average speed of opening Friday was increased for am peak and mid-day hours of the Eastbound in comparison with the Fridays before opening. After the opening, the average speed records were increased again, after the opening for both am peak and mid-day hours of this bound. For the Westbound, however, these two periods of the day experienced a decrease on the opening Friday, and this decrease pattern continued after the opening Friday too. For the pm peak hours, the same increase pattern was recorded for this bound.

As illustrated in Figure 25, the low-speed records of NJ Route 3 were confined majorly during the pm periods of Northbound and distributed almost during the entire day for Southbound.

For NJ Route 120, as summarized in Tables 11 and 12, the average speed records recorded an increase during mid-day and pm peak hours on the opening Friday for both Northbound and Southbound in comparison with the previous Fridays. However, the am peak hours showed a decrease for this corridor on the opening Friday. After the opening, the am peak hours of the Northbound and the am and pm peak hours of the Southbound experienced an increase when compared to the opening Friday. Other day periods recorded a decreasing pattern after the opening of the complex.

Similar to the CIMTT heatmaps, data loss was observed from 10 pm to 6 am for all average speed heatmaps. Also, some data loss during the entire day was observed for Meadowlands Pkwy specifically.

According to Table 13, Interstate 95 experienced a decrease in speeds from September to October for all peak hours in both Northbound and Southbound. However, from October to November, average speeds increased for both am, and pm peak jours of Southbound and the am peak hours of Northbound.

As shown in Table 14 for Meadowlands Pkwy, average speeds during am peak hours of Northbound and pm peak hours of Southbound increased from September to November. The average speeds during om peak hours of Northbound and the am peak hours of the Southbound decreased from September to October and then increased from October to November.

As presented in Table 15, the entire NJ Route 3 experienced an increasing pattern in average speeds from September to October during both am and pm peak hours. However, during the pm peak hours of Northbound and am peak hours of Southbound, a decreasing pattern was observed from October to November.

For NJ Route 120, the average speeds of the entire Northbound experienced a decreasing pattern during both am and pm peak hours. At the same time, the Southbound corridor increased average speed from September to October. From October to November, the entire NJ Route 120 experienced a decreasing pattern during both am and pm peak hours (shown in Table 16).
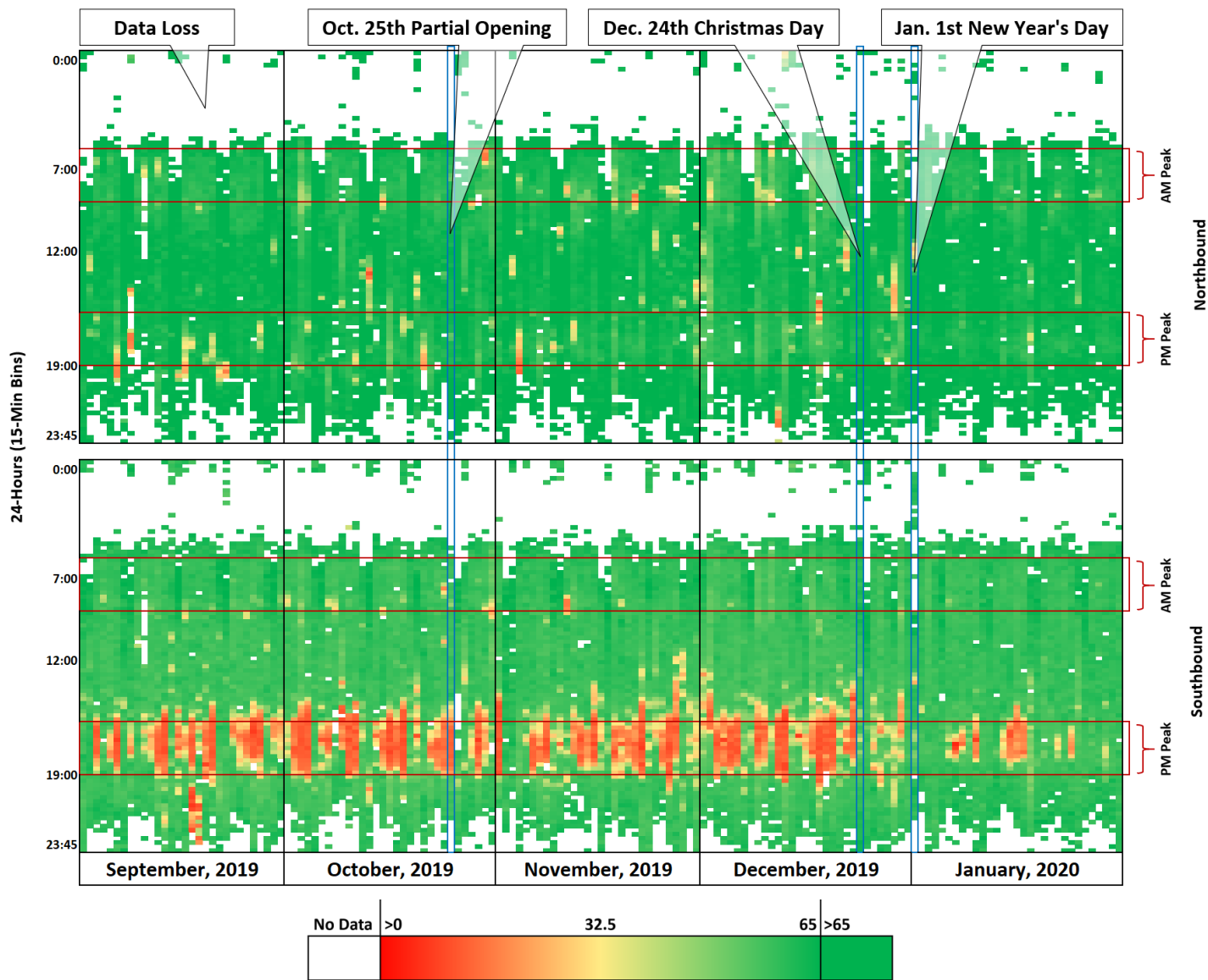
Figure 22 Daily average speed heatmap for Interstate 95 in 15-min bin
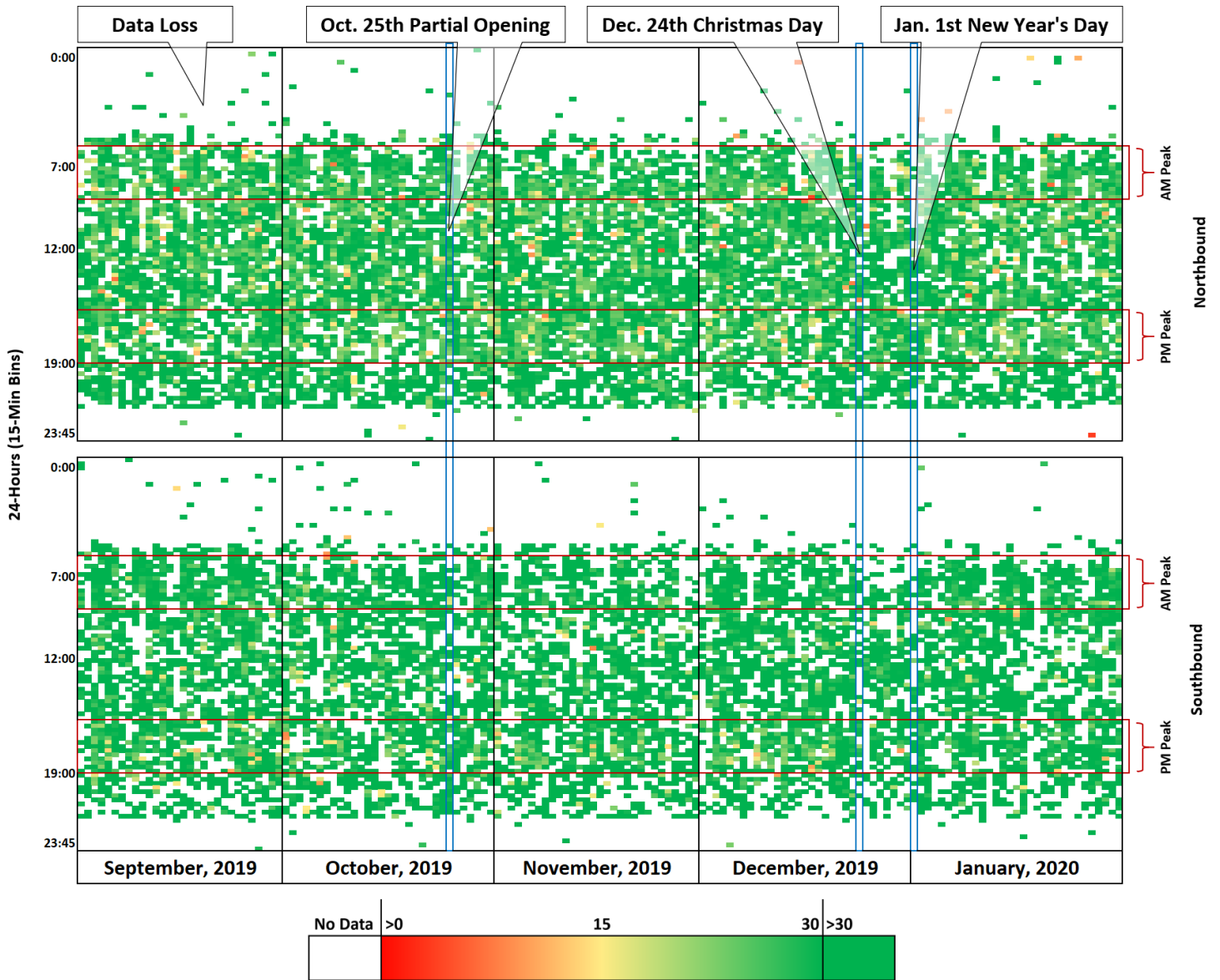
Figure 23 Daily average speed heatmap for Meadowlands Pkwy in 15-min bin
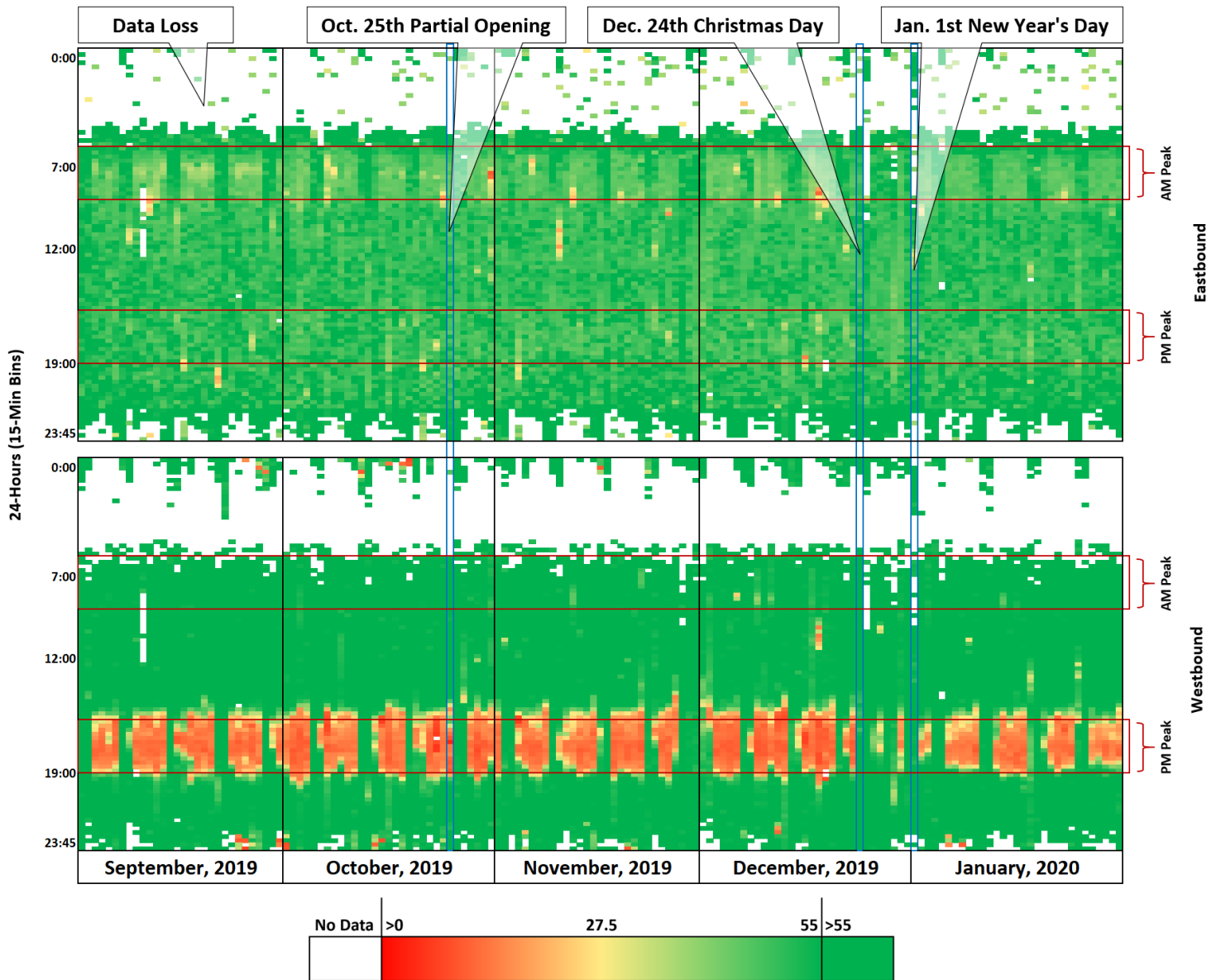
Figure 24 Daily average speed heatmap for NJ Route 3 in 15-min bin
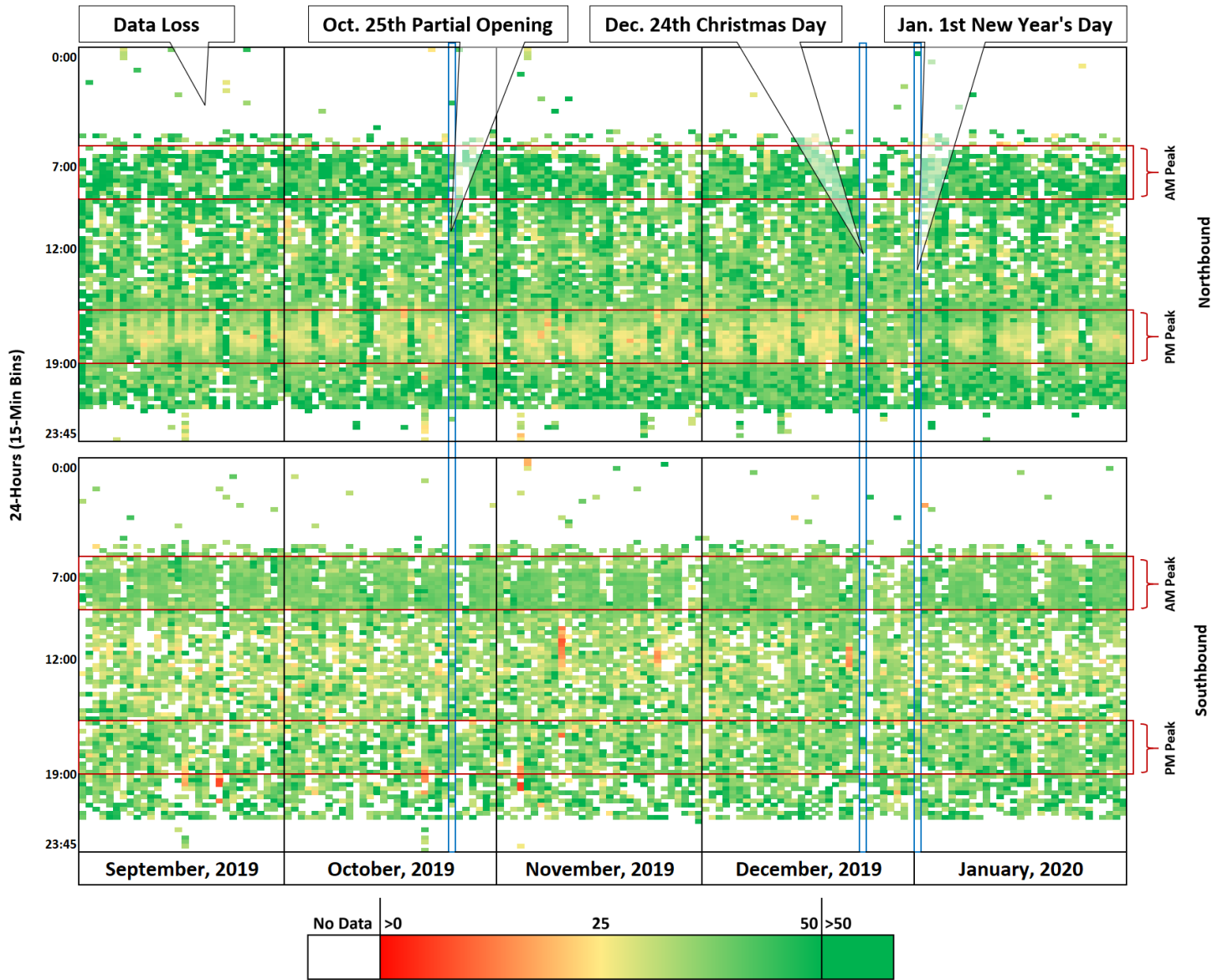
Figure 25 Daily average speed heatmap for NJ Route 120 in 15-min bin

Table 5 Average speed records for all Fridays from September to December for Interstate 95

Bound	Day Time	September, Fridays				October, Fridays				November, Fridays					December, Fridays			
		1st	2nd	3rd	4th	1st	2nd	3rd	Opening Friday	1st	2nd	3rd	4th	5th	1st	2nd	3rd	4th
NB	AM	61.97	60.66	61.30	61.23	57.59	60.21	59.87	**59.87**	61.23	61.36	60.48	61.66	66.75	60.78	60.37	59.06	65.51
	Mid-Day	61.77	63.45	63.37	63.57	61.64	62.02	62.06	**63.30**	62.42	62.32	62.51	60.36	65.02	63.51	61.25	61.11	62.42
	PM	46.82	62.34	50.97	50.95	56.93	54.07	52.91	**60.94**	61.52	60.05	60.09	59.46	61.47	62.14	53.97	60.70	60.70
SB	AM	58.65	58.50	57.45	57.41	57.36	58.08	55.37	**55.62**	57.68	59.05	59.34	58.69	61.60	57.30	57.53	56.86	56.90
	Mid-Day	54.27	52.66	50.57	52.25	48.16	50.85	48.64	**52.52**	45.41	52.28	46.63	44.71	54.81	52.77	49.14	50.19	54.20
	PM	15.36	13.11	13.71	18.75	13.39	14.56	11.60	**14.62**	11.85	17.41	18.88	11.94	45.70	19.94	12.26	14.00	40.92

Table 6 Average of all Fridays for each month for Interstate 95

Bound	Day Time	Ave Sep.	Ave Oct.	Ave. Sep. & Oct.	Opening Friday	Ave Nov.	Ave Dec.	Ave Nov. & Dec.
NB	AM	61.29	59.22	60.40	**59.87**	62.30	61.43	61.91
	Mid-Day	63.04	61.91	62.56	**63.30**	62.53	62.07	62.32
	PM	52.77	54.64	53.57	**60.94**	60.52	59.38	60.01
SB	AM	58.00	56.94	57.55	**55.62**	59.27	57.15	58.33
	Mid-Day	52.44	49.22	51.06	**52.52**	48.77	51.57	50.01
	PM	15.23	13.18	14.35	**14.62**	21.16	21.78	21.43

Table 7 Average speed records for all Fridays from September to December for Meadowlands Pkwy

Bound	Day Time	September, Fridays				October, Fridays				November, Fridays					December, Fridays			
		1st	2nd	3rd	4th	1st	2nd	3rd	Opening Friday	1st	2nd	3rd	4th	5th	1st	2nd	3rd	4th
NB	AM	28.01	27.71	27.64	29.59	26.14	29.23	25.61	**26.98**	27.56	30.37	23.86	28.06	29.07	28.05	26.76	31.98	29.24
	Mid-Day	24.12	25.28	26.93	27.23	25.11	28.46	27.87	**28.29**	27.75	28.37	27.38	26.53	30.93	28.10	27.30	26.94	30.31
	PM	27.04	25.02	28.08	30.79	25.60	24.02	27.56	**26.48**	23.02	25.15	24.74	26.10	28.84	28.85	20.23	27.68	27.90
SB	AM	28.61	29.19	29.09	30.93	26.09	30.36	30.97	**28.14**	32.31	29.97	29.68	30.23	33.34	30.69	31.58	30.65	32.78
	Mid-Day	31.20	27.89	30.49	28.61	30.86	30.92	31.23	**31.68**	28.99	29.68	29.15	31.35	31.11	30.58	30.74	31.61	31.56
	PM	30.20	26.67	29.58	27.70	29.50	31.59	27.05	**28.23**	25.28	30.40	26.17	26.36	32.24	26.49	25.74	26.94	30.69

Table 8 Average of all Fridays for each month for Meadowlands Pkwy

Bound	Day Time	Ave Sep.	Ave Oct.	Ave. Sep. & Oct.	Opening Friday	Ave Nov.	Ave Dec.	Ave Nov. & Dec.
NB	AM	28.24	26.99	27.71	**26.98**	27.78	29.01	28.33
	Mid-Day	25.89	27.15	26.43	**28.29**	28.19	28.16	28.18
	PM	27.73	25.73	26.87	**26.48**	25.57	26.16	25.83
SB	AM	29.46	29.14	29.32	**28.14**	31.11	31.42	31.25
	Mid-Day	29.55	31.00	30.17	**31.68**	30.06	31.12	30.53
	PM	28.54	29.38	28.90	**28.23**	28.09	27.47	27.81

Table 9 Average speed records for all Fridays from September to December for NJ Route 3

Bound	Day Time	September, Fridays				October, Fridays				November, Fridays					December, Fridays			
		1st	2nd	3rd	4th	1st	2nd	3rd	Opening Friday	1st	2nd	3rd	4th	5th	1st	2nd	3rd	4th
EB	AM	48.89	44.08	44.85	43.81	44.96	46.39	46.22	**46.88**	47.52	47.86	47.05	46.84	54.20	44.00	48.57	46.36	52.69
	Mid-Day	49.22	49.79	50.02	48.64	50.20	50.31	49.35	**49.95**	50.78	49.57	50.53	50.30	49.94	50.35	51.31	48.81	48.77
	PM	49.86	49.21	51.35	50.18	48.89	51.87	47.39	**49.67**	51.25	50.98	49.71	51.63	49.59	50.73	43.83	49.64	48.80
WB	AM	58.99	59.29	58.96	58.45	58.08	58.67	57.25	**57.81**	56.78	58.16	58.93	53.92	59.70	53.41	57.85	56.98	58.72
	Mid-Day	55.45	54.43	53.62	55.12	52.53	55.36	52.90	**52.32**	53.17	51.12	52.11	48.89	58.41	52.04	47.85	50.05	53.83
	PM	15.97	16.59	15.26	19.12	13.47	16.00	14.48	**15.93**	13.77	18.79	15.63	13.54	55.27	13.14	13.00	16.08	39.78

Table 10 Average of all Fridays for each month for NJ Route 3

Bound	Day Time	Ave Sep.	Ave Oct.	Ave. Sep. & Oct.	Opening Friday	Ave Nov.	Ave Dec.	Ave Nov. & Dec.
EB	AM	45.41	45.86	45.60	**46.88**	48.69	47.91	48.34
	Mid-Day	49.42	49.95	49.65	**49.95**	50.22	49.81	50.04
	PM	50.15	49.38	49.82	**49.67**	50.63	48.25	49.57
WB	AM	58.92	58.00	58.53	**57.81**	57.50	56.74	57.16
	Mid-Day	54.65	53.60	54.20	**52.32**	52.74	50.94	51.94
	PM	16.74	14.65	15.84	**15.93**	23.40	20.50	22.11

Table 11 Average speed records for all Fridays from September to December for NJ Route 120

Bound	Day Time	September, Fridays				October, Fridays				November, Fridays					December, Fridays			
		1st	2nd	3rd	4th	1st	2nd	3rd	Opening Friday	1st	2nd	3rd	4th	5th	1st	2nd	3rd	4th
NB	AM	42.72	42.45	42.61	41.63	40.73	46.22	41.10	**41.85**	43.04	46.92	44.32	37.63	30.04	42.82	44.81	44.10	43.74
	Mid-Day	37.42	38.77	41.93	36.88	40.66	37.63	37.31	**39.70**	40.42	39.66	38.84	38.18	36.13	38.35	35.59	39.30	39.46
	PM	33.25	32.48	30.67	34.93	32.02	34.84	28.55	**33.52**	31.67	29.43	32.54	31.18	35.16	31.85	28.86	29.19	36.07
SB	AM	37.47	37.54	36.59	37.34	37.88	37.53	38.06	**36.73**	37.55	37.77	38.48	38.03	33.03	38.23	37.56	37.48	34.94
	Mid-Day	34.09	33.83	33.23	34.96	35.79	33.14	35.25	**36.24**	35.29	35.58	35.40	35.99	35.98	35.69	34.13	38.72	35.50
	PM	34.98	34.45	36.11	36.40	35.31	35.43	36.03	**36.91**	37.69	39.27	34.36	37.61	36.12	36.96	36.68	39.91	36.23

Table 12 Average of all Fridays for each month for NJ Route 120

Bound	Day Time	Ave Sep.	Ave Oct.	Ave. Sep. & Oct.	Opening Friday	Ave Nov.	Ave Dec.	Ave Nov. & Dec.
NB	AM	42.35	42.68	42.49	**41.85**	40.39	43.87	41.94
	Mid-Day	38.75	38.53	38.66	**39.70**	38.65	38.18	38.44
	PM	32.83	31.80	32.39	**33.52**	32.00	31.49	31.77
SB	AM	37.23	37.82	37.49	**36.73**	36.97	37.05	37.01
	Mid-Day	34.03	34.73	34.33	**36.24**	35.65	36.01	35.81
	PM	35.48	35.59	35.53	**36.91**	37.01	37.45	37.20

Table 13 Average of speed during entire peak hours for each month for Interstate 95

Direction	AM/PM Peak	Sep.	Oct.	Nov.	Dec.	Jan.
Northbound	AM	62.98	61.22	61.70	60.16	62.85
	PM	61.08	60.86	60.47	60.22	63.13
Southbound	AM	59.15	57.22	59.24	58.20	59.04
	PM	37.26	32.77	34.75	34.45	49.78

Table 14 Average of speed during entire peak hours for each month for Meadowlands Pkwy

Direction	AM/PM Peak	Sep.	Oct.	Nov.	Dec.	Jan.
Northbound	AM	27.57	28.48	28.85	27.90	28.30
	PM	29.25	27.38	27.78	28.08	27.53
Southbound	AM	30.52	30.49	31.15	31.07	30.35
	PM	29.22	29.94	30.06	29.21	30.82

Table 15 Average of speed during entire peak hours for each month for NJ Route 3

Direction	AM/PM Peak	Sep.	Oct.	Nov.	Dec.	Jan.
Eastbound	AM	49.26	47.41	49.31	48.64	49.31
	PM	51.05	49.83	49.52	48.66	49.91
Westbound	AM	59.28	58.73	58.59	57.17	58.11
	PM	30.01	26.32	30.18	31.64	32.86

Table 16 Average of speed during entire peak hours for each month for NJ Route 120

Direction	AM/PM Peak	Sep.	Oct.	Nov.	Dec.	Jan.
Northbound	AM	43.77	43.34	42.50	42.38	43.59
	PM	36.10	34.74	34.56	34.05	36.35
Southbound	AM	37.97	38.16	38.07	37.68	38.88
	PM	36.86	37.51	37.18	37.30	37.69

4.2 StreetLight Data

In terms of evaluating a roadway system's performance measure using StreetLight Inc. data, origin or pass-through gates were created on all routes leading to American Dream Complex. In this study, StreetLight volume trip data was extracted for 120 days before and 120 days after the complex's opening. Figure 26 represents the total number of StreetLight volume trips for all days between June, 27th 2019, and February, 22nd 2020. Wherein the data showed an increase in the Street Light Volume trips after the opening.
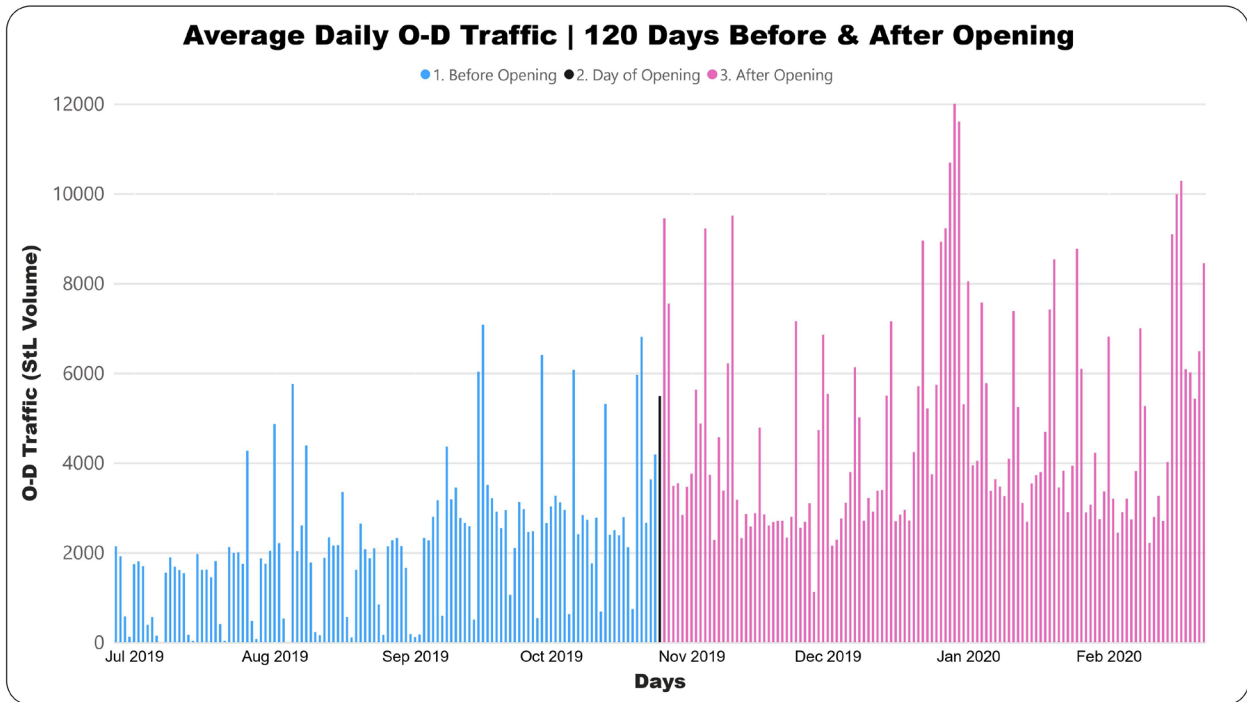
Figure 26 StreetLight volume trips for before and after opening

As shown in Figure 26, StreetLight volume trips during the weekends were low. After the complex opening, the weekend StreetLight Volume trips had increased, and showed many of the weekends had above 2000 StreetLight vehicle volume trips. Detailed information about the daily trip counts is attached in Appendix A.

Further, to understand the StreetLight Inc. data in detail, the StreetLight vehicle volume trips were grouped into 30 days. As shown in Figure 27, groups 1, 2, 3, and 4 represent data for before the opening, groups 5 show the data for the day of opening, and groups 6, 7, 8, and 9 demonstrate data for after the opening.
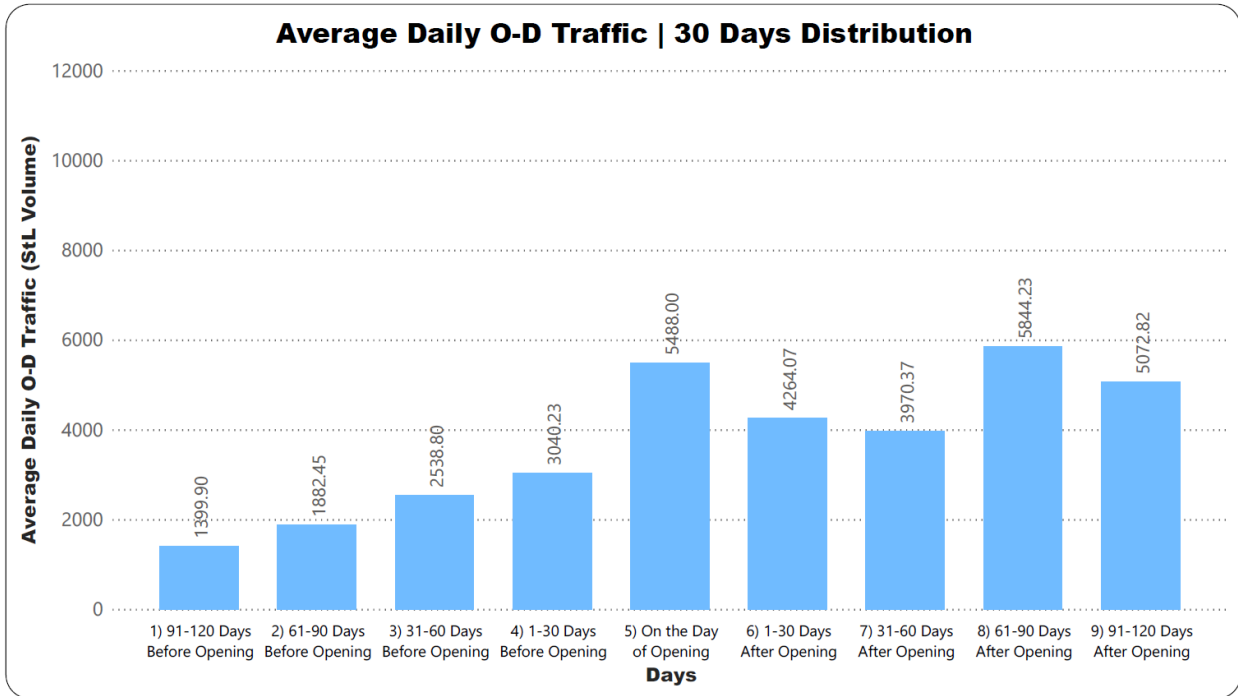
Figure 27 StreetLight volume trips 30 days distribution groups

Based on the average StreetLight volume trips data, groups 1, 2, 3, and 4 showed a gradual increase in the trip that ended at American Dream Complex. On the other hand, groups 6, 7, 8, and 9 did not increase after the opening but had more average StreetLight volume trips than groups 1, 2, 3, and 4. It is important to note that the days clustered for group 8 had many holidays included, due to which the average StreetLight volume trips have been recorded as the highest.

In addition to the trip counts, the trips' purpose was also explored to distinguish the visitors and work-based trips. As seen in Figure 28, home-based work trips account for more than 20 percent of the groups represented before the complex's opening. While after the complex opening, the home-based work trips were reduced to below 15 percent of the average trips, demonstrating an increase in the trips that were not related to work purposes. In terms of the home-based other trips, which can be considered a trip made as a visitor, are gradually increasing. This pattern shows that there has been an increase in the portion of visitors after the opening of the complex. It should be noted that the portion of the non-home-based trip is the maximum because its home or work locations are not identifiable for those trips. However, those trips did end at the American Dream Complex.
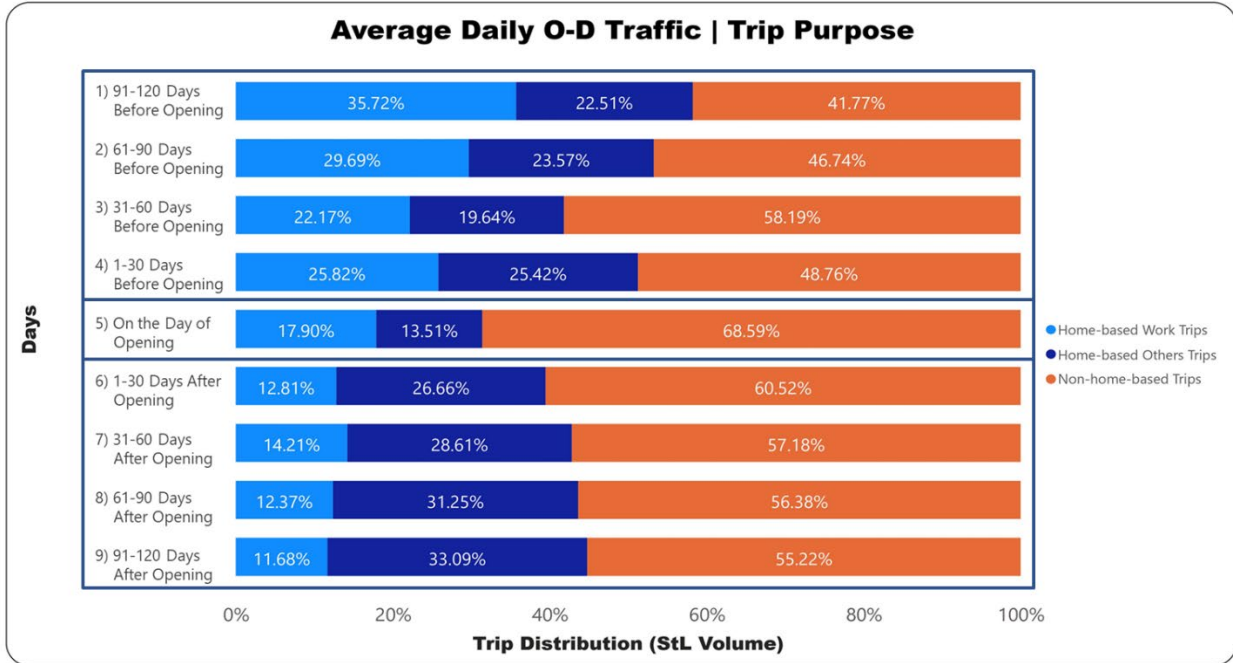
Figure 28 StreetLight volume trips purpose

Besides visualizing trip volume from the Streetlight Inc. database, a change in the travel duration was also accessed. To do so, major routes were chosen based on the trip volume. Only weekday data was considered for performing a normalized statistical analysis and identifying the significant changes. Based on the distribution of travel duration bin, it can be observed that the majority of the trips took 0-10 minutes of travel time from the origin or pass through gates. It should be noted that, as discussed previously in Table 4, the base travel time from all the origin or passthrough grates to the complex is less than 5 minutes.

For the travel duration of 0-10 minutes, results showed a significant increase in the StreetLight volume trips for Interstate 95, whereas a significant reduction in StreetLight volume trips after the opening of the complex was observed on NJ Route 3. Based on the result, it can be determined that after the opening of the complex, an increase in the trips may have caused an increase in travel time on NJ Route 3. For NJ Route 120, there was a reduction in the trip proportion after the opening of the complex, but it did not show a significant difference.

Results of travel duration of 10-20 minutes showed a significant reduction in StreetLight volume trips at Interstate 95. As can be seen in Table 13, the proposition of the trips has moved to 0-10 minutes so resulting in reduced travel time. For NJ Route 3 and NJ Route 120, no significant changes in the StreetLight volume trips were observed.

For the travel duration of 20-30 minutes, NJ Route 120 showed a significant increase in the StreetLight volume trips. Based on the finding, it can be stated that after the opening of the complex, NJ Route 120 has experienced a reduction in the proportion of StreetLight volume trips

in 0.-10 and 10-20 minutes travel duration bin. Changes observed in the proportion of StreetLight volume trips in relation to travel duration are summarized in Table 13.

Table 13 Changes in the proportion of the StreetLight volume trips based on the travel durations
Note: StL Trips = StreetLight volume trips

| Routes | Travel Duration (mins) | Average StL Trip | | Change | | |
		Before Opening	After Opening	Difference	P-Value	Signification Test
Interstate 95	0-10	36.84%	45.77%	8.93%	0.00	Significant Increase
	10-20	46.76%	36.87%	-9.89%	0.00	Significant Reduction
	20-30	10.20%	10.88%	0.68%	0.29	Insignificant Increase
	30-40	3.60%	3.03%	-0.57%	0.34	Insignificant Reduction
	40-50	0.69%	1.29%	0.59%	0.22	Insignificant Increase
	50-60	0.42%	0.94%	0.52%	0.27	Insignificant Increase
NJ Route 3	0-10	52.71%	48.57%	-4.14%	0.03	Significant Reduction
	10-20	30.97%	32.17%	1.20%	0.26	Insignificant Increase
	20-30	8.44%	10.67%	2.23%	0.07	Insignificant Increase
	30-40	4.89%	2.97%	-1.92%	0.06	Insignificant Reduction
	40-50	0.76%	1.39%	0.63%	0.16	Insignificant Increase
	50-60	1.55%	1.89%	0.34%	0.37	Insignificant Increase
NJ Route 120	0-10	57.99%	54.69%	-3.29%	0.15	Insignificant Reduction
	10-20	29.41%	28.62%	-0.79%	0.40	Insignificant Reduction
	20-30	7.02%	11.65%	4.63%	0.01	Significant Increase
	30-40	2.99%	3.82%	0.83%	0.29	Insignificant Increase
	40-50	1.38%	0.46%	-0.92%	0.18	Insignificant Reduction
	50-60	0.18%	0.62%	0.44%	0.22	Insignificant Increase

Other than the trip attribute, Streetlight Inc. database also provided traveler attributes, including the level of income, level of education, and trips involving kids or not. Based on the level of income, results demonstrated that 16.3 percent of travelers had an income between 50K to 75K, 13.5 percent of travelers had income less the 20K, 12.5 percent of travelers had an income between 75K and 100K, 12.1 percent of travelers had an income between 20K and 35K, 11.4 percent of travelers had an income between 35K and 50K, 10.4 percent of travelers had an income between 100K and 125K, travelers having income between 125K to 150K,150K to 200K, and more than 200K accounted to be 23.8 percent. Figure 29 shows a detailed distribution of travelers' level of income.
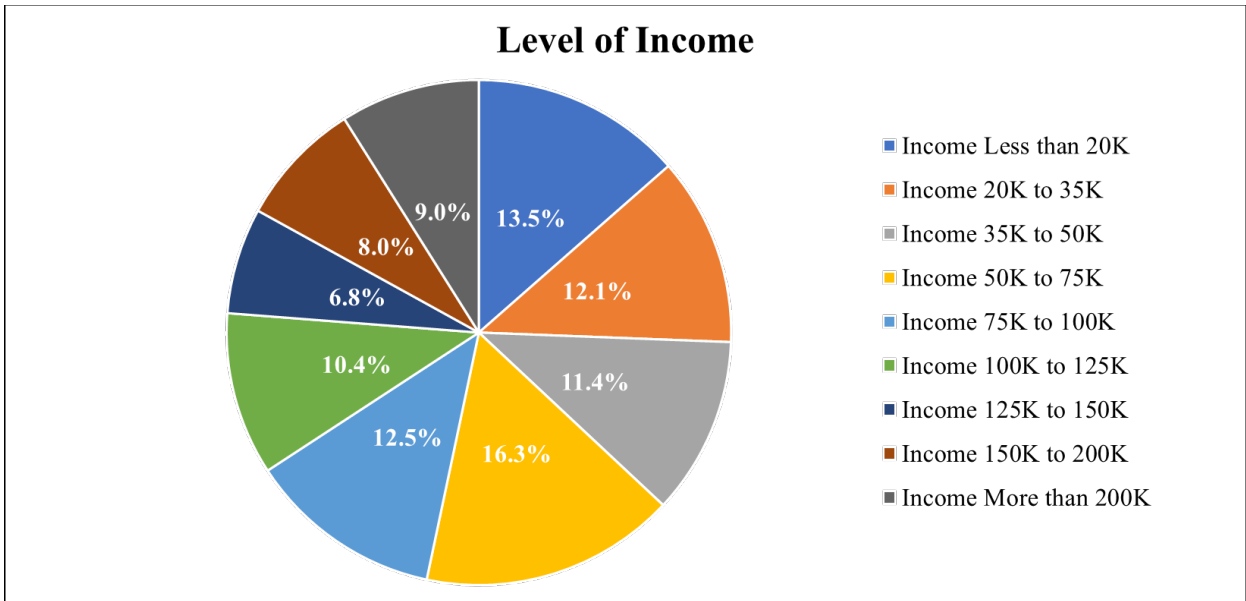
Figure 29 Traveler Attribute: Level of Income

In terms of the level of education of the travelers, the majority of the travelers had high school diplomas (28.4 percent), followed by bachelor's degree (22.7 percent), some college (21.6 percent), No high school diploma (13.7 percent), and graduate degree (13.5 percent). For the trips that involved kids/no kids showed that 37.9 percent of the trips involved kids. Figure 30 and 31 shows a detailed distribution of the level of education and involvement of kids.
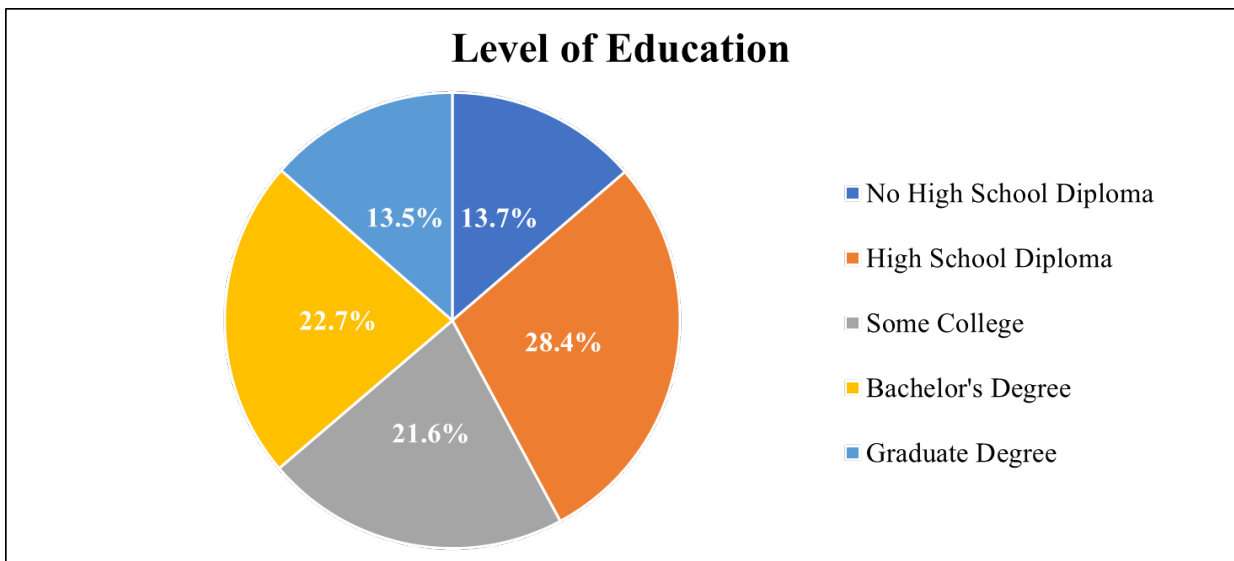
Figure 30 Traveler Attribute: Level of Education
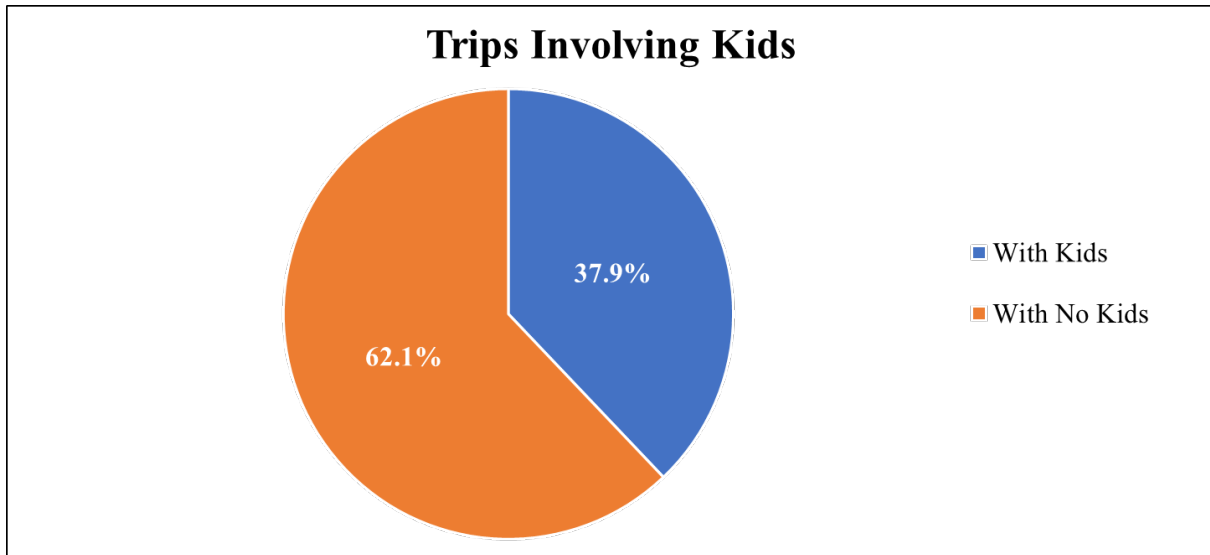
Figure 31 Traveler Attribute: Trips involving kids

4.3 Safety Analysis

The developed safety analysis methodology was applied to a video data collection from two intersections near the American dream complex. Results from a 180-minute video detected and tracked 7195 vehicles and 7 pedestrian trajectories at Hampton Inn at Paterson Plank Rd. and 8901 vehicles and 99 pedestrian trajectories at Murray Hill Pkwy and Paterson Plank Rd. in daytime conditions. Trajectories were extracted with the detection confidence threshold of 0.80 for vehicles and 0.6 for pedestrians. It is recommended that detection thresholds be modified depending on the camera's position and height. Based on the data obtained from the trajectories, data was validated, and relative accuracy was calculated to gauge the algorithm's performance.

Detection and tracking were validated for 60 minutes of video for both intersections. Table 14 shows the relative accuracy and error by comparing the values of detected counts and manual counts for the Hampton Inn at Paterson Plank Rd. Intersection. Based on the result, the vehicles initially tracked in the South and North showed fewer cars than the manual count, demonstrating an error of 0.02 and 0.03, respectively. However, the East and West start directions detected more cars compared to the manual count, showing an error of 0.11 and 0.08, respectively. Overall, it was observed that the detection and tracking algorithm showed an accuracy of 98 percent.

Table 14 Detection and tracking accuracy results (Location: Hampton Inn at Pateson Plank Road)

Start Direction	Detected Counts	Manual Count	Accuracy	Error
North	865	892	0.97	0.03
South	1262	1265	0.98	0.02
East	51	46	1.11	0.11
West	103	95	1.08	0.08
Total	2263	2298	0.98	0.02

For the Murray Hill Pkwy. and Paterson Plank Rd., only North showed fewer vehicle detection counts compared to a manual count, showing an error of 0.02. While start direction from South, East, and West showed more vehicle detection counts than manual counts, representing an error of 0.05, 0.04, and 0.19, respectively. Inclusive, it was observed that the detection and tracking algorithm exhibited an error of 0.04, i.e., an accuracy of 96 percent. Table 15 shows the relative accuracy and the error by comparing the values of detected counts and manual counts for the Murray Hill Pkwy. and Paterson Plank Rd.

Table 15 Detection and tracking accuracy results (Location: Murray Hill Pkwy & Paterson Plank Road)

Start Direction	Detected Counts	Manual Count	Accuracy	Error
North	864	886	0.98	0.02
South	965	923	1.05	0.05
East	198	191	1.04	0.04
West	418	351	1.19	0.19
Total	2245	2351	1.04	0.04

Further, based on the objective of this study, firstly, a directional-based traffic count was extracted by defining the zone parameters during the analysis. Tables 16 and 17 demonstrate the directional traffic count by identifying the starting and ending points of the detected trajectories for Hampton Inn at Paterson Plank Rd. and Murry hill Pkwy and Paterson Plank Rd., respectively. Start and endpoints for each completely tracked road user are extracted and matched with the zone parameter to determine the direction flow. The result showed that most vehicles entered the intersections from the southbound zone and exited from the northbound zone at both intersections. In

comparison, start and endpoints for the vehicles in eastbound and westbound were reported to be less. Note that both locations do not permit left turning at the intersections, and also Paterson Plank Rd. has divergent or a dedicated right turning lane, which may cause the following results. For instance, to interpret the result, the value 3973 in table 16 demonstrates that 3973 vehicles entered the intersection from the southbound and exited the intersection from northbound.

Table 16 Detection results: direction-based traffic count (Location: Hampton Inn at Pateson Plank Road)

Direction	North	South	East	West	Total
North	0	2734	0	0	2734
South	3973	0	0	0	3973
East	144	18	0	0	163
West	310	0	15	0	325
Total	4445	2753	15	0	7195

Table 17 Detection results: direction-based traffic count (Location: Murray Hill Pkwy & Paterson Plank Road)

Direction	North	South	East	West	Total
North	0	2323	0	436	2759
South	3871	0	0	0	3871
East	108	300	0	408	816
West	483	713	258	0	1455
Total	4462	3336	258	845	8901

Secondly, the non-compliance behavior of road users has been calculated and validated. To calculate the vehicle-based non-compliance events, running red light vehicles where events were counted. To do so, the traffic signal phase was detected based on one of the traffic lights at the intersection, and an associated condition algorithm was implemented to extract red light running events. Table 18 and 19 shows the recorded red light running events every 60 minutes for both locations. Figure 32 shows an illustration of the detected vehicle non-compliance event.

Table 18 Detection results: vehicle non-compliance counts (Location: Hampton Inn at Paterson Plank Road)

Time	Total Vehicle Counts	Vehicle Non-Compliance Counts
2:40 PM – 3:40 PM	2263	14
3:40 PM – 4:40 PM	2145	11
4:40 PM – 5:40 PM	2787	31
Total	2263	56

Table 19 Detection results: vehicle non-compliance counts (Location: Murray Hill Pkwy & Paterson Plank Road)

Time	Total Vehicle Counts	Vehicle Non-Compliance Counts
2:40 PM – 3:40 PM	2713	19
3:40 PM – 4:40 PM	3121	34
4:40 PM – 5:40 PM	3067	28
Total	8901	81

Figure 32 An illustration of the detected vehicle non-compliance event

Regarding the pedestrian's non-compliance counts, pedestrians not using the crosswalk or jaywalking are considered non-compliance events. Based on the analysis, it was observed that all the pedestrians at the Hampton Inn at Paterson Plank Rd did jaywalks, and 46.6 percent of the pedestrian at the Murray Hill Pkwy and Patterson Plank Rd. Intersection did not comply. Table 20 and 21 shows the recorded jaywalking or non-compliance behavior of pedestrians every 60 minutes. Figure 33 shows an illustration of the detected pedestrian non-compliance events.

Table 20 Detection results: pedestrian non-compliance counts (Location: Hampton Inn at Paterson Plank Road)

Time	Total Pedestrian Counts	Pedestrian Non-compliance Counts
2:40 PM – 3:40 PM	1	1
3:40 PM – 4:40 PM	2	2
4:40 PM – 5:40 PM	4	4
Total	7	7

Table 21 Detection results: pedestrian non-compliance counts (Location: Murray Hill Pkwy & Paterson Plank Road)

Time	Total Pedestrian Counts	Pedestrian Non-compliance Counts
2:40 PM – 3:40 PM	21	8
3:40 PM – 4:40 PM	38	10
4:40 PM – 5:40 PM	40	28
Total	99	46

Figure 33 An illustration of the detected pedestrian non-compliance event

Lastly, vehicle-to-vehicle traffic conflict exposure was identified using the Surrogate Safety Measure, Post-Encroachment time (PET) based on the extracted trajectory data. As the scope of this study, conflict analysis intends to determine the conflict frequency and severity at a defined conflict region. PET less than 1.5 seconds demonstrates a higher probability of a crash occurring and a dangerous conflict. While a PET event with less than 5 seconds is a possible conflict. Based on the results from the test video, the intersection at Hampton Inn at Paterson Plank Rd. had 39 possible PET vehicle-to-vehicle conflict events and 8 dangerous conflict events. On the other hand, Murray Hill Pkwy. And Paterson Plank Rd. reported 283 possible conflicts and 94 dangerous conflicts. The intersection at Murray Hill Pkwy and Paterson Plank Rd. showed more conflicts compared to the intersection at the Hampton Inn at Paterson Plank Rd. which may be due to several reasons, including traffic volume and intersection geometry. Table 22 provides a summary of the PET event counts based on the severity.

Table 22 Analysis result: Post-Encroachment Time (PET)

PET Threshold (Seconds)	PET Event Count (*Hampton Inn at Paterson Plank Road*)	PET Event Count (*Location: Murray Hill Pkwy & Paterson Plank Road*)	Description
PET Events < 20	106	451	Arbitrary Count
PET Events < 5	39	283	Possible Conflict
PET Events < 1.5	8	94	Dangerous Conflict

CHAPTER 5. CONCLUSIONS

The main objective of this research is to evaluate the mobility and safety impacts of the transportation network in the vicinity of the partial opening of the 3-Million Square Foot American Dream Complex. For this goal, initially, the performance of four surrounding corridors was explored by incorporating travel time inflation (TI) and it counterpart, the Corridor Travel Time Inflation (CTI), as performance measures using probe vehicle data. Then, the changes in the trip duration were also evaluated using Streetlight data with different visualizations of the congestion based on a monthly, and daily basis was provided. Thereafter, safety video analysis was developed to evaluate the intersection safety based on Surrogate Safety Measures (SSM).

Based on the results obtained on a monthly basis CTI, Interstate 95, NJ Route 3, and NJ Route 120 were found to experience 42%, 24%, and 42% increase during non-peak hours and 21%, 27%, and 22% during peak hours in CTI from October to November, respectively.. However, Meadowlands Pkwy, Northbound, followed a slightly decreasing pattern during non-peak hours and an increasing pattern during peak hours. CTI for the entire corridor (Meadowlands Pkwy) remained almost the same (a minor increase of 0.05 hours) during non-peak hours and increased slightly during peak hours. CTI for all corridors dropped with the beginning of the new year's holidays during both non-peak and peak hours, except for the Meadowlands Pkwy Southbound during non-peak hours. TI distributions for all corridors' TMCs during the entire study period were also calculated. It was concluded that only TI of some TMCs along the NJ Route 3 and Interstate 95 experienced high values.

Moreover, results obtained from developed CIMTT heatmaps showed that the partial opening of the complex did not considerably affect the congestion of the surrounding corridors since no obvious decrease or increase in congestion was recorded following the opening of the complex. This result can be attributed to the fact that the complex was only partially opened and was not operated in full capacity. Also, there were many delays in the complex's opening, and it could have been a reason why there was not any considerable change in congestion in terms of visitors coming to the complex. It is noted that the complex was also shut down in March due to COVID-19 pandemic, and during that time, there was a dramatic decrease in congestion in the region (Remache-Patino, and Brennan, 2020). New year's holidays, on the other, majorly affected all the surrounding corridors by decreasing their congestion. This decrease can be explained by the fact that during holidays usually no specific congestion is experienced on the roadways.

The speed heatmaps did not show any considerable pattern of increase or decrease for the opening day too. The comparisons of the Fridays before and after the opening Fridays did not show a consistent pattern. For some cases, the average speed records decreased on the opening Friday, and some others increased.

Based on the StreetLight volume trip data, an increase in the StreetLight volume trips was observed after the complex's opening. Further, based on the statistical analysis results, NJ Route 3 showed

a significant reduction in the StreetLight volume trips for the travel duration of 0 -10 minutes after the opening of the complex. While, NJ Route 120 showed an insignificant reduction in the StreetLight volume trips for the travel duration 0-10 minutes and 10-20 minutes. NJ Route 120 showed a significant increase in the StreetLight volume trips for the travel duration of 20-30 minutes. This shift in the StreetLight volume trips demonstrates that NJ Route 3 and NJ Route 120 had an increase in travel time after the opening of the complex. However, Interstate 95 had a significant increase in the StreetLight volume trips for the travel duration of 0-10 minutes, showing no impact on the travel time after the opening.

In terms of the safety analysis, this study developed an automated video-based methodology to detect, track, count, evaluate non-compliance behavior, and identify vehicle-to-vehicle conflicts and conflict severity. The proposed work can be implemented at the intersection to evaluate safety. Based on the validation result of the safety analysis, the detection and tracking algorithm, i.e., YOLO-V5 and DeepSORT, showed an accuracy between 95 and 98 percent. Further, based on the developed automated non-compliance evaluation methodology (i.e., pedestrian jaywalking and vehicles running a red light) provides a detailed understanding of road users' non-compliance behavior. Lastly, the Post-Encroachment Time (PET) helps to identify the conflict events and severity based on the PET thresholds. The proposed work and the safety measure developed in this study could be adapted to analyze a signalized intersection.

REFERENCES

American Dream Meadowlands. In Wikipedia. https://en.wikipedia.org/wiki/American_Dream_Meadowlands. Accessed on July 29, 2020

Bechtel AJ, Brennan Jr TM, de Araujo JM. Characterizing bridge functional obsolescence using congestion performance measures determined from anonymous probe-vehicle data. Journal of Performance of Constructed Facilities. 2016 April 1;30(2):04015027.

Brennan Jr TM, Remias SM, Grimmer GM, Horton DK, Cox ED, Bullock DM. Probe Vehicle–Based Statewide Mobility Performance Measures for Decision Makers. Transportation research record. 2013 Jan;2338(1):78-90.

Brennan Jr TM, Remias SM, Manili L. Performance measures to characterize corridor travel time delay based on probe vehicle data. Transportation Research Record. 2015 Jan;2526(1):39-50.

Brennan Jr TM, Venigalla MM, Hyde A, LaRegina A. Performance Measures For Characterizing Regional Congestion Using Aggregated Multi-Year Probe Vehicle Data. Transportation Research Record. 2018 Dec;2672(42):170-9.

Brennan TM, Gurriell RA, Bechtel AJ, Venigalla MM. Visualizing and evaluating interdependent regional traffic congestion and system resiliency, a case study using big data from probe vehicles. Journal of Big Data Analytics in Transportation. 2019 June 1;1(1):25-36.

Chen M, Chien SI. Dynamic freeway travel-time prediction with probe vehicle data: Link based versus path based. Transportation Research Record. 2001;1768(1):157-61.

Chen P, Tong R, Lu G, Wang Y. Exploring travel time distribution and variability patterns using probe vehicle data: case study in Beijing. Journal of Advanced Transportation. 2018 January 1;2018.

Hainen AM, Remias SM, Brennan TM, Day CM, Bullock DM. Probe vehicle data for characterizing road conditions associated with inclement weather to improve road maintenance decisions. In2012 IEEE Intelligent Vehicles Symposium 2012 June 3 (pp. 730-735). IEEE.

Hellinga B, Izadpanah P, Takada H, Fu L. Decomposing travel times measured by probe-based traffic monitoring systems to individual road segments. Transportation Research Part C: Emerging Technologies. 2008 Dec 1;16(6):768-82.

Jenelius E, Koutsopoulos HN. Travel time estimation for urban road networks using low frequency probe vehicle data. Transportation Research Part B: Methodological. 2013 July 1;53:64-81.

Jie L, Van Zuylen H, Chunhua L, Shoufeng L. Monitoring travel times in an urban network using video, GPS and Bluetooth. Procedia-Social and Behavioral Sciences. 2011 January 1;20:630-7.

Jintanakul K, Chu L, Jayakrishnan R. Bayesian mixture model for estimating freeway travel time distributions from small probe samples from multiple days. Transportation Research Record. 2009;2136(1):37-44.

Liu K, Yamamoto T, Morikawa T. Estimating delay time at signalized intersections by probe vehicles. Proceedings of ICTTS. 2006 Aug:644-55.

Nanthawichit C, Nakatsuji T, Suzuki H. Application of probe-vehicle data for real-time traffic-state estimation and short-term travel-time prediction on a freeway. Transportation research record. 2003;1855(1):49-59.

Regional Integrated Transportation Information System (RITIS). www.ritis.org. Accessed on July 29, 2020

Remias SM, Brennan TM, Day CM, Summers HT, Horton DK, Cox ED, Bullock DM. Spatially referenced probe data performance measures for infrastructure investment decision makers. Transportation Research Record. 2014 Jan;2420(1):33-44.

Thompson KR. Probe vehicle performance measures for assessing travel time reliability.

Yamamoto T, Liu K, Morikawa T. Variability of travel time estimates using probe vehicle data. InProceedings of the Fourth International Conference on Traffic and Transportation Studies (ICTTS) 2006 August 2 (pp. 278-287).

Zhang Z, Wang Y, Chen P, He Z, Yu G. Probe data-driven travel time forecasting for urban expressways by matching similar spatiotemporal traffic patterns. Transportation Research Part C: Emerging Technologies. 2017 Dec 1;85:476-93.

Zheng F, Van Zuylen H. Urban link travel time estimation based on sparse probe vehicle data. Transportation Research Part C: Emerging Technologies. 2013 June 1;31:145-57.

Zhu X, Fan Y, Zhang F, Ye X, Chen C, Yue H. Multiple-factor based sparse urban travel time prediction. Applied Sciences. 2018 Feb;8(2):279.

Wikipedia contributors. American Dream Meadowlands. Wikipedia, The Free Encyclopedia. Wikipedia, The Free Encyclopedia, 10 Mar. 2021. Web. 14 Mar. 2021.

Chen P, Zeng W, Yu G, Wang Y. Surrogate safety analysis of pedestrian-vehicle conflict at intersections using unmanned aerial vehicle videos. Journal of advanced transportation. 2017 Jan 1;2017.

Tak S, Kim S, Lee D, Yeo H. A comparison analysis of surrogate safety measures with car-following perspectives for advanced driver assistance system. Journal of Advanced Transportation. 2018 Jan 1;2018.

Fu T, Stipancic J, Zangenehpour S, Miranda-Moreno L, Saunier N. Automatic traffic data collection under varying lighting and temperature conditions in multimodal environments: Thermal versus visible spectrum video-based systems. Journal of advanced transportation. 2017 Jan 1;2017.

Li Y, Wu D, Lee J, Yang M, Shi Y. Analysis of the transition condition of rear-end collisions using time-to-collision index and vehicle trajectory data. Accident Analysis & Prevention. 2020 Sep 1;144:105676.

Olszewski P, Dąbkowski P, Szagała P, Czajewski W, Buttler I. Surrogate safety indicator for unsignalised pedestrian crossings. Transportation research part F: traffic psychology and behaviour. 2020 Apr 1;70:25-36.

Guo Y, Sayed T, Zaki MH, Liu P. Safety evaluation of unconventional outside left-turn lane using automated traffic conflict techniques. Canadian Journal of Civil Engineering. 2016;43(7):631-42.

Scholl L, Elagaty M, Ledezma-Navarro B, Zamora E, Miranda-Moreno L. A Surrogate Video-Based Safety Methodology for Diagnosis and Evaluation of Low-Cost Pedestrian-Safety Countermeasures: The Case of Cochabamba, Bolivia. Sustainability. 2019 Jan;11(17):4737.

St-Aubin P, Saunier N, Miranda-Moreno L. Large-scale automated proactive road safety analysis using video data. Transportation Research Part C: Emerging Technologies. 2015 Sep 1;58:363-79.

Li Y, Wu D, Lee J, Yang M, Shi Y. Analysis of the transition condition of rear-end collisions using time-to-collision index and vehicle trajectory data. Accident Analysis & Prevention. 2020 Sep 1;144:105676.

Nadimi N, Behbahani H, Shahbazi H. Calibration and validation of a new time-based surrogate safety measure using fuzzy inference system. Journal of traffic and transportation engineering (English edition). 2016 Feb 1;3(1):51-8.

Qi W, Wang W, Shen B, Wu J. A Modified Post Encroachment Time Model of Urban Road Merging Area Based on Lane-Change Characteristics. IEEE Access. 2020 Apr 16;8:72835-46.

Fu T, Miranda-Moreno L, Saunier N. Measuring crosswalk safety at nonsignalized crossings during nighttime based on surrogate measures of safety: Case study in Montreal, Canada. InTransportation Research Board Annual Meeting Compendium of Papers 2016.

Peesapati LN, Hunter MP, Rodgers MO. Can post encroachment time substitute intersection characteristics in crash prediction models?. Journal of safety research. 2018 Sep 1;66:205-11.

Gettman D, Head L. Surrogate safety measures from traffic simulation models. Transportation Research Record. 2003;1840(1):104-15.

Perkins SR, Harris JI. Criteria for Traffic Conflict Characteristics, Signalized Intersections. Research Laboratories, General Motors Corporation; 1967.

Gettman D, Pu L, Sayed T, Shelby SG, Energy S. Surrogate safety assessment model and validation. No. FHWA-HRT-08-051. Turner-Fairbank Highway Research Center; 2008 Jun 1.

Redmon J, Divvala S, Girshick R, Farhadi A. You only look once: Unified, real-time object detection. InProceedings of the IEEE conference on computer vision and pattern recognition 2016 (pp. 779-788).

Redmon J, Farhadi A. Yolov3: An incremental improvement. arXiv preprint arXiv:1804.02767. 2018 Apr 8.

Wang H, Tong X, Lu F. Deep learning based target detection algorithm for motion capture applications. InJournal of Physics: Conference Series 2020 Nov 1 (Vol. 1682, No. 1, p. 012032). IOP Publishing.

Bewley A, Ge Z, Ott L, Ramos F, Upcroft B. Simple online and real-time tracking. In2016 IEEE international conference on image processing (ICIP) 2016 Sep 25 (pp. 3464-3468). IEEE.

Hou X, Wang Y, Chau LP. Vehicle tracking using deep SORT with low confidence track filtering. In2019 16th IEEE International Conference on Advanced Video and Signal Based Surveillance (AVSS) 2019 Sep 18 (pp. 1-6). IEEE.

Glenn Jocher, Alex Stoken, Jirka Borovec, NanoCode012, ChristopherSTAN, Liu Changyu, et al. ultralytics/yolov5: v4.0 - nn.SiLU() activations, Weights & Biases logging, PyTorch Hub integration. Zenodo; 2021 (https://github.com/ultralytics/yolov5).

StreetLight Data. Resources: success stories. Available: https://www.streetlightdata.com/transportation-planning-success-stories/

StreetLight Data. Why StreetLight: our data. Available: https://www.streetlightdata. com/our-data/ Truckinginfo. (2019). New Jersey has the Worst Traffic Bottleneck in the country. Retrieved from: https://www.truckinginfo.com/325014/new-jersey-has-the-worst-traffic-bottleneck-in-the-country. Accessed on May 07, 2021

Regional Integrated Transportation Information System (RITIS). www.ritis.org. Accessed on July 29, 2020

National Highway Traffic Safety Administration (NHTSA). (2018). State of New Jersey Highway Safety Plan.. https://www.nhtsa.gov/sites/nhtsa.dot.gov/files/documents/new_jersey_fy2018_hsp.pdf). Accessed on July 29, 2021.

Remache-Patino, B., & Brennan, T. (2020). Characterization of the Coronavirus Pandemic on Signalized Intersections Using Probe Vehicle Data. Journal of Modern Mobility Systems, 1, 101-109.

Appendix: A (Average daily O-D StreetLight volume trips for each month)

Average Daily O-D Traffic | July, 2019

● Weekdays ● Weekends

O-D Traffic (StL Volume) vs Days

Values: 1741, 1806, 1691, 392, 563, 146, 1552, 1894, 1681, 1609, 1541, 164, 33, 1963, 1615, 1621, 1449, 1810, 405, 34, 2119, 1992, 2005, 1747, 4269, 478, 72, 1867, 1749, 2035

Average line: 1401

Average Daily O-D Traffic | August, 2019

● Weekdays ● Weekends

O-D Traffic (StL Volume) vs Days

Values: 4861, 2206, 527, 5759, 2030, 2605, 4385, 1774, 228, 156, 1884, 2338, 2157, 2165, 3347, 565, 103, 1616, 2642, 2075, 1867, 2094, 843, 163, 2138, 2272, 2325, 2144, 1657, 181

Average line: 1970

Average Daily O-D Traffic | September, 2019

● Weekdays ● Weekends

O-D Traffic (StL Volume)

2765

Day	Value
1	114
2	173
3	2327
4	2269
5	2796
6	3163
7	589
8	4362
9	3181
10	3444
11	2773
12	2657
13	2587
14	504
15	6031
16	7079
17	3507
18	3212
19	2908
20	2542
21	2948
22	1054
23	2100
24	3127
25	2967
26	2456
27	2472
28	535
29	6403
30	2655

Days

Average Daily O-D Traffic | October, 2019

● Before Opening ● Day Of Opening ● After Opening

O-D Traffic (StL Volume)

3532

Day	Value
1	3030
2	3121
3	3121
4	—
5	623
6	6070
7	2410
8	2832
9	—
10	1756
11	2778
12	683
13	5314
14	2393
15	2381
16	—
17	2789
18	2116
19	742
20	5961
21	6807
22	2659
23	3627
24	4187
25	5488
26	9449
27	7549
28	3487
29	—
30	2834
31	3464

Days

Average Daily O-D Traffic | November, 2019

Weekdays Weekends

O-D Traffic (StL Volume) vs Days

3954

Day	Value
1	3757
2	5627
3	4878
4	9222
5	3732
6	2278
7	4568
8	3382
9	6217
10	9506
11	3173
12	2323
13	2859
14	2577
15	2877
16	4786
17	2852
18	2604
19	2682
20	2706
21	2708
22	2333
23	2795
24	7157
25	2550
26	2687
27	3095
28	1121
29	4729
30	6852

Average Daily O-D Traffic | December, 2019

Weekdays Weekends

O-D Traffic (StL Volume) vs Days

5348

Day	Value
1	5534
2	2152
3	2284
4	2756
5	3109
6	3790
7	6130
8	5011
9	2709
10	3218
11	2909
12	3378
13	3395
14	5498
15	7151
16	2698
17	2843
18	2952
19	2713
20	4235
21	5706
22	8952
23	5208
24	3746
25	5735
26	8929
27	9225
28	10692
29	16217
30	11604
31	5301

Average Daily O-D Traffic | January, 2020

Average Daily O-D Traffic | February, 2020